



10
I29A

#402 CIVIL ENGINEERING STUDIES

C.2 STRUCTURAL RESEARCH SERIES NO. 402

A PROBABILISTIC STUDY OF SAFETY AND DESIGN OF EARTH SLOPES

By

M. S. YUCEMEN

W. H. TANG

A. H-S. ANG

Metz Reference Room
Civil Engineering Department
B106 C. E. Building
University of Illinois
Urbana, Illinois 61801

Issued as a
Technical Report
of Research Supported by the
NATIONAL SCIENCE FOUNDATION
under
Grants GK-1812X and GK-36378

UNIVERSITY OF ILLINOIS
URBANA, ILLINOIS
JULY 1973

A PROBABILISTIC STUDY OF SAFETY AND DESIGN OF EARTH SLOPES

by

M. S. Yucemen

W. H. Tang

and

A. H-S. Ang

Issued as a
Technical Report
of Research Supported by the
NATIONAL SCIENCE FOUNDATION
under
Grants GK-1812X and GK-36378

University of Illinois
Urbana, Illinois
July 1973

ACKNOWLEDGMENTS

This report is based on the doctoral dissertation of M. S. Yucemen submitted to the Graduate College, University of Illinois at Urbana-Champaign, for partial fulfillment of the Ph.D. degree. The study was conducted under the directions of Professors A. H-S. Ang and W. H. Tang, as part of a research program on the probabilistic methods in engineering design, supported by the National Science Foundation (currently) under grant GK-36378.

The authors acknowledge the advice provided by the staff in soil and rock mechanics; in particular, Professors M. T. Davisson, A. J. Hendron, and H. O. Ireland.

The numerical work was performed on the IBM 360/75 system of the Computing Service Office of the University.

TABLE OF CONTENTS

Chapter		Page
1	INTRODUCTION AND BACKGROUND	1
	1.1 General Remarks	1
	1.2 Review of Previous Work.	2
	1.3 Objectives and Scope of Study.	5
	1.4 Notation.	7
2	BASIC RELIABILITY MODELS	11
	2.1 General Remarks	11
	2.2 Bases of Reliability Analysis.	12
	2.3 Estimation and Updating of Uncertainties	21
3	PROBABILISTIC MODELS FOR STABILITY ANALYSIS OF SLOPES	29
	3.1 General Remarks	29
	3.2 Probabilistic Models for the Total Stress Analysis of Slopes	30
	3.3 Probabilistic Models for the Effective Stress Analysis of Slopes	39
4	EVALUATION OF SHORT-TERM STABILITY OF SLOPES	51
	4.1 Inherent Variability and Uncertainty Due to Insufficient Sampling	51
	4.2 Discrepancies Between Laboratory and In Situ Undrained Strengths	51
	4.3 Model Uncertainty.	74
	4.4 Analysis of Results	76
	4.5 Recommended Safety Factors for Design	83
5	EVALUATION OF LONG-TERM STABILITY OF SLOPES.	89
	5.1 Inherent Variability and Uncertainty Due to Insufficient Sampling	89
	5.2 Discrepancies Between Laboratory and In Situ Peak Effective Stress Parameters	89
	5.3 Uncertainty Associated with the Estimation of Pore Pressure Distribution.	104
	5.4 Uncertainty Due to the Method of Analysis (Model Uncertainty)	108
	5.5 Analysis of Results	111
	5.6 Recommended Safety Factors for Design	117

	Page
6	APPLICATIONS TO ACTUAL FAILURE CASES 119
	6.1 General Remarks 119
	6.2 An Example of Short-Term Slope Stability: The Congress Street Open Cut in Chicago 119
	6.3 An Example of Long-Term Slope Stability: Landslide at Selset 132
7	SUMMARY AND CONCLUSIONS 142
	LIST OF REFERENCES 145
APPENDIX	
A	COMPUTATION OF \bar{N}_2 AND Δ_2 FOR s FROM PECK'S DATA 184
B	COMPUTATION OF THE SPATIAL CORRELATION PARAMETER v FROM HOOPER AND BUTLER'S DATA 187
C	DERIVATION OF AN APPROXIMATE EXPRESSION FOR $\rho_{N_i N_j}$ 194
D	MEAN, VARIANCE AND COVARIANCE OF \hat{s}_i BASED ON REGRESSION ANALYSIS. 197
E	RELATION BETWEEN MEAN SAFETY FACTOR AND CORRECTIVE FACTOR N_f FOR SHORT-TERM SLOPE STABILITY 199
F	COMPUTATION OF THE STATISTICAL PARAMETERS OF s FOR THE FIRST LAYER BASED ON REGRES- SION ANALYSIS. 200
G	ANALYSIS OF THE COHESIONLESS LAYER. 202

LIST OF TABLES

Table		Page
2.1	Mean and Coefficient of Variation of N_j Corresponding to Different Distributions Assumed Over Its Range	23
4.1	Values of δ_s from Various Sources	52
4.2	Mean Correction and Sampling Error Due to Changes in Stress State.	54
4.3	Comparison Between Shear Strengths of Borehole Samples and Block Specimens for London Clay at Ashford Common Shaft.	56
4.4	Data for $N_2(s)$ from Different Sites.	58
4.5	Mean Correction and Sampling Error Due to Mechanical Disturbance	59
4.6	Size Effect on Undrained Strength of Blue London Clay	60
4.7	Data for $N_3(s)$ from Different Sites.	61
4.8	Mean Correction and Sampling Error Due to Specimen Size.	62
4.9	Data for $N_4(s)$ from Different Sites.	64
4.10	Corrections for Rate of Shearing.	65
4.11	Data for $N_5(s)$ from Different Sites.	69
4.12	Corrections for Orientation and Anisotropy	71
4.13	Data for $N_6(s)$ from Different Sites	72
4.14	Values of the Corrective Factors for the Slip at Bradwell.	73
4.15	Safety Factors in End-of-Construction Failures in Excavations.	75
4.16	Corrections to Computed Shear Strength for Various Soil Conditions	78

	Page	
4.17	Failure Probabilities of Slopes Designed with Current Safety Factors	83
4.18	Recommended Values of the Safety Factor for Design (With Minimum Soil Exploration)	85
4.19	Recommended Values of the Safety Factor for Design (With Extensive Soil Exploration, Stiff-Fissured Clays)	86
4.20	Recommended Values of the Safety Factor for Design (With Extensive Soil Exploration, Intact Clays).	87
5.1	Data for the Effect of Specimen Size on c and ϕ	91
5.2	Mean Correction and Sampling Error Due to Specimen Size.	93
5.3	Data for $N_4(c)$ and $N_4(\phi)$ from Different Sites	94
5.4	Corrections for Rate of Shearing	95
5.5	Data for $N_5(c)$ and $N_5(\phi)$ from Different Sites	96
5.6	Data for $N_6(c)$ and $N_6(\phi)$ from Different Sites	97
5.7	Summary of Available Data for the Computation of N_{sf}	100
5.8	Comparison of $\hat{\phi}_r$ Values from Different Testing Methods ^r	103
5.9	Mean Corrections and Prediction Errors Due to Progressive Failure	105
5.10	Corrections to Estimated Pore Pressures for Different Sites.	107
5.11	Available Data for N_f	109
5.12	Statistical Parameters of N_{MR} for Different Soil Conditions (With Minimum Soil Exploration)	113
5.13	Failure Probabilities of Slopes Designed with the Current Safety Factor of 1.5	116

	Page
5.14 Recommended Values of the Safety Factor for Design	118
6.1 Data for the Undrained Strengths at Congress Street	121
6.2 Data for \hat{s} from Different Borings	122
6.3 Statistical Parameters of s Based on Regression Analysis	123
6.4 Comparison of the Statistical Parameters of s as Obtained from Two Different Methods	124
6.5 Failure Probabilities Computed from the Original and New Slope Profiles	130
6.6 Summary of Test Results at Selsset	133
6.7 Mean Resisting Moments Corresponding to Different Pore Pressure Distributions	138
A.1 Comparison of Shear Strengths of Undisturbed and Shelby Tube Samples at Chicago Subway.	185
B.1 Summary of Shear Strength Data	188
B.2 Values of $\rho(\lambda)$	191

LIST OF FIGURES

Figure		Page
3.1	Circular Arc Analysis of Slope Stability	154
3.2	Equivalent Number of Statistically Independent Soil Elements	155
3.3	Forces Considered in the Fellenius Method of Slices	156
4.1	A Typical Histogram for the Undrained Shear Strength of London Clay.	157
4.2	Unconfined Compression Tests from Chicago Subway.	157
4.3	Relation Between Undrained Strengths Mea- sured on 4 in. x 8 in. and 1-1/2 in. x 3 in. Specimens for Brown London Clay at Kensal Green.	158
4.4	Strength Ratio Versus Elapsed Time to Failure	158
4.5	The Variation in Strength with Time to Failure for Undrained Tests on Weald Clay and Boston Blue Clay	159
4.6	(a) Orientation of Specimens at Various Locations of the Failure Surface, (b) Definition of Geometric Parameters Related to the Orientation of Specimens, (c) Variation of α and β for a Typical Slip Circle.	160
4.7	Variation of Maximum Deviator Stress with Orientation of Failure Plane in UU Triaxial Tests: (a) for Over- Consolidated Kaolinite Clay; (b) for Normally Consolidated San Francisco Bay Mud	161
4.8	Variation of Undrained Strength with Specimen Orientation (Isotropic Clays).	162

	Page
4.9	Variation of Undrained Strength with Specimen Orientation (Clays with C-Anisotropy) 163
4.10	Variation of Undrained Strength with Specimen Orientation (Clays with M-Anisotropy) 164
4.11	Example to Illustrate the Computation of $N_5(s)$ 165
4.12	Variation of p_f with Mean Safety Factor for Stiff-Fissured Clays (with Minimum Soil Exploration) 166
4.13	Variation of p_f with Mean Safety Factor for Intact Clays (with Minimum Soil Exploration). 167
4.14a	Variation of Mean Safety Factor with Number of Specimens ($p_f = 10^{-1}$) 168
4.14b	Variation of Mean Safety Factor with Number of Specimens ($p_f = 10^{-3}$) 169
4.15	Variation of p_f with Mean Safety Factor Considering the Degree of Soil Exploration (Stiff-Fissured Clays) 170
5.1	Variation in Strength with Time to Failure in Drained Compression Tests on Remoulded Weald Clay 171
5.2	Variation of ϕ and c with Specimen Orientation 172
5.3	Comparison of Strengths for Plane Strain and Triaxial Specimens in Terms of Effective Stresses for Remoulded Weald Clay 173
5.4	Stress Strain Curve Considering Large Displacements 173
5.5	Variation of p_f with Mean Safety Factor for First-Time Slides in Intact Clays (with Minimum Soil Exploration) 174
5.6	Variation of p_f with Mean Safety Factor for First-Time Slides in Stiff-Fissured Clays (with Minimum Soil Exploration) 175

	Page	
5.7	Variation of p_f with Mean Safety Factor for Slides on Pre-Existing Slip Surfaces in Stiff- Fissured Clays (with Minimum Soil Exploration)	176
5.8	Variation of p_f with Mean Safety Factor Considering the Degree of Soil Exploration (First-Time Slides in Stiff-Fissured Clays)	177
6.1	Approximate Cross Section of the Cut and the Approximate Position of the Actual Slip Surface at Congress Street Open Cut	178
6.2	Segments Along the Failure Surface	179
6.3	Undrained Shear Strength Versus Depth	180
6.4	Original and New Slope Profiles, the Location of the Rotation Centers and the Position of the Actual and Critical Slip Surfaces (Congress Street)	181
6.5	Average Cross Section of the Slope and the Position of the Most Critical Potential Failure Surface at Selset	182
6.6	Flow Nets A and B.	183
B.1	U4 Sampling.	192
B.2	U1-1/2 Sampling	193
G.1	Resistance Due to Cohesionless Layer	204

Chapter 1

INTRODUCTION AND BACKGROUND

1.1 General Remarks

Soil and foundation engineering are characterized by numerous uncertainties, resulting from insufficient information and inadequate knowledge of the subsoil conditions. Properties of soil generally vary from location to location and also may change with time.

The design and analysis of earthworks, earth retaining structures and foundations involve large soil masses. In conventional practice, based on the results of soil exploration and testing, a large soil mass is divided into smaller regions (layers and slices) within which the soil properties may be assumed to be homogeneous. For each of these smaller regions, the soil properties are represented by their spatial averages within the region. However, due to limited sampling efforts, the estimates of these spatial averages will involve some uncertainty.

Additional uncertainties are introduced due to the estimation of the in situ soil properties from the results of laboratory soil tests. In such tests the actual conditions in the field would not be simulated perfectly. For example, the average shear strength parameters obtained from the laboratory triaxial tests differ from the in situ values due to factors such as changes in the stress system, disturbance during sampling, anisotropy, plane strain and progressive failure. The total uncertainty would also include those associated with the estimation of pore pressures and loads acting in the field and various simplifying assumptions and idealizations in the analysis.

In the field of soil and foundation engineering, these uncertainties are well recognized (Feld,³⁴ Jumikis,⁴⁷ Peck,⁸¹ and Sowers¹⁰¹) and are implicitly accounted for through the use of the traditional safety factors in designs. Conventional design relies heavily on the subjective choice of the design parameters, design load specifications and design models, supplemented with a safety factor selected on the basis of experience and judgment. Certain shortcomings may be observed in this procedure; namely:

1. The associated reliability level or risk of design is unknown and there is no quantitative and consistent basis for comparing the relative risk or safety of various designs.
2. There is no systematic way of analyzing the degree of uncertainty and its effect on the safety of design.
3. Additional information obtained through intensive soil exploration, improved testing techniques, or better correlation studies cannot be incorporated systematically in the evaluation of uncertainty and subsequent reduction of the required safety factor for design.

These shortcomings can be overcome through the application of probability concepts, which are the proper tools for the modeling and analysis of uncertainties. Probabilistic concepts also provide a consistent basis for combining various sources of information to update the uncertainties for risk evaluation. Furthermore, the expression of safety in terms of risk facilitates the application of decision analysis in the selection of optimal design.

1.2 Review of Previous Work

During the last few years, increasing interest has been shown in

the application of probabilistic procedures to soil mechanics and foundation engineering problems. The previous work in this area may be divided into three main groups:

1. Those that employ statistical methods for estimating soil parameters for the development of empirical relations among various soil properties. Most of the studies in this group are in the form of regression analyses on soil properties (e.g., Cozzolini,²⁴ Holtz and Krizek,⁴⁰ Ladd et al.,⁵⁶ Lumb,⁶⁴ and Terzaghi and Peck¹⁰⁸). Work has also been done to fit probability distributions to soil data. Confidence intervals of the mean were applied to calculate the number of specimens that were required for a satisfactory estimation of various soil parameters such as compressibility, shear strength, etc. (Hooper and Butler,⁴¹ Kay and Krizek,⁴⁸ Lumb,^{65,67} Nelson et al.,⁷⁶ and Schultze⁸⁶).
2. Those that treat the subject of safety factor probabilistically. These include the analyses of earthworks, earth retaining structures and foundations (Biernatowski,⁵ Cornell,²² Klein and Karavaev,⁵³ Langejan,⁶⁰ Lumb,⁶⁶ Lytton,⁶⁸ Meyerhof,⁷¹ Nishida et al.,⁷⁷ Resendiz and Herrera,⁸⁴ Shuk,⁸⁹ Singh,⁹¹ Tang et al.,¹⁰⁵ and Wu and Kraft¹¹⁸⁻¹²⁰).
3. Those that apply the concepts of statistical decision theory. Most of these are based on the Bayesian approach (Costello and Laguros,²³ Folayan et al.,³⁶ Rosenblueth,⁸⁵ Tang,¹⁰⁴ Turkstra,¹¹⁰ and Wu and Kraft^{119,120}).

These studies serve to indicate the potential applications of statistical and probabilistic concepts in soil and foundation engineering. However, most of these works assumed highly idealized conditions, and thus the applications are limited to simple cases. Also, few are design-oriented or made use of available field experience and laboratory data.

Probabilistic analysis of slopes has been pursued by Wu and Kraft^{11,19,120} and Cornell.²² Wu and Kraft studied the static and seismic stability of slopes using the total stress analysis. The spatial correlation of undrained strength was not considered. The errors in the method of analysis (referred to as the mechanism errors) arising from factors such as anisotropy, plane strain, progressive failure, sampling disturbance and shape of failure surface were estimated from a limited survey of data reported in the literature. Moreover, the effects of rate of shearing and specimen size were not taken into consideration. Probability distributions were assigned to each of the random variables involved in the stability model, and the probability distribution of the safety margin was determined. As expected, the resulting equations are quite complex, and thus the practical applications are limited.

The static stability analysis of slopes by Cornell was based on the first-order probability theory, which leads to simple computations. Linear regression analysis was used to determine any significant spatial trend in the soil properties and also to obtain the mean-value functions and the variances and covariances of the estimators. However, Cornell's study lacks a thorough evaluation of various uncertainties involved in the slope stability problem.

In these studies no probabilistic model has been suggested for the effective stress analysis of slopes under long-term conditions.

In the last 20 years, various records of slope failures have been documented and studied extensively by researchers all over the world (Bjerrum and Kjaernsli,¹⁶ Henkel and Skempton,³⁸ Ireland,⁴³ Kjaernsli and Simons,⁵² Sevaldson,⁸⁸ Skempton and Brown,⁹⁴ Skempton,⁹⁶ Skempton and La Rochelle,⁹⁷ Wolfskill and Lambe,¹¹⁶ and Wright and Duncan¹¹⁷). The published results of these investigations and related works offer a valuable source for the analysis of uncertainties involved in the short and long-term static stability of slopes.

1.3 Objectives and Scope of Study

The purpose of this investigation is to formulate a probabilistic method by which all sources of uncertainties can be modeled and systematically analyzed relative to the slope stability problem. It is intended to develop a practical risk-based design procedure that can be used by the practicing engineer. For these purposes, the proposed format will be based on the approximate first-order probability theory. The problems of short and long-term stability of slopes are developed to illustrate the proposed probabilistic procedure.

Based on an extensive literature survey, this study summarizes the research results relevant to the evaluation of the effect of various uncertainties encountered in the slope stability problem. Attempts to suggest general guidelines for evaluating the uncertainties in different soil types are also made.

In Chapter 2 the probabilistic concepts that will be used in the formulation of a risk-based design are reviewed. The general equations for

the analysis of uncertainties and risk-based design are derived using first-order probability theory. A procedure for updating information is also developed and its application illustrated.

Chapter 3 contains the formulation of the probabilistic models for the total and effective stress analysis of slopes. The spatial correlation of shear strength parameters are described by taking into account the two cases where the variation in strength is assumed to be with and without any significant spatial trend.

In Chapter 4, the uncertainties involved in the short-term stability analysis of slopes are investigated and evaluated quantitatively using information reported in the literature. The relative contribution from different sources of uncertainty and their effect on the reliability of slopes are studied with a typical example. The level of reliability underlying present design of slopes and the range of existing uncertainty are also evaluated. Safety factors for the design of slopes in various types of soil conditions that are commonly encountered in practice are developed for specified risk levels.

Chapter 5 contains a study similar to that of Chapter 4 for the long-term stability of slopes based on the effective stress method.

In Chapter 6, two case studies of slope failures are presented to illustrate the proposed probabilistic method. These are specifically

1. The Congress Street Open Cut, Chicago (short-term) and
2. The Selset Landslide, Yorkshire, England (long-term).

Each case is analyzed in detail, based on a realistic evaluation of all the underlying uncertainties. In both cases, redesigns are suggested to meet certain specified reliability levels.

Chapter 7 contains a summary of the results of this research.

Appendix A illustrates a typical procedure evaluating the corrective factor. The effect of mechanical disturbance on undrained shear strength is analyzed using the data given by Peck.⁷⁹ Appendix B describes the estimation of the spatial correlation of undrained shear strength based on the data reported by Hooper and Butler.⁴¹ In Appendix C an approximate expression is derived for estimating the correlation coefficient between two corrective factors which are functions of other corrective factors. Appendix D contains the equations for the mean, variance and covariance of the undrained shear strength for the case when the strength is a function of depth. In Appendix E a relation between the safety factor and the corrective factor for the design model is derived for the short-term slope stability. Appendices F and G complement the analysis of the Congress Street Open Cut presented in Chapter 6.

1.4 Notation

For convenient reference, the principal symbols used in this text are listed below. A bar over the variable denotes its mean value.

C	in situ peak effective cohesion intercept
c	spatial average of in situ peak effective cohesion intercept
c_r	spatial average of in situ residual cohesion intercept
\bar{F}	computed mean safety factor

l_i	length of the i th segment of the failure arc
M_O	overturning moment
M_R	resisting moment
N	corrective factor with mean \bar{N} and c.o.v. Δ
n_e	equivalent number of statistically independent soil elements
n_s	number of specimens
p_f	probability of failure
r	radius of failure surface
S	in situ undrained shear strength
S_f	in situ peak shear strength
S_t	sensitivity
s	spatial average of in situ undrained shear strength
s_f	spatial average of in situ peak shear strength
s_m	average shear strength mobilized at the site
s_r	spatial average of in situ residual shear strength
\bar{u}_i	average pore pressure for the i th slice computed from the best estimate of the pore pressure distribution along the failure surface

v	spatial correlation parameter
X	a design variable describing a spatial average in situ soil property
\hat{X}	model of X with mean \bar{X} and c.o.v. δ_X
γ	average unit weight of soil deposit
Δ_X	c.o.v. of N_X ; a measure of the prediction and modeling uncertainty in \bar{X}
δ_X	c.o.v. of \hat{X} ; a measure of the inherent variability in X
η	ratio of the cohesive and frictional components of M_R
μ_F	"actual" mean safety factor
μ_k	true mean value of X_k
ρ	coefficient of correlation
σ	standard deviation
$\Phi(x)$	standard normal probability distribution function evaluated at x
$\Phi^{-1}(1-p_f)$	value of the standard normal variate corresponding to a cumulative probability of $(1-p_f)$
ϕ	in situ peak effective angle of shearing resistance
ϕ	spatial average of in situ peak effective angle of shearing resistance

ϕ_r spatial average of in situ residual angle of shearing resistance

Ω_X c.o.v. denoting the overall uncertainty in X

Chapter 2

BASIC RELIABILITY MODELS

2.1 General Remarks

The reliability of an engineering system or a component of the system is determined by comparing the resistance of the system (or component) to the applied load or load effect. In the probabilistic formulation developed here, the reliability of a slope at a certain section is analyzed by comparing the resisting moment, M_R , and the overturning moment, M_O , acting per unit of width at that particular section of the slope. A shear failure will occur when M_O exceeds M_R , causing a portion of the slope to move along a surface relative to the rest of the soil mass. Considering M_R and M_O as random variables, the risk of failure can be defined as

$$p_f = \text{Pr} (M_R \leq M_O) \quad (2.1)$$

or

$$p_f = \int_0^{\infty} \int_0^{m_o} f_{M_R, M_O} (m_R, m_o) dm_R dm_o \quad (2.2)$$

where $f_{M_R, M_O} (m_R, m_o)$ is the joint density function of M_R and M_O . For statistically independent M_R and M_O

$$f_{M_R, M_O} (m_R, m_o) = f_{M_R} (m_R) f_{M_O} (m_o)$$

and

$$p_f = \int_0^{\infty} \int_0^{m_o} f_{M_R} (m_R) f_{M_O} (m_o) dm_R dm_o \quad (2.2a)$$

For prescribed or assumed distributions of M_R and M_O , expressions relating p_f to the means and variances (or coefficients of variation) of M_R and M_O can be derived (Ang³). From these expressions design equations corresponding to a specified risk level may be obtained in terms of the required mean resisting moment and associated uncertainty (see Section 2.2.2).

In actual earthwork design, of course, there is not enough data to justify or ascertain a particular probability distribution. It is well-known that a design will be sensitive to the assumed distribution at low risks, say $\ll 10^{-3}$ (Ang,² Ellingwood and Ang,³² and Turkstra¹⁰⁹). Fortunately, as indicated by Meyerhof⁷¹ and as found in this study, the customary overall safety factors used in the design of slopes correspond to probabilities of failure greater than 10^{-3} . Thus, due to high risk levels ($> 10^{-3}$) involved in the design of earth slopes, the distribution sensitivity is not too important (Ang²).

2.2 Bases of Reliability Analysis

2.2.1 First-Order Approximate Analysis

In the stability analysis of slopes, both the resisting and overturning moments will depend on other variables. For example, the resisting moment is a function of the undrained strength and the geometry of the slope under short-term conditions. Since the geometry of a slope is usually well-defined, the dimensions associated with the slope profile will be considered as constants in this study; however, if necessary, the dimensions can be treated also as random variables. The stability analysis of slopes generally involves a large soil mass. In conventional practice, this large soil mass

is divided into smaller regions (layers and slices); over each of these smaller regions the soil medium is assumed to be homogeneous, and the soil properties are represented by the spatial averages of the corresponding soil parameters. Therefore, consistent with this approach, the spatial averages of the respective soil parameters will be used in the stability model. For example, the resisting moment, M_R , will be a function of the spatial averages of the in situ soil properties, X_i 's, as

$$M_R = f(X_1, X_2, \dots, X_n) \quad (2.3)$$

If the model for the resisting moment as expressed by the function in Eq. 2.3 represents reality perfectly, and if X_1, X_2, \dots, X_n are free from any prediction errors, then the uncertainty in M_R will consist only of the inherent spatial variabilities in the soil properties. However, because of the various simplifying assumptions and approximations, the model of the resisting moment used in design will not describe reality exactly. Furthermore, the soil parameters involved in the computation of M_R will be subject also to estimation errors. For these modeling and estimation errors, non-dimensional corrective factors N_f and N_{X_i} are introduced (Ang²) such that

$$f = N_f \hat{f} \quad (2.4)$$

$$X_i = N_{X_i} \hat{X}_i \quad i = 1, 2, \dots, n \quad (2.4a)$$

where \hat{f} is the empirical or theoretical function adopted for determining M_R , and \hat{X}_i is a random variable assumed to model X_i . The use of corrective factors was suggested by Ang¹⁻³ in developing the extended reliability concept. Hence, Eq. 2.3 becomes

$$M_R = N_f \hat{f}(N_{X_1} \hat{X}_1, N_{X_2} \hat{X}_2, \dots, N_{X_n} \hat{X}_n) \quad (2.5)$$

Here \hat{X}_i 's, N_f and N_{X_i} 's are assumed as random variables with means \bar{X}_i , \bar{N}_f , \bar{N}_{X_i} , and coefficients of variation δ_{X_i} , Ω_f , Δ_{X_i} , respectively.

The uncertainties associated with the basic variability in X_i therefore is measured by δ_{X_i} . \bar{X}_i and δ_{X_i} would be evaluated from observed data, although engineering judgment is sometimes also needed especially when data is limited (Tang and Ang¹⁰⁶). Δ_{X_i} represents a measure of the prediction uncertainty in X_i . Consistent with the first-order approximation (Ang,² and Tang and Ang¹⁰⁶), Δ_{X_i} will be ascribed entirely to the errors in the predicted mean value \bar{X}_i . Accordingly, one can write

$$N_{X_i} = \frac{X_i}{\bar{X}_i} \approx \frac{\mu_i}{\bar{X}_i} \quad (2.6)$$

where μ_i denotes the true mean of X_i . \bar{N}_f and Ω_f describe respectively, the mean bias and the uncertainty in the functional model of the resisting moment.

Here

$$\Omega_f = \sqrt{\delta_f^2 + \Delta_f^2} \quad (2.7)$$

where δ_f represents the basic variability about the proposed function, and Δ_f denotes any imperfections in the form of the equation used.

The functional relationship adopted in conventional design could be rather complex; hence, an exact statistical analysis of M_R based on Eq. 2.3 might be infeasible. However, an approximate but systematic method of analysis should be satisfactory for practical engineering purposes. Suppose M_R is expanded in a Taylor series about the true means of X_1, X_2, \dots, X_n , respectively.

Keeping only the linear terms in the expansion, the mean value of M_R is given approximately as (Ang,² and Tang and Ang¹⁰⁶)

$$\mu_{M_R} \approx \bar{N}_f \hat{f}(\mu_1, \mu_2, \dots, \mu_n) \quad (2.8)$$

in which $\mu_i = \bar{N}_{X_i} \bar{X}_i$, assuming N_{X_i} and \hat{X}_i are statistically independent.

Similarly, a first-order approximation of the uncertainty in M_R can be obtained. Assuming N_f to be uncorrelated with all of the other random variables involved in M_R , it is shown that (Tang and Ang¹⁰⁶)

$$\begin{aligned} \Omega_{M_R}^2 &\approx \Omega_f^2 + \frac{1}{2} \left[\sum_{i=1}^n \left(\frac{\partial f}{\partial X_i} \right)_0^2 \bar{N}_{X_i}^2 \bar{X}_i^2 \Omega_{X_i}^2 \right. \\ &+ 2 \sum_{i=1}^n \sum_{j=i+1}^n \left(\frac{\partial f}{\partial X_i} \right)_0 \left(\frac{\partial f}{\partial X_j} \right)_0 \bar{N}_{X_i} \bar{N}_{X_j} \bar{X}_i \bar{X}_j (\rho_{N_i N_j} \Delta_{X_i} \Delta_{X_j} \\ &\left. + \rho_{\hat{X}_i \hat{X}_j} \delta_{X_i} \delta_{X_j} \right) \left. \right] \quad (2.9) \end{aligned}$$

where the first partial derivatives of f are evaluated at the mean values, $\mu_1, \mu_2, \dots, \mu_n$; Ω_{X_i} is the total uncertainty associated with the basic variability in and prediction error of X_i and is given as

$$\Omega_{X_i} = \sqrt{\delta_{X_i}^2 + \Delta_{X_i}^2} \quad (2.10)$$

$\rho_{N_i N_j}$ and $\rho_{\hat{X}_i \hat{X}_j}$ are the correlation coefficients between the corrective factors N_{X_i} and N_{X_j} and between the models \hat{X}_i and \hat{X}_j , respectively.

In cases where n pairs of observations are available on \hat{X}_i and \hat{X}_j , then $\rho_{\hat{X}_i \hat{X}_j}$ would be computed from

$$\rho_{\hat{X}_i \hat{X}_j} = \frac{\frac{1}{n} \sum_{k=1}^n [(\hat{X}_{ik} - \bar{X}_i)(\hat{X}_{jk} - \bar{X}_j)]}{\sqrt{\text{VAR}(\hat{X}_i) \text{VAR}(\hat{X}_j)}} \quad (2.11)$$

in which \hat{X}_{ik} and \hat{X}_{jk} are the k th observed values of \hat{X}_i and \hat{X}_j , respectively. The evaluation of $\rho_{N_i N_j}$ is more difficult; a simplified method for estimating $\rho_{N_i N_j}$ is given in Appendix C, where N_{X_i} and N_{X_j} are each a product of other corrective factors.

In a similar way, a first-order approximation of μ_{M_0} and Ω_{M_0} can be obtained in terms of functions of the first and second-moments of the variables used in modeling M_0 .

If necessary the corrective factor N_{X_i} may be assumed to be the product of several component factors. For example, in estimating the spatial average of an in situ shear strength parameter based on laboratory tests, there will be prediction errors due to rate of shearing, disturbance during sampling, specimen size, etc. The corrective factor associated with \hat{X}_i should represent the combined effect of these factors. For this purpose N_{X_i} will be written in the following form

$$N_{X_i} = \prod_{j=1}^{n_0} N_j \quad (2.12)$$

where N_j represents the corrective factor to compensate for the prediction error in X_i due to the j th effect, and n_0 is the number of independent corrective factors. In conformity with the first-order approximation for statistically independent N_j 's, one gets

$$E(N_{X_i}) = \bar{N}_{X_i} = \prod_{j=1}^{n_0} \bar{N}_j \quad (2.13)$$

and,

$$\Delta_{X_i}^2 \approx \sum_{j=1}^{n_0} \Delta_j^2 \quad (2.14)$$

where Δ_j is the c.o.v. of N_j .

2.2.2 Evaluation of Risk

Once the mean and the total uncertainty of M_R and M_O are evaluated, the failure probability of a slope at a particular section can be computed by using Eq. 2.1 for prescribed distributions of M_R and M_O . Since in earth slopes p_f is moderately high ($> 10^{-3}$), the choice of these distributions will not be too important; hence, any distribution (or sets of distributions) that will facilitate the calculation of the failure probability will suffice. Throughout this study M_R and M_O are assumed to be lognormal variates.

The mean resisting and overturning moments \bar{M}_R and \bar{M}_O , computed by using the laboratory test results and the imperfect design equations without any corrections, will generally be different than the corresponding in situ values μ_{M_R} and μ_{M_O} due to the existence of systematic biases. For slopes where the weight of soil above the sliding surface is the only external load, the uncertainty in the overturning moment is small relative to that in the resisting moment* (Cornell²² and Singh⁹¹); thus, the discrepancy between \bar{M}_O and μ_{M_O} is expected to be small (i.e., $\mu_{M_O} \approx \bar{M}_O$). On the other hand, the discrepancy between \bar{M}_R and μ_{M_R} may be significant due to the systematic biases involved in the basic design variables and in the design equations. Thus,

* For example, in the analysis of the slide at Selset Ω_{M_O} is estimated to be less than 0.01 compared to $\Omega_{M_R} = 0.12$.

$$\mu_{M_R} = N_{M_R} \bar{M}_R \quad (2.15)$$

where N_{M_R} is the corrective factor that accounts for the overall bias in the mean resisting moment resulting from the combined effects of the systematic biases in the component design variables and in the design equations.

Assuming M_R and M_o to be statistically independent lognormal variates, the probability of failure is

$$p_f = 1 - \Phi \left\{ \frac{\ln \left[\frac{\mu_{M_R}}{\mu_{M_o}} \sqrt{\frac{1 + \Omega_{M_o}^2}{1 + \Omega_{M_R}^2}} \right]}{\sqrt{\ln[(1 + \Omega_{M_R}^2)(1 + \Omega_{M_o}^2)]}} \right\} \quad (2.16)$$

where $\Phi(\cdot)$ is the standard normal probability distribution function. If Ω_{M_R} and Ω_{M_o} are small (say ≤ 0.30)

$$\ln(1 + \Omega^2) \approx \Omega^2 \quad (2.17)$$

Using Eq. 2.17 and introducing

$$\mu_F = \frac{\mu_{M_R}}{\mu_{M_o}} \approx \frac{\bar{N}_{M_R} \bar{M}_R}{\bar{M}_o} = \bar{N}_{M_R} \bar{F} \quad (2.18)$$

into Eq. 2.16, the probability of failure becomes

$$p_f \approx 1 - \Phi \left[\frac{\ln \mu_F - \frac{1}{2} (\Omega_{M_R}^2 - \Omega_{M_o}^2)}{\sqrt{\Omega_{M_R}^2 + \Omega_{M_o}^2}} \right] \quad (2.19)$$

or in terms of \bar{F}

$$p_f \approx 1 - \Phi \left[\frac{\ln(\bar{N}_{M_R} \bar{F}) - \frac{1}{2}(\Omega_{M_R}^2 - \Omega_{M_0}^2)}{\sqrt{\Omega_{M_R}^2 + \Omega_{M_0}^2}} \right] \quad (2.19a)$$

Since μ_F is the ratio of the "actual" mean resisting moment to the "actual" mean overturning moment, it may be called the "actual mean safety factor" (in the sense that the values of the design variables have been corrected for various systematic errors). On the other hand, the calculated $\bar{F} = \bar{M}_R/\bar{M}_O$ does not reflect any corrections for errors in modeling and prediction, and will be referred to as the "computed mean safety factor."

The term $1/2(\Omega_{M_R}^2 - \Omega_{M_0}^2)$ in Eq. 2.19 could be significant. This is due to the fact that, Ω_{M_0} will be very small in this case compared to Ω_{M_R} , and $1/2(\Omega_{M_R}^2 - \Omega_{M_0}^2)$ will not be negligible compared to $\ln \mu_F$ especially when μ_F is close to 1.0. For example, for $\Omega_{M_R} = 0.20$, $\Omega_{M_0} = 0$ and $\mu_F = 1.1$, the failure probability computed from Eq. 2.19 is in error by 10 percent if $1/2(\Omega_{M_R}^2 - \Omega_{M_0}^2)$ is omitted in Eq. 2.19.

In applying the above probabilistic procedure to the reliability analysis of earth slopes, we need to search for the surface with the largest failure probability (minimum reliability). From the standpoint of system reliability analysis, the reliability of a slope (taken as a system) is not equal to the reliability of the most critical potential failure surface; however, it cannot be greater than that of the failure surface with the smallest reliability. Theoretically, there are infinite potential failure surfaces and each one of them could be considered as a possible failure surface. It is reasonable to assume that only those surfaces with failure probabilities close to the maximum failure probability will contribute to the system failure probability.

Cornell²² indicated that the correlation among the safety factors of different surfaces are expected to be high. Accordingly, even if there are infinitely many potential failure surfaces, their contribution to the system failure probability, with the exception of the one with maximum failure probability, may be small. There is no information available in the literature on the degree of correlation among the safety factors of different surfaces. However, at the Congress Street Open Cut (analyzed in detail in Chapter 6), the correlation among the safety factors of different surfaces are found to be very high^{*} due to the common variables and parameters. In this study, consistent with the conventional method in which the critical surface with the smallest safety factor is examined, the reliability of the most critical potential failure surface at a required section will be analyzed.

2.2.3 Evaluation of Design Safety Factor

The required actual mean safety factor for a specified risk can be obtained by solving Eq. 2.19, yielding

$$\mu_F = \exp \left[\Phi^{-1}(1 - p_f) \sqrt{\Omega_{M_R}^2 + \Omega_{M_0}^2} + \frac{1}{2} (\Omega_{M_R}^2 - \Omega_{M_0}^2) \right] \quad (2.20)$$

where $\Phi^{-1}(1 - p_f)$ denotes the inverse of $\Phi(\cdot)$ and is the value of the standard normal variate corresponding to a cumulative probability of $(1 - p_f)$. Eq. 2.20 could also be written in terms of the computed mean safety factor as

* For the 13 potential failure surfaces considered at the Congress Street Open Cut the coefficients of correlation between the safety factors of different surfaces are found to be very high due to the common corrective factors. Even in the case where the laboratory-measured undrained strength of different potential failure surfaces are assumed to be uncorrelated, the coefficients of correlation are all greater than 0.96.

$$\bar{F} = \frac{\bar{M}_R}{\bar{M}_0} = \frac{1}{\bar{N}_{M_R}} \exp \left[\Phi^{-1}(1 - p_f) \sqrt{\Omega_{M_R}^2 + \Omega_{M_0}^2} + \frac{1}{2}(\Omega_{M_R}^2 - \Omega_{M_0}^2) \right] \quad (2.20a)$$

Generally, the computed mean safety factor is a biased estimate of the actual mean safety factor; thus, \bar{N}_{M_R} usually will not be unity.

2.3 Estimation and Updating of Uncertainties

2.3.1 Estimation of Uncertainties

To design a slope or to evaluate the safety of a given slope using the proposed probabilistic approach, a necessary first step is to assess the uncertainties of the variables involved, as well as their mean values. It should be emphasized that not all available data (from different sites) should be arbitrarily lumped together in the statistical analysis. Judgment has to be exercised to distinguish which of the observed data are directly applicable to the site under consideration. There may exist other observed data which would require further analysis; these may be treated as indirect observations in the statistical analysis. Procedures for assessing the mean and variance based on various types of information have been suggested in Tang and Ang.¹⁰⁶

Procedures for estimating the inherent variability of soil parameters are illustrated in the next chapter. These include conventional methods of statistical estimation.

It is necessary also to determine the prediction biases and errors, in terms of the means and variances of the corrective factors N_j 's and N_{X_i} . If no data are collected from the site to estimate the prediction errors, then the mean and variance of the corrective factors have to be estimated purely on the basis of previous experience and judgment.

In this study, using data reported in the literature, the range for each of the N_j 's were estimated for various soil types. Then, depending on the engineer's opinion as to whether the expected value of N_j lies closer to the lower limit, n_l , or to the upper limit, n_u , or to the middle of the range, an appropriate triangular distribution may be prescribed. On the other hand, if any value of N_j is equally likely over the selected range, a uniform distribution may be more appropriate. Based on these assumed distributions for N_j 's, their respective means and c.o.v.'s can be computed from the formulae tabulated in Table 2.1.

2.3.2 Combining Information from Different Sources

When dealing with a specific site, it is possible that additional information from different sources may be applicable to the particular site. This information could be an expert's opinion, or reported values from other sites with similar soil properties, or test data from the site under consideration, or any combination of these. In this case the prior estimates (as computed from the estimated ranges suggested earlier) should be updated in the light of the additional information.

In this section a procedure for combining two different sources of information for assessing the mean correction and error is presented.

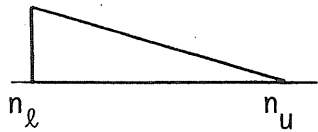
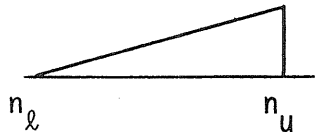
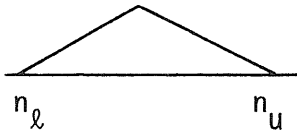
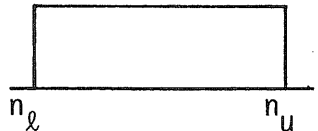
Based on Eqs. 2.6 and 2.13, the true mean of X_i can be expressed as

$$\mu_i \approx N_{X_i} \bar{X}_i = (N_1 \cdot N_2 \cdot \dots \cdot N_{n_0}) \bar{X}_i \quad (2.21)$$

Suppose two independent sources of information are available on one of the

Table 2.1

Mean and Coefficient of Variation of N_j Corresponding to Different Distributions Assumed Over Its Range

Distribution	Symbol	\bar{N}_j	Δ_j
	Triangular Type 1 (TT1)	$0.333(2n_l + n_u)$	$0.707 \frac{n_u - n_l}{2n_l + n_u}$
	Triangular Type 2 (TT2)	$0.333(n_l + 2n_u)$	$0.707 \frac{n_u - n_l}{n_l + 2n_u}$
	Triangular Type 3 (TT3)	$0.500(n_l + n_u)$	$0.408 \frac{n_u - n_l}{n_u + n_l}$
	Uniform (Rectangular) (Un.)	$0.500(n_l + n_u)$	$0.578 \frac{n_u - n_l}{n_u + n_l}$

n_l : lower bound of N_j

n_u : upper bound of N_j

corrective factors, for instance, on N_1 . Equation 2.21 can now be written as

$$\mu_i = N_1 \chi_i \quad (2.22)$$

where

$$\chi_i = (N_2 \cdot N_3 \cdot \dots \cdot N_{n_0}) \bar{X}_i \quad (2.23)$$

and χ_i is a constant for given estimates of N_j and the model mean \bar{X}_i . The estimate of N_1 is conveniently represented by its mean value \bar{N}_1 (Tang and Ang¹⁰⁶); hence, for the first source of information,

$$\bar{N}_1' = \frac{\mu_i'}{\chi_i} \quad (2.24)$$

and

$$\text{VAR}(N_1') = \frac{\text{VAR}(\mu_i')}{\chi_i^2} \quad (2.25)$$

where $\text{VAR}(\mu_i')$ is the variance associated with the estimate μ_i' .

Let \bar{N}_1' and \bar{N}_1'' be two independent estimates of N_1 with the associated variances given by $\text{VAR}(N_1')$ and $\text{VAR}(N_1'')$ respectively, and \bar{N}_1''' be the updated corrective factor based on the combined information.

From Eqs. 2.24 and 2.25, it can be observed that the corresponding estimates μ_i' and μ_i'' and their variances $\text{VAR}(\mu_i')$ and $\text{VAR}(\mu_i'')$ exist. Now, assume the combined or updated estimate μ_i''' to be a linear function of the two independent estimates, i.e.,

$$\mu_i''' = a \mu_i' + b \mu_i'' \quad (2.26)$$

If μ_i' , μ_i'' and μ_i''' are restricted to be unbiased estimates of the true

mean, μ_j^* , then

$$E(\mu_j^i) = E(\mu_j^{ii}) = E(\mu_j^{iii}) = \mu_j$$

Taking the expectation of both sides of Eq. 2.26 and using the unbiasedness restriction one gets

$$a + b = 1 \quad (2.27)$$

Imposing minimum variance criterion to obtain the best combined estimate of μ_j requires the minimization of

$$\text{VAR}(\mu_j^{iii}) = a^2 \text{VAR}(\mu_j^i) + b^2 \text{VAR}(\mu_j^{ii}) \quad (2.28)$$

subject to the condition given by Eq. 2.27. The result gives

$$\frac{\text{VAR}(\mu_j^{ii})}{\text{VAR}(\mu_j^i) + \text{VAR}(\mu_j^{ii})}$$

and

$$\frac{\text{VAR}(\mu_j^i)}{\text{VAR}(\mu_j^i) + \text{VAR}(\mu_j^{ii})}$$

as the values of a and b , respectively. Substituting these into Eq. 2.26 yields

$$\mu_j^{iii} = \frac{\text{VAR}(\mu_j^{ii})}{\text{VAR}(\mu_j^i) + \text{VAR}(\mu_j^{ii})} \mu_j^i + \frac{\text{VAR}(\mu_j^i)}{\text{VAR}(\mu_j^i) + \text{VAR}(\mu_j^{ii})} \mu_j^{ii} \quad (2.29)$$

Thus, using Eqs. 2.24 and 2.25, Eq. 2.29 becomes

* An example of unbiased estimate is to use the sample mean of the observed data as the estimator.

$$\bar{N}_1^{''''} = \frac{\text{VAR}(N_1^{''})}{\text{VAR}(N_1) + \text{VAR}(N_1^{''})} \bar{N}_1' + \frac{\text{VAR}(N_1')}{\text{VAR}(N_1) + \text{VAR}(N_1^{''})} \bar{N}_1^{''} \quad (2.30)$$

Similarly Eq. 2.28 can be rewritten as

$$\text{VAR}(N_1^{''''}) = \frac{\text{VAR}(N_1') \text{VAR}(N_1^{''})}{\text{VAR}(N_1) + \text{VAR}(N_1^{''})} \quad (2.31)$$

and using

$$\Delta_1^{,2} = \frac{\text{VAR}(N_1')}{\bar{N}_1'^2}$$

in Eqs. 2.30 and 2.31 yields

$$\bar{N}_1^{''''} = \bar{N}_1' \bar{N}_1^{''} \frac{\Delta_1'^2 \bar{N}_1' + \Delta_1^{''2} \bar{N}_1^{''}}{\Delta_1'^2 \bar{N}_1'^2 + \Delta_1^{''2} \bar{N}_1^{''2}} \quad (2.32)$$

$$\text{VAR}(N_1^{''''}) = \frac{\bar{N}_1'^2 \bar{N}_1^{''2} \Delta_1'^2 \Delta_1^{''2}}{\Delta_1'^2 \bar{N}_1'^2 + \Delta_1^{''2} \bar{N}_1^{''2}} \quad (2.33)$$

or

$$\Delta_1^{''''} = \Delta_1' \Delta_1^{''} \frac{\sqrt{\Delta_1'^2 \bar{N}_1'^2 + \Delta_1^{''2} \bar{N}_1^{''2}}}{\Delta_1'^2 \bar{N}_1'^2 + \Delta_1^{''2} \bar{N}_1^{''2}} \quad (2.34)$$

If new information becomes available, the original estimates for N_j can be revised by repeating the above procedure to update each corrective factor separately. The resulting posterior estimate of μ_j will be

$$\mu_i'''' = \frac{n_0}{\Pi_{j=1}} \bar{N}_j'''' \bar{X}_i \quad (2.35)$$

where \bar{N}_j'''' is the final mean value of the j th corrective factor. Thus, through this procedure, an engineer can continually improve his estimates of μ_i in a systematic manner.

Example

As an illustration, the effect of mechanical disturbance on the undrained strength during tube sampling is analyzed for the Congress Street Open Cut in Chicago. As a first estimate of the corrective factor that accounts for the effect of mechanical disturbance, the values given in Table 4.5 may be used, giving \bar{N}_2^I and Δ_2^I as 1.30 and 0.13, respectively. Peck⁷⁹ reported the results of a series of tests performed in connection with the Chicago Subway soil testing program to determine the loss in strength due to mechanical disturbance. In these tests the undrained strength of the specimens obtained from large block samples by hand trimming are compared with those obtained from the 2 in. Shelby tube samples. Assuming that these data are directly applicable to the site under consideration, one gets $\bar{N}_2^{II} = 1.39$ and $\Delta_2^{II} = 0.025$ (see Appendix A).

Combining these two pieces of information using Eqs. 2.32 and 2.34, the updated mean correction and error due to mechanical disturbance are found to be, respectively,

$$\bar{N}_2'''' = 1.30 \times 1.39 \times \frac{0.13^2 \times 1.30 + 0.025^2 \times 1.39}{0.13^2 \times 1.30^2 + 0.025^2 \times 1.39^2} = 1.38$$

and,

$$\Delta_2''' = 0.025 \times 0.13 \frac{\sqrt{0.13^2 \times 1.30^2 + 0.025^2 \times 1.39^2}}{0.13^2 \times 1.30 + 0.025^2 \times 1.39} = 0.024$$

Chapter 3

PROBABILISTIC MODELS FOR STABILITY ANALYSIS OF SLOPES

3.1 General Remarks

When an excavation is performed in saturated soils, the pore pressure at any point will be influenced by the stress changes resulting from the cutting. If the excavation is carried out rapidly so that no dissipation of the excess pore pressure takes place, the soil will remain in an undrained state during this period. This stage is referred to as the end-of-construction or short-term condition. After the construction, there is a period of pore pressure redistribution during which the pore pressures in the soil gradually adjust themselves, until they are everywhere in equilibrium with the steady seepage flow pattern. This final stage is known as the long-term condition.

All natural slopes are in the long-term condition. For slopes formed by cutting, the condition depends mainly on the permeability of the soil. In clays, especially if they are intact, the permeability is very low and the long-term condition would not be reached until several months or years after excavation. In temporary work, where the end-of-construction is the main concern, or in cases where it is necessary to evaluate the initial safety, the stability of a slope in cohesive soils is analyzed assuming the short-term condition to exist.

The stability of a slope at the end of an excavation does not assure its safety in the future. Actually the increase in pore pressure to compensate for the out-of-balance pore pressures caused by the excavation

and the softening of clay may decrease the shear strength with time, making the long-term stability more critical. Therefore, for permanent cuts and natural slopes which are exposed for long periods of time, the long-term stability should also be examined based on the results of the effective stress analysis.

3.2 Probabilistic Models for the Total Stress Analysis of Slopes

3.2.1 Models of Resisting and Overturning Moments

Under the short-term condition, the stability analysis is based on undrained strength and is often referred to as the total stress analysis. In this case, the shear strength mobilized along the potential failure surface is independent of the total normal stresses, and the analysis does not involve the pore pressures. The potential failure surface is assumed to be cylindrical--an arc of a circle in cross section. Referring to Fig. 3.1, the overturning moment M_o (due to the weight of soil above the assumed rupture surface), per foot of width, about the center of rotation is

$$M_o = \sum_{j=1}^m V_j \gamma_j d_j \quad (3.1)$$

where:

V_j = volume of the j th portion of the sliding soil mass (see Fig. 3.1)

γ_j = average unit weight of soil within the j th volume

d_j = moment arm of the centroid of the j th mass about the center of rotation.

The resisting moment, M_R , is provided by the shear strength of the

soil at the failure surface. For each foot of width of the slope,

$$M_R = r \sum_{i=1}^m \ell_i s_i \quad (3.2)$$

where:

r = radius of the circular failure surface

ℓ_i = length of the i th segment of the failure arc (see Fig. 3.1)

s_i = spatial average in situ undrained shear strength along the i th segment of the failure arc.

Commonly, in stability analysis, the average strength along each segment of the potential failure surface is considered; i.e., the spatial average of the in situ undrained strengths, s_i , $i = 1, 2, \dots, m$, along the segments of the potential failure surface would be a convenient choice of the random variables required for the stability model. This has also been indicated by Langejan⁶⁰ who argued that a general failure in a soil mass depends on the mean strength of the soil, on the grounds that an internal averaging of strength along the failure surface takes place. The spatial averages of soil parameters were also used by Cornell,²² and Wu and Kraft.¹¹⁹

A potential failure surface is assumed to consist of soil elements where the size of each element is taken to be the same as that of the standard triaxial specimen of 1.5 in. diameter by 3 in. high (Wu and Kraft¹¹⁹). Therefore, for every foot of width (perpendicular to the cross section) of the i th segment with arc length ℓ_i feet, there will be m_i soil elements, where m_i is computed from

$$m_i = \frac{\ell_i \times 12}{1.5} \frac{12}{1.5} = 64 \ell_i \quad (3.3)$$

The undrained strength of an element is assumed to be equal to the strength of a 1.5 in. diameter by 3 in. high triaxial specimen. Based on this m_i soil elements, the spatial average undrained strength along the i th strip is

$$\hat{s}_i = \frac{1}{m_i} \sum_{j=1}^{m_i} \hat{S}_j \quad (3.4)$$

in which the undrained strength (laboratory-measured) of each element, \hat{S}_j , is identically distributed with mean \bar{s}_i^* and variance $\sigma_{S_i}^2$, where \bar{s}_i^* is the mean undrained strength of the i th layer, and $\sigma_{S_i}^2$ is the variance of the specimen strength. The expected value of \hat{s}_i then is

$$\begin{aligned} E(\hat{s}_i) &= \bar{s}_i = E\left(\frac{1}{m_i} \sum_{j=1}^{m_i} \hat{S}_j\right) = \frac{1}{m_i} \sum_{j=1}^{m_i} E(\hat{S}_j) \\ &= \frac{1}{m_i} \sum_{j=1}^{m_i} \bar{s}_i^* = \frac{1}{m_i} m_i \bar{s}_i^* = \bar{s}_i^* \end{aligned} \quad (3.5)$$

i.e., the mean of the spatial average undrained strength along the i th segment is taken to be equal to the mean undrained strength of the soil in the i th layer.

Similarly,

$$\begin{aligned}
\text{VAR}(\hat{s}_i) &= \frac{1}{m_i} \sum_{j=1}^{m_i} \text{VAR}(\hat{S}_j) + \frac{2}{m_i} \sum_{k=1}^{m_i} \sum_{j=k+1}^{m_i} \text{COV}(\hat{S}_k, \hat{S}_j) \\
&= \frac{1}{m_i} (m_i \sigma_{S_i}^2) + \frac{2}{m_i} \sigma_{S_i}^2 \sum_{k=1}^{m_i} \sum_{j=k+1}^{m_i} \rho_{kj} \\
&= \frac{\sigma_{S_i}^2}{m_i} \left(1 + \frac{2}{m_i} \sum_{k=1}^{m_i} \sum_{j=k+1}^{m_i} \rho_{kj} \right) \\
&= \frac{\sigma_{S_i}^2}{m_i} \frac{1}{\left(1 + \frac{2}{m_i} \sum_{k=1}^{m_i} \sum_{j=k+1}^{m_i} \rho_{kj} \right)} = \frac{\sigma_{S_i}^2}{n_{e_i}} \tag{3.6}
\end{aligned}$$

where ρ_{kj} is the correlation coefficient between the k th and j th elements that are λ_{kj} inches apart; n_{e_i} denotes the equivalent number of (independent) soil elements, and as observed from Eq. 3.6 is equal to

$$n_{e_i} = \frac{m_i}{\left(1 + \frac{2}{m_i} \sum_{k=1}^{m_i} \sum_{j=k+1}^{m_i} \rho_{kj} \right)} \tag{3.7}$$

Based on the results of Appendix B, ρ_{kj} can be expressed as

$$\rho_{kj} = \rho(\lambda_{kj}) = e^{-v\lambda_{kj}} \tag{3.8}$$

where v is a spatial correlation parameter to be estimated from soils data.

Combining Eqs. 3.3, 3.7 and 3.8 one obtains

$$n_{e_i} = \frac{64\ell_i}{\left(1 + \frac{2}{64\ell_i} \sum_{k=1}^{m_i} \sum_{j=k+1}^{m_i} e^{-v_i \lambda_{kj}}\right)} \quad (3.9)$$

Figure 3.2 gives the values of n_e corresponding to eight different values of v for ℓ up to 200 ft. In this study v is taken as 0.21 based on the data given by Hooper and Butler⁴¹ (see Appendix B).

In practice, the average undrained strength of a layer is estimated by testing specimens only at a limited number of locations throughout that layer. Therefore, due to this insufficient sampling, there will be an error in the prediction of the mean of the spatial average undrained strength along the i th strip, obtained from Eq. 3.5 as

$$\text{VAR}(\bar{s}_i) = \text{VAR}(\bar{s}_i^*) = \frac{\sigma_{S_i}^2}{n_{S_i}} \quad (3.10)$$

or in terms of c.o.v.

$$\Delta_0 = \frac{\delta_{S_i}}{\sqrt{n_{S_i}}} \quad (3.10a)$$

where n_{S_i} specimens tested throughout the i th layer are assumed to be uncorrelated because of random sampling. To account for the error resulting from insufficient sampling, a corrective factor designated by N_0 is used, with a mean of 1.0 and a c.o.v. Δ_0 , where Δ_0 is given by Eq. 3.10a.

Thus, in its final form the in situ spatial average undrained strength, s_i , can be written as

$$s_i = \left(N_0 \prod_{j=1}^{n_0} N_j \right) \hat{s}_i = \left(\prod_{j=0}^{n_0} N_j \right) \hat{s}_i \quad (3.11)$$

where N_j 's, $j = 1, 2, \dots, n_0$, are the corrective factors accounting for the various factors which will be evaluated in Chapter 4. The total uncertainty in s_i is given by Eq. 2.10 where

$$\Delta_{s_i} = \sqrt{\frac{\delta_{S_i}^2}{n_{s_i}} + \sum_{j=1}^{n_0} \Delta_j^2} = \sqrt{\Delta_0^2 + \Delta_q^2} \quad (3.12)$$

and

$$\delta_{s_i} = \frac{\delta_{S_i}}{\sqrt{n_{e_i}}} \quad (3.13)$$

Δ_q is the total sampling and prediction error in s_i due to the discrepancies between the in situ and laboratory-measured strengths.

The mean and coefficient of variation of M_R can now be obtained using Eqs. 2.8 and 2.9, respectively. If the potential failure surface passes through m layers, then from Eq. 3.2

$$\mu_{M_R} = \bar{N}_f r \sum_{i=1}^m \ell_i \bar{N}_{s_i} \bar{s}_i = \bar{N}_f \bar{M}_R^* \quad (3.14)$$

where

$$\bar{M}_R^* = r \sum_{i=1}^m \ell_i \bar{N}_{s_i} \bar{s}_i \quad (3.15)$$

$\rho_{N_i N_j}$, the coefficient of correlation between N_{s_i} and N_{s_j} , is found in Appendix C as

$$\rho_{N_i N_j} \approx \frac{\Delta_{ij}^2 (s)}{\Delta_{s_i} \Delta_{s_j}} \quad (3.16)$$

Thus, the total uncertainty in M_R is

$$\begin{aligned} \Omega_{M_R}^2 &\approx \Omega_f^2 + \frac{r^2}{\bar{M}_R^{*2}} \left[\sum_{i=1}^m \lambda_i^2 \bar{N}_{s_i}^2 \bar{s}_i^2 \Omega_{s_i}^2 \right. \\ &\quad + 2 \sum_{i=1}^m \sum_{j=i+1}^m \lambda_i \lambda_j \bar{N}_{s_i} \bar{N}_{s_j} \bar{s}_i \bar{s}_j \rho_{\hat{s}_i \hat{s}_j} \delta_{s_i} \delta_{s_j} \\ &\quad \left. + 2 \sum_{i=1}^m \sum_{j=i+1}^m \lambda_i \lambda_j \bar{N}_{s_i} \bar{N}_{s_j} \bar{s}_i \bar{s}_j \Delta_{ij}^2 (s) \right] \quad (3.17) \end{aligned}$$

where \bar{M}_R^* is defined in Eq. 3.15

If the whole potential failure surface is located in one layer, (i.e., $m = 1$) then

$$\mu_{M_R} = \bar{N}_f r L \bar{N}_s \bar{s} \quad (3.18)$$

$$\Omega_{M_R}^2 \approx \Omega_f^2 + \Omega_s^2 \quad (3.19)$$

where L is the total length of the failure arc.

Similarly, from Eq. 3.1

$$\mu_{M_0} = \bar{N}_g \sum_{j=1}^m V_j d_j \bar{N}_{\gamma_j} \bar{\gamma}_j = \bar{N}_g \bar{M}_0^* \quad (3.20)$$

and

$$\begin{aligned}
\Omega_{M_0}^2 &\approx \Omega_g^2 + \frac{1}{\bar{M}_0^2} \left[\sum_{j=1}^m V_j^2 d_j^2 \bar{N}_{\gamma_j}^2 \bar{\gamma}_j^2 \Omega_{\gamma_j}^2 \right. \\
&+ 2 \sum_{i=1}^m \sum_{j=i+1}^m V_i V_j d_i d_j \bar{N}_{\gamma_i} \bar{N}_{\gamma_j} \bar{\gamma}_i \bar{\gamma}_j \rho_{\hat{\gamma}_i \hat{\gamma}_j} \delta_{\gamma_i} \delta_{\gamma_j} \\
&\left. + 2 \sum_{i=1}^m \sum_{j=i+1}^m V_i V_j d_i d_j \bar{N}_{\gamma_i} \bar{N}_{\gamma_j} \bar{\gamma}_i \bar{\gamma}_j \Delta_{ij}^2(\gamma) \right] \quad (3.21)
\end{aligned}$$

where $\Delta_{ij}^2(\gamma)$ is the squared sum of the coefficients of variation of the corrective factors that are the same for both γ_i and γ_j . Since the variability in $\hat{\gamma}$ (for example at Selset $\delta_{\gamma} = 0.007$) and the modeling and prediction errors in M_0 are negligible compared to the uncertainties involved in M_R , Ω_{M_0} may be assumed to be zero and

$$\mu_{M_0} \approx \bar{M}_0 = \sum_{j=1}^m V_j \bar{\gamma}_j d_j \quad (3.20a)$$

3.2.2 Consideration of Spatial Trend

In obtaining the spatial average strength of the soil along the portions of the potential failure surface the variation of soil strength within a stratum may indicate a marked spatial trend. If this trend is assumed to be a linear function of the depth (z) as well as of the two plan directions (x, y), then the undrained soil strength may be modeled as

$$\hat{S}(x,y,z) = a + b_1 z + b_2 x + b_3 y \quad (3.22)$$

Based on this linear model, the observed data (i.e., the test results from the n_s specimens obtained from the field) could be analyzed by using multiple linear regression analysis. This regression analysis will give the best estimates of a , the b_i 's ($i = 1, 2, 3$) and σ_S^2 which is the variance of \hat{S} given the x, y, z values. These estimates will give indications of whether the dependence of the soil strength on any one or more of these directions is significant. This may be done for any of the b_i 's, for example, b_3 , by examining whether it is significantly different than zero using methods of hypothesis testing (for an application see Cornell²²).

For a specified significance level, the choice of which is subjective, the t-statistic indicates whether a null hypothesis will be accepted or rejected. According to the outcome of this hypothesis testing, the engineer may decide to keep or eliminate b_3 from his model. For more information on this topic the reader is referred to Mood and Graybill.⁷²

Generally, the soil strength would depend mainly on the depth, z , and the strength model for a specific soil stratum may be simplified to

$$\hat{S}(z) = a + b_1 z \quad (3.23)$$

If the portion of the potential failure surface that is passing through this stratum is divided into m smaller segments, then the spatial average undrained strength for the i th segment will be given as

$$\hat{s}_i = E(\hat{S}_i | z_i) = a + b_1 z_i \quad (3.24)$$

where z_i is the depth to the centroid of the i th segment. Linear regression analysis gives the best estimates of the parameters, namely \hat{a} , \hat{b}_1 . The variance of the undrained strength σ_S^2 which is assumed to be constant can also be

estimated from the regression analysis. Based on the results of this regression analysis, the best estimate of \hat{s}_i will be as given in Eq. 3.24. Expressions for evaluating the mean, variance and covariance of \hat{s}_i from the results of regression analysis are derived in Appendix D.

The spatial correlation between the average undrained strengths of two segments (for instance, i th and j th) within the same soil stratum may also be obtained by using the results of the regression analysis. From Eqs. D.5 and D.6 (see Appendix D)

$$\begin{aligned} \rho_{\hat{s}_i \hat{s}_j} &= \frac{\text{COV}(\hat{s}_i, \hat{s}_j)}{\sqrt{\text{VAR}(\hat{s}_i) \text{VAR}(\hat{s}_j)}} \\ &= \frac{1 + \frac{(z_i - \bar{z})(z_j - \bar{z})}{\text{VAR}(z)}}{\sqrt{\left(1 + \frac{(z_i - \bar{z})^2}{\text{VAR}(z)}\right) \left(1 + \frac{(z_j - \bar{z})^2}{\text{VAR}(z)}\right)}} \end{aligned} \quad (3.25)$$

where

\bar{z} = mean depth of soil samples

$\text{VAR}(z)$ = variance of depth of soil samples

For example, according to Eq. 3.25, $\rho_{\hat{s}_i \hat{s}_j}$ will be 1.0 for two segments having the same depth (i.e., $z_i = z_j$).

3.3 Probabilistic Models for the Effective Stress Analysis of Slopes

3.3.1 Models of Resisting and Overturning Moments

In terms of the effective normal stresses, the peak shear strength S_f of a saturated clay can be represented by the Coulomb-Terzaghi equation

$$\begin{aligned}
 S_f &= C + (p - u) \tan \phi \\
 &= C + p' \tan \phi
 \end{aligned}
 \tag{3.26}$$

where:

- C = peak effective cohesion intercept
- ϕ = peak effective angle of shearing resistance
- p = normal stress
- u = pore pressure
- p' = (p - u) effective normal stress

A stability analysis in terms of effective stresses requires knowledge of the total normal stress and the pore pressure at all points of the failure surface, as well as the in situ values of the effective cohesion intercept and angle of shearing resistance. Due to the variation of p' along the slip surface and to the possibility of the failure surface passing through several materials with different values of shear strength parameters, the method of slices is convenient for effective stress analysis of slopes.

In routine stability investigations it is a common practice to analyze the safety of a slope based on the peak strength. For the i th segment, the spatial average in situ peak strength is

$$s_{f_i} = c_i + \bar{p}_i' \tan \phi_i \tag{3.27}$$

where c_i and ϕ_i designate the true in situ spatial averages of the peak shear strength parameters; \bar{p}_i' represents the in situ value of the average effective normal stress along the base of the i th slice, expressed as

$$\bar{p}_i' = \bar{p}_i - \bar{u}_i \tag{3.28}$$

where \bar{u}_i is the average pore pressure for the i th slice computed from the best estimate of the pore pressure distribution along the actual or assumed failure surface.

Considering the soil mass above the circular failure arc as a free body (see Fig. 3.1) the overturning and resisting moments per foot of slope about the center of rotation are, respectively

$$M_O = \sum_{i=1}^m V_i \gamma_i d_i \quad (3.29)$$

and

$$\begin{aligned} M_R &= \sum_{i=1}^m r l_i s_{f_i} = \sum_{i=1}^m r l_i (c_i + \bar{p}_i' \tan \phi_i) \\ &= \sum_{i=1}^m r (c_i l_i + \bar{p}_i' l_i \tan \phi_i) \\ &= \sum_{i=1}^m r (c_i l_i + \bar{P}_i' \tan \phi_i) \end{aligned} \quad (3.30)$$

If the i th slice is sufficiently narrow, the curved boundary can be approximated by a straight line that makes an angle θ_i with the horizontal axis. The moment arm for the weight of the i th slice is then equal to $r \sin \theta_i$, and Eq. 3.29 becomes

$$M_O = r \sum_{i=1}^m V_i \gamma_i \sin \theta_i \quad (3.31)$$

In the case where the whole failure surface is located in one material, c_i and ϕ_i will have the same value (c and ϕ) along the base of all the slices; in this case M_R is

$$M_R = r (cL + \tan \phi \sum_{i=1}^m \bar{P}_i') \quad (3.32)$$

If the assumed failure mass is indeed the actual failure mass, Eqs. 3.30 and 3.31 are exact expressions of the resisting and overturning moments of the soil in the failure mass. However, M_R involves the unknown distribution of \bar{P}_i' along the failure surface. The approximate methods of slope stability analysis applied in practice do not necessarily use the values of \bar{P}_i' which satisfy statics and thus introduce modeling errors. Among the various approximate methods, the ordinary method of slices developed by Fellenius (also known as the Swedish Circle method) is widely used in practice because of its simplicity. More rigorous methods based on refined assumptions about the earth pressures acting on the sides of the slices have also been developed. For detailed descriptions of various methods of stability analysis of slopes, the reader is referred to Bishop,⁶ Morgenstern and Price,⁷³ Taylor,¹⁰⁷ Terzaghi and Peck,¹⁰⁸ Whitman and Moore,¹¹⁴ and Whitman and Bailey.¹¹⁵

3.3.2 Formulation Based on the Fellenius Method

In this study the equations used to compute M_O and M_R are based on the Fellenius method because of its popularity and simplicity. A shortcoming of this method is that it may involve large errors under certain extreme conditions. However, as indicated by Turnbull and Hvorslev,¹¹¹ "all currently available methods for stability analysis may yield questionable results for special or unusual conditions."

In the Fellenius method, a simplifying assumption is made so that the forces acting on the sides of any slice have zero resultant normal to the

failure arc for that slice. For the i th slice, considering the equilibrium of forces in the direction perpendicular to the failure arc, one gets (see Fig. 3.3)

$$\begin{aligned}\bar{W}_i \cos \theta_i &= \bar{P}_i' + \bar{u}_i l_i \\ \therefore \bar{P}_i' &= \bar{W}_i \cos \theta_i - \bar{u}_i l_i\end{aligned}\quad (3.33)$$

Using Eq. 3.33 in Eq. 3.30 gives

$$M_R = \sum_{i=1}^m r [c_i l_i + (\bar{W}_i \cos \theta_i - \bar{u}_i l_i) \tan \phi_i] \quad (3.34)$$

and for homogenous soils, from Eq. 3.32

$$M_R = r [cL + \tan \phi \sum_{i=1}^m (\bar{W}_i \cos \theta_i - \bar{u}_i l_i)] \quad (3.35)$$

Due to such factors as disturbance during sampling, specimen size, rate of shearing, anisotropy, and plain strain assumption, the spatial average peak effective stress parameters in the field (c , ϕ) will be different than those measured in the laboratory (\hat{c} , $\hat{\phi}$) (Peck,⁸² and Skempton and Hutchinson⁹⁹). In addition to these factors, Bishop,¹² Bjerrum,¹⁸ Skempton,⁹⁶ and other investigators have demonstrated that the average shear strength mobilized in many long-term failures of slopes could be smaller than the average peak shear strength due to progressive failure mechanism. Therefore, it is necessary first to analyze the effects of various factors that cause discrepancies between the laboratory and in situ values of the peak shear strength parameters, and secondly to estimate the effect of progressive failure

in reducing the average peak strength, based on data from actual failure cases. The in situ spatial averages c and ϕ along any segment of the potential failure surface may be written as

$$c_i = [N_0(c_i) \prod_{j=1}^{n_0} N_j(c_i)] \hat{c}_i = [\prod_{j=0}^{n_0} N_j(c_i)] \hat{c}_i \quad (3.36)$$

$$\phi_i = [N_0(\phi_i) \prod_{j=1}^{n_0} N_j(\phi_i)] \hat{\phi}_i = [\prod_{j=0}^{n_0} N_j(\phi_i)] \hat{\phi}_i \quad (3.37)$$

where $N_0(c_i)$ and $N_0(\phi_i)$ are the corrective factors to account for the prediction errors in c_i and ϕ_i , respectively, due to insufficient sampling. $N_0(c_i)$ and $N_0(\phi_i)$ will both have a mean equal to unity; the corresponding uncertainties, $\Delta_0(c)$ and $\Delta_0(\phi)$, will be equal to δ_{C_i} and δ_{ϕ_i} divided by the square root of the number of specimens tested over the i th soil mass.

The methods and related equations given in Section 3.2 about the spatial variation and correlation of s_i apply as well for c_i and ϕ_i . In this section these topics are not discussed again, but the corresponding equations are directly used by replacing s_i with c_i or ϕ_i .

A first-order approximation of the mean of c_i is

$$\mu_{C_i} = [\prod_{j=0}^{n_0} \bar{N}_j(c_i)] \bar{c}_i = \bar{N}_{C_i} \bar{c}_i \quad (3.38)$$

where

$$\bar{N}(c_i) = \prod_{j=1}^{n_0} \bar{N}_j(c_i) \quad (3.39)$$

and its coefficient of variation is expressed as

$$\Omega_{c_i} = \sqrt{\Delta_{c_i}^2 + \delta_{c_i}^2} \quad (3.40)$$

where

$$\Delta_{c_i} = \sqrt{\frac{\delta_{c_i}^2}{n_{s_i}} + \sum_{j=1}^{n_0} \Delta_j^2(c_i)} \quad (3.41)$$

and

$$\delta_{c_i} = \frac{\delta_{c_i}}{\sqrt{n_{e_i}}} \quad (3.42)$$

Similarly for ϕ_i

$$\mu_{\phi_i} = \bar{N}_{\phi_i} \bar{\phi}_i \quad (3.43)$$

$$\Omega_{\phi_i} = \sqrt{\Delta_{\phi_i}^2 + \delta_{\phi_i}^2} \quad (3.44)$$

where

$$\bar{N}_{\phi_i} = \prod_{j=1}^{n_0} \bar{N}_j(\phi_i) \quad (3.45)$$

$$\Delta_{\phi_i} = \sqrt{\frac{\delta_{\phi_i}^2}{n_{s_i}} + \sum_{j=1}^{n_0} \Delta_j^2(\phi_i)} \quad (3.46)$$

and

$$\delta_{\phi_i} = \frac{\delta_{\phi_i}}{\sqrt{n_{e_i}}} \quad (3.47)$$

Note that the spatial correlation for the peak effective stress parameters is assumed to be described by Eq. 3.8; therefore, the values of n_{e_i} for c_i and ϕ_i corresponding to different ℓ_i 's can be obtained from Fig. 3.2 provided the spatial correlation parameters v_c and v_ϕ are known. There appears to be no data available for estimating the values of v_c and v_ϕ . However, for large ℓ_i 's it is reasonable to assume the value of n_{e_i} to be large for both c_i and ϕ_i compared to n_{s_i} . Therefore, δ_{c_i} and δ_{ϕ_i} will be insignificant compared to Δ_{c_i} and Δ_{ϕ_i} ; accordingly, one can write

$$\Omega_{c_i} \approx \Delta_{c_i} \quad (3.40a)$$

$$\Omega_{\phi_i} \approx \Delta_{\phi_i} \quad (3.44a)$$

The corrective factor N_{S_f} , with a mean \bar{N}_{S_f} and a coefficient of variation Δ_{S_f} (see Section 5.2.6 for more details) is used to account for the discrepancy between the spatial average peak strength, s_f , and the average strength actually mobilized in the field, s_m . Similarly, the uncertainty associated with the inaccurate estimation of pore pressures along the failure surface is taken into consideration by N_u (mean \bar{N}_u and c.o.v. Δ_u). On the other hand, the error introduced into the reliability analysis by the approximate Fellenius method is corrected by N_f , which has a mean \bar{N}_f and a coefficient of variation Ω_f . The insertion of these corrective factors brings the expression of M_R into the following form:

$$M_R = N_f N_u N_{S_f} r \sum_{i=1}^m [N_{c_i} \hat{c}_i \ell_i + (\bar{w}_i \cos \theta_i - \bar{u}_i \ell_i) \tan (N_{\phi_i} \hat{\phi}_i)] \quad (3.48)$$

For slopes located in one material Eq. 3.48 becomes

$$M_R = N_f N_u N_{s_f} r [N_c \hat{c} L + \tan(N_\phi \hat{\phi}) \sum_{i=1}^m (\bar{W}_i \cos \theta_i - \bar{u}_i \lambda_i)] \quad (3.49)$$

In Eqs. 3.48 and 3.49, \bar{P}_i' ($= \bar{W}_i \cos \theta_i - \bar{u}_i \lambda_i$) will be treated as a deterministic quantity since the uncertainty associated with \bar{W}_i is negligible, and the error and uncertainty due to \bar{u}_i are accounted for by the corrective factor N_u .

A first-order approximation of μ_{M_R} and Ω_{M_R} can be obtained according to the format given by Eqs. 2.8 and 2.9, with M_R expressed by either Eq. 3.49 or Eq. 3.48, depending on whether the failure surface passes through one or more layers of soil. In the example given in Chapter 6 and in the general slope model considered in Chapter 5 the failure surface passes through one material. Therefore, based on Eq. 3.49

$$\mu_{M_R} \approx \bar{N}_f \bar{N}_u \bar{N}_{s_f} r [L \bar{N}_c \bar{c} + \tan(\bar{N}_\phi \bar{\phi}) \sum_{i=1}^m \bar{P}_i'] \quad (3.50)$$

and

$$\begin{aligned}
\Omega_{M_R}^2 &\approx \Omega_f^2 + \Delta_u^2 + \Delta_{S_f}^2 + \frac{r^2}{\bar{M}_R^{*2}} \left([L \bar{N}_c \bar{c}]^2 \Omega_c^2 \right. \\
&+ \left[\sum_{i=1}^m \bar{p}_i' \right]^2 [\bar{N}_\phi \sec^2 (\bar{N}_\phi \bar{\phi}) \bar{\phi}]^2 \Omega_\phi^2 \\
&+ 2 [L \bar{N}_c \bar{c}] \left[\sum_{i=1}^m \bar{p}_i' \right] [\bar{N}_\phi \sec^2 (\bar{N}_\phi \bar{\phi}) \bar{\phi}] \rho_{\hat{c}\hat{\phi}} \delta_c \delta_\phi \\
&+ \left. 2 [L \bar{N}_c \bar{c}] \left[\sum_{i=1}^m \bar{p}_i' \right] [\bar{N}_\phi \sec^2 (\bar{N}_\phi \bar{\phi}) \bar{\phi}] \rho_{N_c N_\phi} \Delta_c \Delta_\phi \right)
\end{aligned} \tag{3.51}$$

where

$$\bar{M}_R^* = r L \bar{N}_c \bar{c} + r \tan (\bar{N}_\phi \bar{\phi}) \sum_{i=1}^m \bar{p}_i' \tag{3.52}$$

$\rho_{N_c N_\phi}$, is the correlation between N_c and N_ϕ , and will be given by Eq. C.6 (see Appendix C)

$$\rho_{N_c N_\phi} \approx \frac{\sum_{k=0}^{n_0} \rho_k \Delta_k(c) \Delta_k(\phi)}{\Delta_c \Delta_\phi} \tag{3.53}$$

where ρ_k is the coefficient of correlation between $N_k(c)$ and $N_k(\phi)$. Substitution of Eq. 3.53 into Eq. 3.51 gives

$$\begin{aligned} \Omega_{M_R}^2 = & \Omega_f^2 + \Delta_u^2 + \Delta_{s_f}^2 + \frac{1}{M_R^{*2}} \left(K_c^2 \Omega_c^2 + K_\phi^2 \Omega_\phi^2 \right. \\ & \left. + 2 K_c K_\phi \left[\rho_{\hat{c}\hat{\phi}} \delta_c \delta_\phi + \sum_{k=0}^{n_0} \rho_k \Delta_k(c) \Delta_k(\phi) \right] \right) \end{aligned} \quad (3.54)$$

in which

$$K_c = r L \bar{N}_c \bar{c} \quad (3.55a)$$

and

$$K_\phi = r \left[\sum_{i=1}^m \bar{p}_i' \right] \left[\bar{N}_\phi \sec^2 (\bar{N}_\phi \bar{\phi}) \bar{\phi} \right] \quad (3.55b)$$

In order to compute the uncertainty resulting from the correlation among the random variables, one should estimate the values of $\rho_{\hat{c}\hat{\phi}}$ and ρ_k 's, $k = 1, 2, \dots, n_0$. Some reported values indicate that \hat{c} and $\hat{\phi}$ are probably negatively correlated, with low values of \hat{c} associated with high values of $\hat{\phi}$, and vice versa. For Selset $\rho_{\hat{c}\hat{\phi}}$ is computed to be -0.40 using Eq. 2.11. Lumb⁶⁶ gave an average correlation coefficient of -0.244 based on data from strength tests conducted for residual decomposed granite from Hong Kong, Penang (Malaysia), and Snowy Mountains (Australia), and on residual decomposed volcanic rocks from Hong Kong. Holtz and Krizek⁴⁰ reported -0.49 as the correlation coefficient for impervious borrow material at Oroville Dam. The assumption of statistically independent \hat{c} and $\hat{\phi}$ simplifies the computations, and it is also on the conservative side if the correlation is negative. Besides, as mentioned earlier, δ_c and δ_ϕ will be small due to the large value of n_e . Therefore, in Eq. 3.54 one could neglect the term associated with $\rho_{\hat{c}\hat{\phi}} \delta_c \delta_\phi$.

Generally, there is no data available to estimate the value of ρ_k 's. In this study, limited data was available for anisotropy, for which the correlation coefficient, ρ_5 , was determined to be -0.32. Due to the possibility that some of the ρ_k 's may be negative and some positive, the net contribution of the uncertainty resulting from the correlations is expected to be small. Hence, the last term in Eq. 3.54 may be eliminated, giving

$$\Omega_{M_R}^2 = \Omega_f^2 + \Delta_u^2 + \Delta_{S_f}^2 + \frac{1}{M_R^2} [K_C^2 \Omega_C^2 + K_\phi^2 \Omega_\phi^2] \quad (3.56)$$

Based on Eq. 3.31, the mean overturning moment is given as

$$\mu_{M_0} \approx \bar{M}_0 = r \sum_{i=1}^m V_i \bar{\gamma}_i \sin \theta_i \quad (3.57)$$

whereas $\Omega_{M_0} \approx 0$.

Chapter 4

EVALUATION OF SHORT-TERM STABILITY OF SLOPES

4.1 Inherent Variability and Uncertainty Due to Insufficient Sampling

Due to the heterogeneity of soil deposits, natural variations in the undrained strength exist within a soil strata which can be conveniently measured by the coefficient of variation δ_S . For instance, tests by Hooper and Butler⁴¹ on London clay taken at a number of different sites indicate that δ_S varies between 0.11 and 0.33. In Fig. 4.1a typical histogram for one of the sites is shown. Various other investigators have also determined δ_S within a particular soil zone. The reported results are given in Table 4.1. As described in Section 3.2.1, the variability in the spatial average undrained strength, δ_S , will be equal to $\frac{\delta_S}{\sqrt{n_e}}$. The equivalent number of independent soil elements can be obtained from Fig. 3.2 in terms of the spatial correlation parameter, v , and the arc length of the failure surface.

The uncertainty in the spatial average undrained shear strength resulting from insufficient sampling, Δ_o , is equal to $\frac{\delta_S}{\sqrt{n_s}}$, which is observed to decrease with the square root of the number of test specimens (Cornell,²² Kay and Krizek,⁴⁸ and Langejan⁶⁰).

4.2 Discrepancies Between Laboratory and In Situ Undrained Strengths4.2.1 Introductory Remarks

The soil strength measured in the laboratory by testing triaxial specimens could differ from the field (in situ) strength; the major factors contributing to these discrepancies are (Skempton and Hutchinson⁹⁹):

Table 4.1
 Values of δ_S from Various Sources

Reference	Soil Type and Site	δ_S
Hooper and Butler ⁴¹	London clay, Barbican site	0.11 - 0.33
Ireland ⁴³	Chicago clay, Congress Street Open Cut	0.18 - 0.34
Ladd et al. ⁵⁶	Soft Bangkok clay	0.23 - 0.41
Lumb ⁶⁴	Hong Kong marine clay	0.18
Morse ⁷⁵	Glacial tills, Illinois	0.15 - 0.31
Singh ⁹¹	General	0.20 - 0.40
Ward et al. ¹¹²	London clay, various sites	0.11 - 0.21

1. Disturbance during sampling,
2. Size of specimen,
3. Rate of shearing,
4. Sample orientation and anisotropy,
5. Plane strain failure,
6. Progressive failure.

In the following sections, each factor is discussed briefly using results reported in the literature. The expected values of $N_j(s)$'s and their c.o.v.'s computed by assuming various simple distributions over the estimated ranges, are tabulated for each case. These values can be updated if additional information becomes available as described in Section 2.3.2.

4.2.2 Disturbance During Sampling

Poor and inadequate methods of sampling are the most important source of error in the estimation of in situ soil strength. Most commonly, the soil samples are obtained by using thin-walled tube samplers. In practice, it has generally been assumed that sampling disturbance reduces the shearing strength of clays (Lambe and Whitman,⁵⁹ and Skempton and Hutchinson⁹⁹). Therefore, the undrained shear strength obtained by testing tube samples will be consistently lower than the in situ undrained shear strength. The disturbances that take place in a soil sample starting with its removal from the field until it is placed in a testing apparatus are due to the following:

1. The inevitable changes in the stress system because of the removal of the sample from the ground,
2. The mechanical disturbances resulting during sampling and preparation of the specimen.

The corrective factors necessary for these two types of disturbances will be designated by $N_1(s)$ and $N_2(s)$, respectively.

Disturbance Due to Changes in the Stress System

This type of disturbance will occur even in the case of perfect sampling.* Skempton and Sowa⁹⁵ indicated that for a saturated normally consolidated clay, in spite of the considerable changes in stress, the undrained shear strength of a perfect sample is practically the same as the corresponding strength in the ground provided no change in water content occurs. According

* The term "perfect sample" denotes a specimen where no disturbance has occurred other than that accompanied with the release of in situ stresses.

to their research, for soils having a low sensitivity ($S_t = 2$), the change in the undrained strength due to the release of stresses is on the order of 1 to 2 percent (i.e., $N_1(s) = 1.01-1.02$). Ladd and Lambe⁵⁴ reported that the undrained strength of a perfect sample is only slightly lower than the undisturbed strength for medium sensitive ($S_t = 2-4$) clays. Noorany and Seed⁷⁸ analyzed the sampling disturbance resulting from the release of stresses for the San Francisco Bay mud ($S_t \approx 8$). They indicated that the undrained strength of perfectly undisturbed samples is about 6 to 8 percent less than the in situ strength for this sensitive clay (meaning $N_1(s) = 1.06-1.08$).

The values of S_t for most clays range between 2 and 4, and for sensitive clays they range from 4 to 8. Thus, except for extra sensitive and quick clays, the range of $N_1(s)$ could be taken to be between 1.0 and 1.10. Table 4.2 gives the values of $\bar{N}_1(s)$ and $\Delta_1(s)$ for clays with different sensitivities.

Table 4.2
Mean Correction and Sampling Error Due to
Changes in Stress State

Sensitivity of Clay	Estimated Range of $N_1(s)$	Assumed Distribution	$\bar{N}_1(s)$	$\Delta_1(s)$
Low Sensitivity ($S_t = 1-2$)	1.0-1.10	TT1	1.03	0.02
Medium Sensitivity ($S_t = 2-4$)	1.0-1.10	TT3	1.05	0.02
Sensitive ($S_t = 4-8$)	1.0-1.10	TT2	1.07	0.02
General Case ($S_t = 1-8$)	1.0-1.10	Un.	1.05	0.03

Mechanical Disturbance

The mechanical disturbance results from the driving of the sampler into the soil, the removal of soil from the sampling tube, the trimming of the sample to the size required for a strength test and the mounting of the specimen in the triaxial apparatus. Even the best sampling techniques cannot avoid some mechanical disturbance. It has been observed by various authors (Skempton and Sowa,⁹⁵ and Ward et al.¹¹²) that the least disturbed samples are obtained by trimming specimens by hand from large blocks of clay which have been carefully excavated. The block specimens would be subjected to some unknown degree of disturbance and weakening, but this disturbance is generally considered small. The comparison of the undrained strength of the block specimens with those obtained from tube or borehole samples will lead to an estimate of the degree of discrepancy between in situ and laboratory values of the undrained strength due to mechanical disturbance. The term "borehole samples" is used to define those samples that are obtained in the following manner: A steel sampling tube about 4 in. in diameter is driven into the bottom of a borehole, and then in the laboratory, specimens are obtained from the 4 in. core by means of 1-1/2 in. diameter tubes. Therefore, borehole samples are subjected twice to the action of the driving of sampling tubes before they are tested, whereas in tube sampling this happens only once.

An extensive series of tests were performed by Peck⁸⁰ in connection with the Chicago Subway soil testing program to determine the loss in strength due to mechanical disturbance. Figure 4.2 shows the plotted results for the entire investigation. In this figure the line marked "Shelby Tube Samples"

describes the correlation between the undisturbed strength (the undrained strength of the specimens prepared from large block specimens by hand trimming) and the strength measured from the 2 in. Shelby tube specimens. This line indicates that the undrained strength obtained from the 2 in. Shelby tube specimens should be increased by a factor of 1.35 to get the undisturbed strength (i.e., $N_2(s) = 1.35$).*

The shear strength of the borehole samples and the block specimens are compared by Ward et al.¹¹³ for London clay at Ashford Common Shaft (see Table 4.3). Excluding level B, where the clay is very highly fissured, the ratio of the block to borehole strength varies between 1.16 to 1.48 (i.e., $N_2(s) = 1.16$ to 1.48).

Table 4.3

Comparison Between Shear Strengths of Borehole Samples
and Block Specimens for London Clay at Ashford
Common Shaft (from Ward et al.¹¹³)

Level	Vertical Block Specimens			Borehole Samples			Strength Ratio Block/Borehole
	Depth ft	Mean Water Content %	Shear Strength lb/sq in.	Mean Water Content %	Shear Strength lb/sq in.	Depth Zone ft	
A	30	22.4	36.6± 5.7	22.5	25.4± 5.8	20- 40	1.44
B	50	25.8	32.9± 8.7	23.6	35.0±13.1	40- 60	0.94
C	66	24.8	44.1±10.0	24.7	31.8±13.4	55- 75	1.39
D	91	22.8	54.4±11.6	23.6	46.9±17.7	80-100	1.16
E	114	24.2	59.9±20.2	23.9	47.3±17.5	111-120	1.26
F	138	23.6	81.0±19.5	23.7	54.6±19.4	130-150	1.48

* The analysis of the same data based on a least square linear fit through the origin (i.e., dependent variable intercept restricted to be zero) gives $N_2(s) = 1.40$.

Data from various sites about $N_2(s)$ are summarized in Table 4.4. In view of these data, $N_2(s)$ is estimated to range from 1.0 to 1.60 for tube specimens, and from 1.15 and 2.25 for borehole specimens where the mechanical disturbance is higher. The values of $\bar{N}_2(s)$ and $\Delta_2(s)$ that would be obtained assuming different distributions over the estimated ranges, are summarized in Table 4.5 for tube and borehole samplings.

4.2.3 Size of Specimen

It is desirable that the test specimens be large enough to contain a representative selection of the composition and all the discontinuities in the soil. However, the most common specimen used in the laboratory strength tests, which is 1-1/2 in. in diameter and 3 in. high, is generally not large enough to reflect the influence of joints and fissures on the strength of clays. In addition, when a small triaxial specimen is found to contain an obvious fissure, the specimen is usually discarded (Duncan and Dunlop,³⁰ and Skempton and Hutchinson⁹⁹). In other words, the 1-1/2 in. by 3 in. specimens usually consist of intact clay, whereas the in situ strength is controlled to some extent by the fissures and joints which exist in the soil mass with varying degrees. Therefore, the undrained strength obtained from the 1-1/2 in. by 3 in. specimens are consistently higher than the actual strength of the clay in the soil mass.

In the spatial average undrained strength estimated from the 1-1/2 in. by 3 in. specimens, the error resulting from the size of the test specimens is accounted for by the corrective factor $N_3(s)$. To estimate the influence of the specimen size on the soil strength, the results obtained from

Table 4.4

Data for $N_2(s)$ from Different Sites

Reference	Soil Type, Site and Comments	Block Specimens Compared With	$N_2(s)$
Ladd and Lambe ⁵⁴	Kawasaki clay, Japan	Tube Specimens	1.23
	Lagunnilas clay, Venezuela	Tube Specimens	1.35
	For normally consolidated clays of moderate sensitivity, depending on type of clay	--	1.25-2.0
Peck ⁸⁰	Chicago clay, Chicago Subway	Tube specimens	1.35
Simons ⁹⁰	Blue London clay	Borehole specimens	1.43
Skempton and La Rochelle ⁹⁷	London clay, Bradwell	Tube specimens	1.05
Ward et al. ¹¹²	London clay, Site O	Tube specimens	1.55
	London clay, Site P	Tube specimens	1.47
	London clay, Site O	Borehole specimens	1.67
	London clay, Site B	Borehole specimens	1.82
	London clay, Site K	Borehole specimens	2.22
	London clay, Paddington, Victoria, South Bank	Borehole specimens	1.82
Ward et al. ¹¹³	London clay, Ashford Common Shaft	Borehole specimens	1.35 (1.16-1.48)

Table 4.5
 Mean Correction and Sampling Error Due
 to Mechanical Disturbance

Type of Sampling	Estimated Range of $N_2(s)$	Assumed Distribution	$\bar{N}_2(s)$	$\Delta_2(s)$
Tube sampling	1.0-1.60	Un.	1.30	0.13
	1.0-1.60	TT1	1.20	0.12
	1.0-1.60	TT3	1.30	0.09
	1.0-1.60	TT2	1.40	0.10
Borehole sampling	1.15-2.25	Un.	1.70	0.19
	1.15-2.25	TT1	1.52	0.17
	1.15-2.25	TT3	1.70	0.13
	1.15-2.25	TT2	1.88	0.14

testing 1-1/2 in. by 3 in. specimens are compared with those measured from the larger specimens which are more representative of the fissures in the clay mass. For instance, from the plotted results shown in Fig. 4.3, the average strength of the 4 in. dia. by 8 in. specimens are observed to be about 13 percent less than that of the 1-1/2 in. dia. by 3 in. specimens for Brown London clay at Kensal Green; thus, for this case $N_3(s)$ could be taken as 0.87.

An extensive series of tests was performed by Simons⁹⁰ to study the effect of specimen size on the undrained strength of stiff-fissured Blue London clay. These tests included specimens of varying sizes, and they were all tested under undrained conditions. For purposes of comparison, the

Metz Reference Room
 Civil Engineering Department
 3106 C. E. Building
 University of Illinois
 Urbana, Illinois 61801

results were corrected to a common moisture content. The following data were reported by Simons.⁹⁰ In this case, the large specimens give approximately

Table 4.6
Size Effect on Undrained Strength of Blue
London Clay (from Simons⁹⁰)

Size of Specimen	Number of Tests	Strength Ratio
12" dia. x 24"	5	0.62
6" dia. x 12"	9	0.56
4" dia. x 8"	11	0.57
1-1/2" dia. x 3"	36	1.00

the same measured strength, which is about 60 percent of that for the 1-1/2 in. by 3 in. specimens; i.e., $N_3(s) = 0.60$. In Table 4.7, the values of $N_3(s)$ from different sites are summarized for stiff-fissured clays. The available data indicates a range approximately between 0.55 to 0.85 for $N_3(s)$ in the case of stiff-fissured clays.

For intact clays, as pointed out by Skempton and Hutchinson,⁹⁹ and Morgenstern,⁷⁴ the 1-1/2 in. by 3 in. specimens are usually adequate to estimate the undrained strength of clays in the soil mass as far as the effect of specimen size is concerned. So, for intact clays $N_3(s)$ is estimated to lie between 0.85 (the maximum value of $N_3(s)$ for stiff-fissured clays) and 1.0. Values of $\bar{N}_3(s)$ and $\Delta_3(s)$ computed for stiff-fissured and intact clays using different distributions are shown in Table 4.8.

Table 4.7

Data for $N_3(s)$ from Different Sites

Reference	Soil Type, Site and Comments	Specimen Size	$N_3(s)$
Bishop and Little ¹³	Brown London Clay, Maldon, Essex (size effect estimated)	--	0.66
Marsland ⁶⁹	London clay, Wraysbury	5" dia. x 10"	0.64
Marsland and Butler ⁷⁰	Barton clay, Fawley, Hampshire	3", 4", 5", dia. specimens	0.67-0.85
Simons ⁹⁰	Blue London clay	4" dia. x 8"	0.57
		6" dia. x 12"	0.56
		12" dia. x 24"	0.62
Skempton and La Rochelle ⁹⁷	London clay, Bradwell	4" dia. x 8"	0.70
	London clay, Kensal Green	4" dia. x 8"	0.87
Skempton and Hutchinson ⁹⁹	London clay, Kensal Green	4" dia. x 8"	0.82

Table 4.8
Mean Correction and Sampling Error
Due to Specimen Size

Type of Clay	Estimated Range of $N_3(s)$	Assumed Distribution	$\bar{N}_3(s)$	$\Delta_3(s)$
Stiff-fissured clay	0.55-0.85	Un.	0.70	0.12
	0.55-0.85	TT2	0.75	0.09
	0.55-0.85	TT3	0.70	0.09
	0.55-0.85	TT1	0.65	0.11
Intact clay	0.85-1.0	Un.	0.93	0.05
	0.85-1.0	TT2	0.95	0.04
	0.85-1.0	TT3	0.93	0.03
	0.85-1.0	TT1	0.90	0.04

4.2.4 Rate of Shearing (Time to Failure)

Undrained tests are usually carried out at a rate of strain where failure occurs in about 15 minutes (Skempton and Hutchinson⁹⁹). However, actual failure of a slope occurs in a much longer period of time. Various authors (Crawford and Eden,²⁵ Lambe and Whitman,⁵⁹ and Skempton and La Rochelle⁹⁷) have indicated that increasing the rate at which a saturated soil is sheared increases the undrained strength. It is generally recognized that undrained strength in a long duration (say several days) test is less than that obtained in a short duration (say several minutes) test. Therefore, due to the difference in the time to failure between laboratory tests and actual field failures, there will be errors involved in the estimation of spatial average in situ

undrained strength based on laboratory measurements. In order to compensate for this error, the corrective factor $N_4(s)$ is used. The magnitude of this error depends on the sensitivity of soil to rate of shearing as well as the time required after excavation for a failure to take place at the site. The strength reduction per log cycle of time may be taken as a measure of the sensitivity of soil to the effect of rate of shearing.

Some research work has been carried out to estimate the influence of this time effect. Casagrande and Wilson²⁰ found that the undrained strength of saturated clays and of clay shales decreases linearly with the logarithm of time. They indicated that the straight line representation is satisfactory within the range of time to failure of from 1 minute to 30 days (see Fig. 4.4). The results of a similar study by Bishop and Henkel⁹ on Boston Blue clay and Weald clay are shown in Fig. 4.5.

In Table 4.9, data about the strength reduction per log cycle of time obtained from various sources are given. In the same table the mean undrained strength from 15-minute laboratory tests is compared with the undrained strength that corresponds to a failure in the field taking place in one day and in one month. The available data indicate that for soils which are exceptionally sensitive to the rate of shearing, such as Cucaracha clay shale and Fornebu clay, the strength reduction per log cycle of time is about 14 percent, whereas for most of the clays this reduction is about 4 to 6 percent. Depending on this rate at which soil strength decreases, four different cases are considered as summarized in Table 4.10. In each case, the range of $N_4(s)$ is assumed to lie between the corresponding values for 30 days and 1 day. $\bar{N}_4(s)$ and $\Delta_4(s)$ values computed for each case are given in Table 4.10.

Table 4.9

Data for $N_4(s)$ from Different Sites

Reference	Soil Type and Site	Strength Reduction (per log cycle of time)	$N_4(s)$ 1 day	$N_4(s)$ 30 days
Bishop and Henkel ⁹	Weald clay (remoulded)	5.5%	0.89	0.81
	Boston Blue clay (remoulded)	5.3%	0.89	0.82
Bjerrum et al. ¹⁷	Fornebu clay	14.0%	0.63	0.50
Casagrande and Wilson ²⁰	Bearpaw clay shale	4.0%	0.89	0.80
	Mexico City clay	4.3%	0.90	0.83
	Cambridge clay	5.3%	0.89	0.80
	Oahe bentonite	9.5%	0.81	0.62
	Cucaracha clay shale	13.0%	0.68	0.45
Simons ⁹⁰	Blue London clay	9.3%	0.81	0.67
Skempton and La Rochelle ⁹⁷	Brown London clay, Bradwell	5.0%	0.89	0.81

Table 4.10
Corrections for Rate of Shearing

Classification		Estimated Range of N_4 (s)	Assumed Distribution	\bar{N}_4 (s)	Δ_4 (s)
Sensitivity to Rate of Shearing	Strength Reduction (per log cycle of time)				
Slightly sensi- tive	less than 3.5%	0.90-1.0	Un.	0.95	0.03
Moderately sensitive	3.5-6.0%	0.80-0.90	Un.	0.85	0.03
Sensitive	6.0-10.0%	0.60-0.80	Un.	0.70	0.08
Very sensitive	10.0-14.0%	0.45-0.70	Un.	0.58	0.12

Slightly sensi- tive-Sensitive	3.0-10.0%	0.60-1.0	Un.	0.80	0.14
Unknown sensi- tivity to shearing rate	3.0-14.0%	0.45-1.0	Un.	0.73	0.22

If the sensitivity of the soil to time effect is unknown, a reasonable range for $N_4(s)$ may be from 0.45 to 1.0, whereas if it is known that the soil is not exceptionally sensitive to the rate of shearing, then $N_4(s)$ may be assumed to range between 0.60 to 1.0. The values of $\bar{N}_4(s)$ and $\Delta_4(s)$ for these cases, computed assuming a uniform distribution over these two ranges, are also given in Table 4.10.

4.2.5 Sample Orientation and Anisotropy

In routine testing of soils for shear strength measurements, tubular samples are obtained from the boreholes with their axes being vertical, and in the laboratory these specimens are tested to fail by increasing the axial stress (with their axes again being vertical). Referring to Fig. 4.6, if the slope is in an incipient state of failure, then all the elements along the circular arc must be in a state of limiting equilibrium. In this case the orientation of the failure plane which coincides with the sliding surface will be different at every point. If the angles that the failure plane and the specimen axis make with the horizontal direction are called α and β respectively, it will be seen that for the slope shown in Fig. 4.6a, α changes from 60° to -30° and β changes from 90° to 0° , for specimens taken at the top of the slope to those at the toe of the slope. In the conventional method of analysis, the effect of the different orientations of the specimens along the failure surface is usually not considered. However, due to varying degrees of anisotropy that exist in clays (Duncan,²⁹ and Skempton and Hutchinson⁹⁹), the strength along a slip surface at the site could be quite different from those measured in the laboratory using the triaxial specimens extracted from the boreholes with vertical axis ($\beta = 90^\circ$).

For the purpose of analyzing this effect, various investigations were performed by trimming test specimens with different orientations and measuring their strengths with undrained triaxial tests. The plotted results of two such investigations are shown in Figs. 4.7a and 4.7b. To avoid any confusion in describing the orientation of a specimen, the terms vertical, horizontal, and inclined will refer to the axis of specimen. A vertical specimen is one that is trimmed in the normal way, with its axis vertical ($\beta = 90^\circ$), and a horizontal specimen is one trimmed so that its axis is horizontal ($\beta = 0^\circ$). An inclined specimen is one that is trimmed so that β is between 0° and 90° .

It is difficult to make generalizations about the magnitude of the effect of anisotropy on undrained strength. However, depending on the ratio of the horizontal strength to the vertical strength the available data is divided into three groups. For consistency, the terminology given by Lo⁶¹ will be used in the following classification:

1. Clays that are isotropic:

For this type of clays, the shear strength is almost the same in all directions. For example, clay from Sala (Sweden) and pre-consolidated Danish Boulder clay show little effect of specimen orientation and can be considered to be isotropic (see Fig. 4.8).

2. Clays with C-Anisotropy ($\frac{S(\beta = 0^\circ)}{S(\beta = 90^\circ)} > 1$):

In this case horizontal strengths are higher than the vertical strengths. Heavily over-consolidated London clay belongs to this group (see Fig. 4.9).

3. Clays with M-Anisotropy ($\frac{S(\beta = 0^\circ)}{S(\beta = 90^\circ)} < 1$):

Clays for which the horizontal strengths are less than the vertical strengths such as San Francisco Bay mud, clays from Surte (Sweden) and from Welland (Ontario) are considered in this group. Other clays that could be included here are: over-consolidated kaolinite clay, clays from Naticoke (Ontario) and Vienna (Austria)(see Fig. 4.10).

To account for the error in the spatial average undrained strength along the potential failure surface resulting from the effects of anisotropy and orientation, the average undrained strength obtained from vertical specimens are corrected by $N_5(s)$. The values of $N_5(s)$ for the sites mentioned above are computed using the corresponding diagrams showing the variation of undrained strength with specimen orientation (see Table 4.11). The $N_5(s)$ values are obtained considering the entire sliding surface, with β changing by 90° between the top and the toe of the slope, and assuming the vertical strength to be constant with depth.

The determination of $N_5(s)$ is illustrated with reference to Fig. 4.11. Since it is assumed that for a typical slope with a cylindrical potential failure surface β changes by 90° between the top and the toe of the slope, the total length of the failure surface is taken into consideration in the RS- β (Relative Strength versus β) diagram. Then, the area under the strength variation curve will approximately give the ratio of the undrained strength averaged along the failure surface (considering the effects of anisotropy and orientation) to the mean vertical strength. Accordingly, this ratio is equal to $N_5(s)$. For the example shown in Fig. 4.11,

Table 4.11
Data for $N_5(s)$ from Different Sites

Reference	Soil Type, Site and Comments	Type of Anisotropy	$N_5(s)$
Jacobsen ⁴⁴	Pre-consolidated Danish boulder clay	Isotropic	0.97
Jakobson ⁴⁶	Swedish post glacial clay from Sala	Isotropic	1.08
Duncan and Seed ²⁷	London clay (the estimated range is not so dependable since the inclined strengths were not measured but estimated)	C-Anisotropy	1.02-1.19
Simons ⁹⁰	London clay, Wraysbury	C-Anisotropy	0.87
Ward et al. ¹¹³	London clay, Ashford Common Shaft	C-Anisotropy	0.96
Duncan and Seed ²⁷	Over-consolidated kaolinite clay	M-Anisotropy	0.83
Duncan and Seed ²⁸	Normally consolidated San Francisco Bay mud	M-Anisotropy	0.87
Hvorslev ⁴²	Clay from Vienna, Austria	M-Anisotropy	0.93
Jakobson ⁴⁵	Clay from Surte, Sweden	M-Anisotropy	0.97
Lo ⁶¹	Clay from Welland, Ontario	M-Anisotropy	0.85
Lo ⁶³	Clay from Naticoke, Ontario	M-Anisotropy	0.91

$$\begin{aligned}
N_5(s) &= \text{Area under curve OPR (with } L = \text{unity)} \\
&= A_1 + A_2 \\
&= \left(\frac{0.75 + 0.90}{2} \right) 0.5 + \left(\frac{0.90 + 1.0}{2} \right) 0.5 \\
&= 0.413 + 0.475 = 0.888
\end{aligned}$$

In case the shear strength varies with depth, the method of slices may be used. The value of $N_5(s)$ for each segment is obtained by first estimating the average value of β for the failure surface in that slice and then computing the corresponding $N_5(s)$ from the RS- β diagrams. For instance, for a slice between A ($\beta \approx 90^\circ$) and B ($\beta \approx 60^\circ$) of Fig. 4.11, the average value of β is 75° and the corresponding value of the relative strength is 0.95. Therefore, for the slice between A and B, $N_5(s)$ is 0.95.

In Table 4.12, the values of $\bar{N}_5(s)$ and $\Delta_5(s)$ corresponding to the three different kinds of anisotropy are shown. For the isotropic case, the triangular TTI distribution with $\bar{N}_5(s) = 1.0$ is chosen because $\bar{N}_5(s)$ is expected to be 1.0 for the isotropic condition. For the C-Anisotropy, the more reliable data given by Simons⁹⁰ and Ward et al.¹¹³ (see Table 4.11) indicate that the expected value of $N_5(s)$ is more likely to be closer to the lower bound of the estimated range; thus, TTI distribution is also used here. For the case with M-Anisotropy, the uniform distribution is assumed.

4.2.6 Plane Strain Failure

For many landslides the stress and deformation conditions in the field are such that displacements take place only in two dimensions. So, in

Table 4.12
 Corrections for Orientation and Anisotropy

Type of Anisotropy	Estimated Range of $N_5(s)$	Assumed Distribution	$\bar{N}_5(s)$	$\Delta_5(s)$
Isotropic	0.97-1.08	TT1	1.0	0.03
C-Anisotropy	0.85-1.20	TT1	0.97	0.09
M-Anisotropy	0.80-1.0	Un.	0.90	0.06

the stability analysis of slopes plane strain condition is assumed. However, laboratory measurements are based mostly on triaxial testing of cylindrical specimens where axially symmetric condition occurs. It has been indicated by various authors (Dickey et al.,²⁶ Henkel and Wade,³⁹ Kinner and Ladd,⁵¹ and Skempton and Hutchinson⁹⁹) that there is some difference between the soil strength obtained under conditions of plane strain and axial symmetry. Hence, an error will be introduced into the stability analysis due to the use of triaxial test results, in spite of the fact that the actual field conditions require plane strain test data. To account for this discrepancy, average undrained strengths from triaxial compression tests will be corrected by the corrective factor $N_6(s)$.

Henkel and Wade³⁹ performed plane strain and triaxial tests under undrained conditions on remoulded Weald clay. They reported that the undrained strengths in plane strain are about 8 percent higher than those obtained from the triaxial tests for saturated Weald clay (i.e., $N_6(s) = 1.08$).

By comparing the average undrained strength in plane strain with

that in triaxial compression, the value of $N_6(s)$ is computed for two other cases (see Table 4.13). On the basis of these results, the range of $N_6(s)$ is chosen to be from 1.0 to 1.10. The assumption of the uniform distribution within this range gives $\bar{N}_6(s) = 1.05$ and $\Delta_6(s) = 0.03$.

Table 4.13
Data for $N_6(s)$ from Different Sites

Reference	Soil Type	$N_6(s)$
Dickey et al. ²⁶	Sedimented Boston Blue clay	1.02
Duncan and Seed ²⁸	San Francisco Bay mud	1.06
Henkel and Wade ³⁹	Remoulded Weald clay	1.08

4.2.7 Progressive Failure Effect

Progressive failure mechanism and the residual strength of soils are discussed in detail for the long-term stability analysis of slopes (see Section 5.2.6). However, progressive failure may also be involved in short-term failures that take place in stiff-fissured clays and shales. An example of this effect is presumably observed in the slip in London clay, at Bradwell; the slip occurred 5 days after the excavation had been completed. The analysis by Skempton and La Rochelle⁹⁷ showed that the mean shear strength mobilized along the slip surface was about 54 percent of the mean strength obtained in conventional triaxial test. In other words, the overall mean correction needed would be $\bar{N}_s = 0.54$.

Let $N_7(s)$ be the corrective factor to account for the error in the

average in situ undrained strength due to the effect of progressive failure. From $\bar{N}_s = \prod_{j=1}^7 \bar{N}_j$, an estimate of $\bar{N}_7(s)$ can be obtained by substituting the values of the other $\bar{N}_j(s)$'s for this site as tabulated in Table 4.14.

Table 4.14

Values of the Corrective Factors for the Slip at Bradwell

$N_j(s)$	$\bar{N}_j(s)$	Source of Information
N_1	1.03	Low sensitivity ($S_t = 2$)
N_2	1.05	Computed from the data given by Skempton and La Rochelle ⁹⁷ ; tube sampling
N_3	0.70	From Skempton and La Rochelle ⁹⁷
N_4	0.81	Computed from the data given by Skempton and La Rochelle ⁹⁷
N_5	0.87	C-Anisotropy, London clay (Simons ⁹⁰)
N_6	1.05	From Section 4.2.6

Thus,

$$0.54 = (1.03)(1.05)(0.70)(0.81)(0.87)(1.05)\bar{N}_7 = 0.56 \bar{N}_7$$

obtaining,

$$\bar{N}_7(s) = 0.96$$

The above value implies that the effect of progressive failure should be

small for the slip at Bradwell. Based on this result, and also as indicated by Duncan and Dunlop,³⁰ it may be said that the effect of progressive failure on the short-term stability of slopes is probably small. Accordingly, the range of $N_7(s)$ is assumed to be between 0.90 and 1.0. A uniform distribution over this range gives $\bar{N}_7(s)$ and $\Delta_7(s)$ as 0.95 and 0.03, respectively.

4.3 Model Uncertainty

Several authors (e.g., Bishop and Bjerrum,⁸ Lambe and Whitman,^{5,9} and Skempton and Hutchinson^{9,9}) have indicated that it is appropriate to use the total stress method for analyzing the stability of slopes in saturated clays immediately after the formation of the slope when an overall change of water content has not taken place. They emphasized that the errors involved in the short-term stability analysis of slopes will stem mainly from the incomplete knowledge of the in situ value of the average undrained strength along the potential failure surface. Accordingly, it may be assumed that the modeling errors in the expressions for M_R and M_O as given by Eqs. 3.1 and 3.2 will be small, provided that the applications are limited to those cases where short-term condition exists in the field, and the assumed or actual potential failure surface is approximately circular in cross section.

Data on the overall mean safety factor for four end-of-construction failures that took place in excavations of intact clays are given in Table 4.15. In all of the four cases the short-term condition was applicable, and the failures took place along circular surfaces. These data may be used to study the modeling error in M_R (the modeling error in M_O is assumed to be negligible) for short-term stability of slopes. In Appendix E it is shown that

if tube sampling has been performed at the site. The statistical parameters of $N_2(s)$ and $N_3(s)$ used above are the ones obtained by assuming a uniform distribution (see Tables 4.5 and 4.8). Similarly, for intact clays, assuming the same conditions, \bar{N}_s and Δ_q are 0.93 and 0.21, respectively.

The values given above for intact and fissured clays will vary, depending on the sensitivity of soil to rate of shearing and the type of anisotropy. The effects of disturbance due to changes in the stress system, plane strain and progressive failure, tend to compensate each other, such that the resultant effect is relatively insignificant. Thus, the \bar{N}_s and Δ_q values given in Table 4.16 for stiff-fissured and intact clays are tabulated only with respect to the sensitivity to rate of shearing and type of anisotropy. In all cases it is assumed that tube sampling has been performed at the site. These values for \bar{N}_s indicate that the average undrained strength from triaxial tests overestimates the average in situ undrained strength by about 25 to 50 percent in stiff-fissured clays; on the other hand, because of compensating errors, the discrepancy is smaller for intact clays.

In order to analyze the difference in the risk levels of designs that are based on the corrected and laboratory-measured average undrained shear strengths, a general example of short-term slope stability is considered. The same general example will be used to analyze the sensitivity of the total uncertainty to additional sampling and to evaluate the reliability level of earth slopes. The slope is assumed to be located in a fairly homogenous clay deposit with the length of the potential failure surface being 100 ft. The number of 1.5 in. diameter by 3 in. soil elements for a strip of the potential failure surface that is 1 ft wide (perpendicular to the cross section

Table 4.16
 Corrections to Computed Shear Strength
 for Various Soil Conditions

Type of Clay	Sensitivity to Rate of Shearing	Type of Anisotropy	\bar{N}_s	Δ_q
Stiff-fissured	Slightly sensitive to sensitive	M-anisotropy	0.69	0.24
Stiff-fissured	Slightly sensitive to sensitive	C-anisotropy or isotropic	0.76	0.24
Stiff-fissured	Very sensitive	M-anisotropy	0.50	0.23
Stiff-fissured	Very sensitive	C-anisotropy or isotropic	0.55	0.23
Intact	Slightly sensitive to sensitive	M-anisotropy	0.93	0.21
Intact	Slightly sensitive to sensitive	C-anisotropy or isotropic	1.03	0.21
Intact	Very sensitive	M-anisotropy	0.68	0.20
Intact	Very sensitive	C-anisotropy or isotropic	0.75	0.20

of the slope) will be large; thus, n_e as given by Eq. 3.9 will also be large. For instance, $n_e = 182$ corresponding to $v = 0.21$. Therefore, δ_s will be very small (less than 0.025 for $\delta_s = 0.30$) and may be neglected. The values of δ_s and n_s are taken equal to 0.30 and 25, respectively (see Table 4.1 for values of δ_s for different sites). For the model uncertainty, \bar{N}_f is taken as 1.0 and Ω_f as 0.08 based on the results obtained in Section 4.3.

In Figs. 4.12 and 4.13 the risk levels corresponding to different values of mean safety factors are shown for stiff-fissured and intact clays respectively, assuming M-anisotropy, moderate sensitivity to rate of shearing and tube sampling. In these figures, Curve I corresponds to the case where the mean safety factor is computed on the basis of the corrected mean undrained shear strength, whereas Curve II represents the case where the analysis is based on the direct use of the average laboratory strength without any correction. Examination of these figures shows that due to the discrepancies between the in situ and laboratory shear strengths, a design based on the direct use of the average laboratory shear strengths will give a false indication of reliability. For a given mean safety factor the difference between the ordinates of Curve II and Curve I shows the difference in the risk levels of a design. This difference is quite significant for stiff-fissured clays (Fig. 4.12) relative to that for intact clays (Fig. 4.13).

4.4.1 Effect of Sample Size

The required mean safety factor as a function of the number of test specimens, n_s , corresponding to a specified risk level, p_f , are shown in Figs. 4.14a and 4.14b for four different values of Δ_q . The resisting moment M_R is assumed to be lognormal. As n_s increases, the uncertainty in the mean strength decreases, resulting in a reduction in the uncertainty of M_R . As a consequence, the required mean safety factor for a specified risk level will be lowered; however, the rate at which the safety factor decreases diminishes considerably for large values of n_s (say $n_s > 25$). For example, from Fig. 4.14b, for $\Delta_q = 0.20$, increasing n_s from 25 to 50 reduces the mean safety factor from 2.05 to 2.02 (only by 1.5 percent). Thus, extensive sampling (large n_s) will

not be efficient; additional sampling will only reduce that portion of the total uncertainty that is associated with insufficient sampling. It will be more effective if additional testing efforts are directed to assessing information about the corrective factors for the particular project. For example, tests performed at a particular site to estimate the effect of mechanical disturbance during tube sampling may reduce $\Delta_2(s)$ from 0.13 to 0.03 (see Section 2.3.2). This, in turn will reduce the total uncertainty in M_R from 0.224 to 0.184, causing the safety factor to decrease from 2.05 to 1.80 (by 12 percent) for the case where $n_s = 25$, $\Delta_q = 0.20$ and $p_f = 10^{-3}$.

In short, the effort spent in soil exploration and testing to reduce the uncertainty in M_R should be a balanced combination of soil sampling to reduce the sampling uncertainty Δ_o , plus information gathering (including testing) for the corrective factors to reduce the uncertainty arising from the discrepancies between laboratory and in situ undrained strengths, i.e., Δ_q . For this purpose, methods of decision analysis may be utilized in choosing the optimum allocation of effort to decrease the overall uncertainty.

4.4.2 Evaluation of Risk

The level of risk implicit in the present method of design of earth slopes can be evaluated on the basis of the minimum safety factor currently in use. Sowers and Sowers¹⁰² consider a safety factor of 1.3 to 1.4 to be satisfactory for cuts and fills as far as the stability of earth masses is concerned. Meyerhof⁷¹ suggested a minimum overall safety factor of 1.3 to 1.5 for shear failure in earthworks, whereas Jumikis⁴⁷ gave 1.5 as the factor of safety against sliding and rotation failures. Lumb⁶⁶ indicated that with

slope stability, the conventional safety factor is commonly less than 2 and often as low as 1.3. The lower value of the recommended safety factor, 1.3, is suggested for temporary works or when the design is based on detailed soil information, such as using the results of failure analyses of slopes with similar soil properties. On the other hand, 1.5 is commonly used in stability analyses under normal service conditions.

In practice, the engineer generally does not base his design on the average strength of the soil deposit; instead, he uses a conservative value of the soil strength in connection with these safety factors. Regarding the choice of soil parameters for design, Sowers and Sowers¹⁰² indicated that:

"In most strata the deviations from the average are so great that unsafe conclusions will be reached from averages. For design, therefore, the lower values are given emphasis. Although some designers argue that the design should be based on the poorest condition observed in each stratum, this is overly conservative because localized bad spots seldom control the behavior of the entire stratum. If the weak areas occur at random, a reasonable basis for design is the lowest quartile--the value for which 25 percent of the data are poorer and 75 percent better."

Thus, based on this statement, the safety factors of 1.3 to 1.5 could be considered as the minimum safety factors corresponding to designs based on the lowest quartile strength. According to the data presented in Table 4.1, $\delta_S = 0.30$ appears to be a representative value for the variability in the undrained strength within a soil deposit. With $\delta_S = 0.30$ and assuming the undrained strength to be normally distributed, the lowest quartile undrained strength is found to be 20 percent below the mean undrained strength. Accordingly, the minimum value of the "actual" mean safety factor, μ_F^* , will be between $\frac{1.3}{0.8} = 1.63$ and $\frac{1.5}{0.8} = 1.88$.

* In the sense that this is based on "corrected" design variables and design equations.

The total uncertainty associated with the discrepancies between the laboratory and in situ undrained strengths, as measured by Δ_q , has been found to vary between 0.20 to 0.24 for the general soil conditions given in Table 4.16. In these cases it is assumed that minimum soil exploration has been performed at the site. However, Δ_q will be less for a particular site than those computed for these general cases, if test data or additional information on the corrective factors are available from the site under consideration. For example, tests performed to estimate the effect of mechanical disturbance during tube sampling may decrease $\Delta_2(s)$ from 0.13 to 0.03 (see Section 2.3.2). Similarly, if the engineer knows that a certain type of soil will be slightly sensitive to the rate of shearing, then $\Delta_4(s)$ will be 0.03 instead of 0.14 which is used in the case of minimum soil exploration. Thus, if extensive soil exploration is performed at the site, it is estimated that Δ_q will be reduced to a range of 0.12 to 0.17 (by assuming triangular distributions for the various corrective factors considering the local soil conditions observed at the site).

For the above values of Δ_q , the failure probabilities corresponding to the recommended conventional design safety factors of $F = 1.3$ ($\mu_F = 1.63$) and $F = 1.5$ ($\mu_F = 1.88$) are given in Table 4.17. It may be seen that the customary safety factors of 1.3 to 1.5 used in earth slopes correspond to a probability of failure between 0.9 percent to 0.006 percent if test data and information from the particular site is used in evaluating the effect of the various systematic errors. On the other hand, in the case of minimum soil exploration, the uncertainty level will be higher, and the failure probability corresponding to the conventional safety factor of 1.5 will be between 0.3

Table 4.17

Failure Probabilities of Slopes Designed
with Current Safety Factors

F	μ_F	Minimum Soil Exploration		Extensive Soil Exploration	
		Ω_{M_R}	P_f^*	Ω_{M_R}	P_f^*
1.3	1.63	0.22	0.018	0.16	0.0015
1.3	1.63	0.26	0.044	0.20	0.0090
1.5	1.88	0.22	0.003	0.16	0.00006
1.5	1.88	0.26	0.011	0.20	0.0010

* Calculated assuming lognormal M_R

percent to 1 percent. Based on the number of failures (by sliding) in earth dams constructed in the last 30 years, Meyerhof⁷¹ estimated the frequency of failure of earth slopes to be around 0.1 percent, which is within the range of failure probabilities calculated above for various degrees of soil exploration. In Fig. 4.15 the risk levels corresponding to different values of mean safety factor are shown for the cases of minimum and extensive soil exploration in relation to stiff-fissured clays.

4.5 Recommended Safety Factors for Design

The value of the computed (laboratory-based) mean safety factor to be used in design for a given level of reliability can be obtained from Eq. 2.20a. The recommended values of the computed mean safety factor \bar{F} for different soil conditions that may be encountered in practice are shown in Table

4.18 corresponding to risk levels of 10^{-1} , 10^{-2} and 10^{-3} (i.e., 10 percent, 1 percent, 0.1 percent). The various soil conditions considered in Table 4.18 are the same as those for Table 4.16. In all these cases, it is assumed that tube sampling will be performed at the site. In the last three columns of Table 4.18 values of the conventional safety factor, assuming that the lowest quartiles of the soil parameters are to be used in design, are also shown. The safety factors given in Table 4.18 correspond to the case where minimum soil exploration has been performed at the site.

In Tables 4.19 and 4.20 the recommended values of the mean and conventional safety factors are given for stiff-fissured and intact clays considering extensive soil exploration. Since Δ_q will be smaller in this case, compared to those given in Table 4.16, the recommended safety factors will also be smaller.

The safety factors given in Tables 4.18, 4.19 and 4.20 are to be used for slopes which are located in one soil deposit. However, a representative value of the recommended safety factor can be obtained for slopes in which the potential failure surface passes through n layers of different soil properties by computing the weighted average of the safety factors recommended for each layer. For example, a representative value of the computed mean safety factor \bar{F} is

$$\bar{F} = \sum_{i=1}^n \left(\frac{\bar{M}_{R_i}}{\sum_{i=1}^n \bar{M}_{R_i}} \right) \bar{F}_i \quad (4.2)$$

where \bar{M}_{R_i} is the mean resisting moment due to the i th layer based on the

Table 4.18

Recommended Values of the Safety Factor for Design
(With Minimum Soil Exploration)

Type of Clay	Sensitivity to * Rate of Shearing	Type of Anisotropy	Mean Safety Factor (based on the <u>average</u> value of the soil parameters) Corresponding to $p_f =$			Conventional Safety Factor (based on the <u>lowest quartile</u> value of the soil parameters) Corresponding to $p_f =$		
			10^{-1}	10^{-2}	10^{-3}	10^{-1}	10^{-2}	10^{-3}
Stiff-fissured	Slightly sensitive to sensitive	M-anisotropy	2.09	2.74	3.36	1.67	2.19	2.69
Stiff-fissured	Slightly sensitive to sensitive	C-anisotropy or isotropic	1.90	2.49	3.05	1.52	1.99	2.44
Stiff-fissured	Very sensitive	M-anisotropy	2.84	3.70	4.48	2.27	2.96	3.58
Stiff-fissured	Very sensitive	C-anisotropy or isotropic	2.58	3.36	4.07	2.06	2.69	3.26
Intact	Slightly sensitive to sensitive	M-anisotropy	1.49	1.90	2.27	1.19	1.52	1.82
Intact	Slightly sensitive to sensitive	C-anisotropy or isotropic	1.35	1.72	2.05	1.08	1.38	1.64
Intact	Very sensitive	M-anisotropy	2.02	2.54	3.02	1.62	2.03	2.42
Intact	Very sensitive	C-anisotropy or isotropic	1.83	2.31	2.73	1.46	1.85	2.18

* Definition of sensitivity in terms of strength reduction (per log cycle of time) is given in Table 4.10.

Table 4.19

Recommended Values of the Safety Factor for Design
(With Extensive Soil Exploration, Stiff-Fissured Clays)

Sensitivity to Rate of Shearing*	Type of Anisotropy	Mean Safety Factor (based on the <u>average</u> value of the soil parameters) Corresponding to $p_f =$			Conventional Safety Factor (based on the <u>lowest quartile</u> value of the soil parameters) Corresponding to $p_f =$		
		10^{-1}	10^{-2}	10^{-3}	10^{-1}	10^{-2}	10^{-3}
Slightly sensitive	M-anisotropy	1.54	1.84	2.07	1.23	1.47	1.66
Slightly sensitive	C-anisotropy or isotropic	1.42	1.71	1.96	1.14	1.37	1.57
Moderately sensitive	M-anisotropy	1.66	1.96	2.21	1.33	1.57	1.77
Moderately sensitive	C-anisotropy or isotropic	1.58	1.90	2.17	1.26	1.52	1.74
Sensitive	M-anisotropy	2.14	2.57	2.93	1.71	2.06	2.35
Sensitive	C-anisotropy or isotropic	1.94	2.36	2.72	1.55	1.89	2.18
Very sensitive	M-anisotropy	2.64	3.26	3.78	2.11	2.61	3.02
Very sensitive	C-anisotropy or isotropic	2.40	2.96	3.44	1.92	2.37	2.75

* See Table 4.18

Table 4.20

Recommended Values of the Safety Factor for Design
(With Extensive Soil Exploration, Intact Clays)

Sensitivity to Rate of Shearing*	Type of Anisotropy	Mean Safety Factor (based on the <u>average</u> value of the soil parameters) Corresponding to $p_f =$			Conventional Safety Factor (based on the <u>lowest quartile</u> value of the soil parameters) Corresponding to $p_f =$		
		10^{-1}	10^{-2}	10^{-3}	10^{-1}	10^{-2}	10^{-3}
Slightly sensitive	M-anisotropy	1.13	1.31	1.48	0.90	1.05	1.18
Slightly sensitive	C-anisotropy or isotropic	1.04	1.23	1.38	0.83	0.98	1.10
Moderately sensitive	M-anisotropy	1.21	1.40	1.58	0.97	1.12	1.26
Moderately sensitive	C-anisotropy or isotropic	1.16	1.36	1.54	0.93	1.09	1.23
Sensitive	M-anisotropy	1.56	1.84	2.08	1.25	1.47	1.66
Sensitive	C-anisotropy or isotropic	1.42	1.70	1.91	1.14	1.36	1.53
Very sensitive	M-anisotropy	1.94	2.33	2.67	1.55	1.86	2.14
Very sensitive	C-anisotropy or isotropic	1.75	2.11	2.41	1.40	1.69	1.93

* See Table 4.18

average laboratory-measured undrained strength, and \bar{F}_i is the required mean safety factor for the i th layer. The weighting factors are assigned with respect to the resisting moment only, since the uncertainty in the overturning moment is small compared to that in the resisting moment. An application of Eq. 4.2 is described in Section 6.2.7.

Chapter 5

EVALUATION OF LONG-TERM STABILITY OF SLOPES

5.1 Inherent Variability and Uncertainty Due to Insufficient Sampling

Within a soil deposit the peak effective stress parameters, C and ϕ , will contain some variability. According to Section 3.2.1, the inherent variability in the spatial average peak effective stress parameters, δ_C and δ_ϕ , will be equal to $\frac{\delta_C}{\sqrt{n_e}}$ and $\frac{\delta_\phi}{\sqrt{n_e}}$, respectively. The equivalent number of independent soil elements n_e may be different for c and ϕ depending on the corresponding values of the correlation parameters, v_c and v_ϕ . Lumb⁶⁶ and Singh⁹¹ indicated that, generally, the variability in cohesion C is larger than that in the angle of shearing resistance ϕ . In general, according to Singh,⁹¹ $\delta_C = 0.20$ to 0.40 , and $\delta_\phi = 0.10$ to 0.20 .

The errors in c and ϕ resulting from insufficient sampling are

$$\Delta_0(c) = \frac{\delta_C}{\sqrt{n_s}}$$

and

$$\Delta_0(\phi) = \frac{\delta_\phi}{\sqrt{n_s}}$$

where n_s is the number of test specimens.

5.2 Discrepancies Between Laboratory and In Situ Peak Effective Stress Parameters

The major factors that cause discrepancies between the field and laboratory-measured values of the peak effective stress parameters are the same as those listed for the undrained strength. The effects of each of these factors on the effective stress parameters are discussed in the following sections.

5.2.1 Disturbance During Sampling

In contrast to the undrained strength, the effective stress parameters C and ϕ are not influenced much by mechanical disturbance and changes in the stress system from sampling (Bishop and Henkel,⁹ Kenney,⁵⁰ and Skempton and Hutchinson⁹⁹).

Disturbance Due to Changes in the Stress System

In their study on a clay with sensitivity $S_t = 2$, Skempton and Sowa⁹⁵ reported that C and ϕ are not influenced by the disturbance caused by the changes in the stress system, indicating that $N_1(c) = N_1(\phi) = 1.0$ for this case. Therefore, the effect of sampling disturbance on c and ϕ , specifically resulting from the changes in the stress system, will be neglected.

Mechanical Disturbance

As far as the influence of mechanical disturbance is concerned, there is no data available to quantify this effect. However, several investigators (e.g., Kenney,⁵⁰ and Skempton and Hutchinson⁹⁹) indicated that the effective stress parameters, especially ϕ , are probably not sensitive to minor sampling disturbances. Accordingly, for the effect of mechanical disturbance on ϕ , $N_2(\phi)$ will be taken to be between 1.0 and 1.20, whereas $N_2(c)$ is assumed to range between 1.0 and 1.30. These ranges are estimated by considering the range of $N_2(s)$ in tube sampling (see Section 4.2.2), and may be justified on the basis that c and especially ϕ are influenced much less than s by mechanical disturbances. A uniform distribution over the suggested ranges gives:

$$\bar{N}_2(c) = 1.15, \Delta_2(c) = 0.08 \text{ and } \bar{N}_2(\phi) = 1.10, \Delta_2(\phi) = 0.05.$$

5.2.2 Size of Specimen

Little information is available about the influence of specimen size on c and ϕ . For stiff-fissured clays this effect could be important. Reported values of c and ϕ for two such clays are given in Table 5.1. From this limited data, it is observed that the effect of specimen size is significant for c , and not so significant for ϕ . In the extreme case, if the in situ

Table 5.1

Data for the Effect of Specimen Size on c and ϕ

Reference	Soil Type	Type of Test	c (psi)	ϕ
Marsland and Butler ⁷⁰	Stiff-fissured Barton clay	1-1/2" x 3" triaxial tests	1.6	24°
		3" x 6" and 5" x 10" triaxial tests	1.05	23.5°
		Along continuous fissures	0.9	18.0°
Skempton ⁹⁶	Stiff-fissured Blue London Clay	1-1/2" x 3" triaxial tests	2.2	20°
Skempton et al. ⁹⁸	Stiff-fissured Blue London clay	Along fissure and joint surfaces	1.0	18.5°

value of the average peak cohesion intercept is assumed to be equal to that measured along fissures and joints, then the 1-1/2 in. x 3 in. triaxial specimens overestimate the value of c by 1.82 times in the case of Barton clay and 2.17 times in the case of Blue London clay. These values are computed from the data given in Table 5.1. Thus, the corresponding correction $N_3(c)$ will be $\frac{1}{1.82} = 0.55$ for the Barton clay and $\frac{1}{2.17} = 0.46$ for the Blue London clay. However, $N_3(c)$ should be higher than these extreme values. For example, for Barton clay, comparing the value of c from 1-1/2 in. x 3 in. specimens with that for larger specimens gives $N_3(c) = 0.66$. Comparing these with $N_3(s)$ of Chapter 4, it may be observed that the effects of specimen size on c and on the undrained strength s are probably of the same order (e.g., for Barton clay $N_3(c) = 0.66$ and $N_3(s) = 0.67$; for Blue London clay $N_3(c) > 0.46$ and $N_3(s) = 0.56$).

The influence of specimen size on ϕ is less marked. Even for the extreme cases in which the strength along fissures is compared with the strength obtained from 1-1/2 in. x 3 in. specimens, $N_3(\phi)$ is found to be greater than 0.75 (for Barton clay $N_3(\phi) = 0.75$, for Blue London clay $N_3(\phi) = 0.93$, and for stiff Italian clays $N_3(\phi) = 0.80$ (Esu³³)). According to these results, reasonable ranges for stiff-fissured clays appear to be between 0.60 and 0.85 for $N_3(c)$, and between 0.85 and 1.0 for $N_3(\phi)$.

For intact clays, the influence of specimen size on ϕ is expected to be negligible ($\bar{N}_3(\phi) \approx 1.0$, $\Delta_3(\phi) \approx 0$), since this effect is small even in fissured clays. Consistent with the assumption for stiff-fissured clays, the range of $N_3(c)$ for intact clays is also taken to be equal to that of $N_3(s)$ which lies between 0.85 and 1.0. The corresponding values of $\bar{N}_3(c)$, $\bar{N}_3(\phi)$, $\Delta_3(c)$ and $\Delta_3(\phi)$ for different cases are given in Table 5.2.

Table 5.2
Mean Correction and Sampling Error Due to Specimen Size

Strength Parameter	Soil Type	Estimated Range of $N_3(\cdot)$	Assumed Distribution	$\bar{N}_3(\cdot)$	$\Delta_3(\cdot)$
c	Stiff-fissured	0.60-0.85	Un.	0.73	0.10
		0.60-0.85	TT2	0.77	0.08
		0.60-0.85	TT3	0.73	0.07
		0.60-0.85	TT1	0.68	0.09
	Intact	0.85-1.0	Un.	0.93	0.05
		0.85-1.0	TT2	0.95	0.04
		0.85-1.0	TT3	0.93	0.03
		0.85-1.0	TT1	0.90	0.04
ϕ	Stiff-fissured	0.85-1.0	Un.	0.93	0.05
		0.85-1.0	TT2	0.95	0.04
		0.85-1.0	TT3	0.93	0.03
		0.85-1.0	TT1	0.90	0.04
	Intact	--	---	1.0	0.0

5.2.3 Rate of Shearing (Time to Failure)

The effects of rate of shearing on C and ϕ are less than that on the undrained strength (Kenney⁵⁰). Bishop and Henkel⁹ reported drained test results on remoulded Weald clay in which the variation in strength with time to failure is studied. The proportional decrease over the range from 6 hours to 1 week amounts to about 3.5 percent per log cycle of time (see Fig. 5.1). According to Skempton and Hutchinson,⁹⁹ the time to failure for peak strength

parameters in drained tests under laboratory condition is of the order of 1 day. Bishop and Henkel⁹ indicated that the drained tests normally used to determine C and Φ are performed in a time varying between 1/2 to 3 days depending on the soil type. On the other hand, failure at the site takes many years (for example, Northolt 19 years, Kensal Green 29 years, Sudbury Hill 49 years).

To estimate the ranges of $N_4(c)$ and $N_4(\phi)$, the effective stress parameters corresponding to laboratory tests, with time to failure assumed to be 1 day, are compared with those corresponding to a long-term failure in the field, with time to failure equal to 1 year and 50 years. The results of this comparison based on data obtained from three different sources are given in Table 5.3. In obtaining these results, it is assumed that the

Table 5.3
Data for $N_4(c)$ and $N_4(\phi)$ from Different Sites

Reference	Soil Type and Site	Strength Reduction (per log cycle of time)	$N_4(c)$		$N_4(\phi)$	
			1 year	50 years	1 year	50 years
Bishop and Henkel ⁹	General case	5.0%	0.87	0.79	0.87	0.79
Bishop and Henkel ⁹	Remoulded Weald clay	3.5%	0.90	0.83	0.90	0.83
Skempton and La Rochelle ⁹⁷	London clay, Bradwell	1.5%	0.96	0.94	0.96	0.94

strength reduction in the cohesive and frictional components are of equal magnitude. From these data the lower bound of $N_4(c)$ and $N_4(\phi)$ could both be taken as 0.80. However, since soils which are more sensitive to the shearing rate (such as Fornebu clay) have not been included, on the basis of Section 4.2.4, the range of $N_4(c)$ and $N_4(\phi)$ are both estimated to lie between 0.60 and 1.0. Since data were limited, no classification with respect to sensitivity to shearing rate is made in this case. The values for \bar{N}_4 and Δ_4 computed by assuming four different distributions over this range are given in Table 5.4.

Table 5.4
Corrections for Rate of Shearing

Strength Parameter	Estimated Range of $N_4(\cdot)$	Assumed Distribution	$\bar{N}_4(c) = \bar{N}_4(\phi)$	$\Delta_4(c) = \Delta_4(\phi)$
c, ϕ	0.60-1.0	Un.	0.80	0.14
	0.60-1.0	TT2	0.87	0.11
	0.60-1.0	TT3	0.80	0.10
	0.60-1.0	TT1	0.73	0.13

5.2.4 Sample Orientation and Anisotropy

Some work has been done to investigate the effect of sample orientation and anisotropy on the effective stress parameters. The reported data from various sites concerning c and ϕ values obtained by testing specimens at different orientations are shown in Fig. 5.2. The corresponding values of

$N_5(c)$ and $N_5(\phi)$ are computed in a similar manner as was done for $N_5(s)$ in Section 4.2.5. The results are summarized in Table 5.5.

Table 5.5
Data for $N_5(c)$ and $N_5(\phi)$ from Different Sites

Reference	Soil Type and Site	$\frac{c(\beta = 0^\circ)}{c(\beta = 90^\circ)}$	$\frac{\phi(\beta = 0^\circ)}{\phi(\beta = 90^\circ)}$	$N_5(c)$	$N_5(\phi)$
Bishop et al. ¹⁰	London clay Ashford Common Shaft,				
	Level C	1.04	1.03	1.02	1.02
	Level E	0.90	1.07	0.95	1.04
Duncan and Seed ²⁸	San Francisco Bay mud	--	0.92	--	0.96
Lo ⁶²	Welland clay	--	0.82	--	0.91
Ranganatham et al. ⁸³	Black cotton soil, India	--	0.90	--	0.95
Skempton and Hutchinson ⁹⁹	Blue London clay, Wraysbury	0.91	1.01	0.96	1.01

Based on the above values, the range of $N_5(c)$ and $N_5(\phi)$ are both estimated to be between 0.90 and 1.05. Due to the limited data, no classification can be made according to the type of anisotropy. A uniform distribution within the indicated range gives $\bar{N}_5(c) = \bar{N}_5(\phi) = 0.98$ and $\Delta_5(c) = \Delta_5(\phi) = 0.04$.

In this case, using the $N_5(c)$ and $N_5(\phi)$ values given for London clay at Ashford Common Shaft (levels C and E) and Wraysbury, the coefficient of correlation between $N_5(c)$ and $N_5(\phi)$ is computed using Eq. 2.11, yielding $\rho_5 = -0.32$.

5.2.5 .Plane Strain Failure

The values of $N_6(c)$ and $N_6(\phi)$ obtained by comparing the effective stress parameters from plane strain tests with those measured in triaxial tests are given in Table 5.6. In each of the four cases, the discrepancy

Table 5.6
Data for $N_6(c)$ and $N_6(\phi)$ from Different Sites

Reference	Soil Type	$N_6(c)$	$N_6(\phi)$
Bishop ⁷	Compacted moraine	1.0	1.06-1.11
Bishop and Henkel ⁹	--	-	1.08-1.14
Duncan and Seed ²⁸	San Francisco Bay mud	-	1.10
Henkel and Wade ³⁹	Remoulded Weald clay	-	1.05

is reported in terms of ϕ since the cohesion intercept is small and assumed to be zero. As an example, data given by Henkel and Wade³⁹ are shown in Fig. 5.3. These data show that for the remoulded Weald clay, the average angle of shearing resistance obtained from the triaxial tests (25.9°) should be corrected by a factor of 1.05 to obtain the average ϕ value of 27.1° measured in the plane strain tests (i.e., $N_6(\phi) = 1.05$). In view of the results given in Table 5.6, the range for $N_6(\phi)$ is estimated to be between 1.0 and 1.15, and $\bar{N}_6(c)$ is taken to be 1.0. A uniform distribution over the stated range gives $\bar{N}_6(\phi) = 1.08$ and $\Delta_6(\phi) = 0.04$. As a conservative estimate $\Delta_6(c)$ will also be taken as 0.04.

5.2.6 Progressive Failure Effect

A typical stress strain curve for a clay tested under drained condition is shown in Fig. 5.4. The peak shear strength, S_f , occurs at a relatively small displacement, and as the displacement increases after the peak strength has been attained, the shearing resistance decreases until it finally reaches a constant value. This constant value of shearing resistance is referred to as the residual strength, S_r .

Recently, various studies (Bishop,¹² Duncan and Dunlop,³⁰ and Dunlop and Duncan³¹) have indicated that the ratio of shear strength to shear stress along a potential failure surface is generally not uniform. Therefore, for a first-time slide the peak strength will not be reached at all points of the potential failure surface. At points where the peak has already been reached, if the clay is forced to pass the peak value, then the strength will decrease according to the stress-strain curve. Owing to the reduction in strength at these points, some additional stress will be passed on to other points in the clay causing the peak strength to be exceeded at these points also. In this way, the soil elements at various portions of the slip surface will be successively strained beyond the peak, and a progressive failure of the slope will occur. Skempton⁹⁶ indicated that microscopic fissures, joints, slickensides and other imperfections in clay act like stress concentrators causing the peak strength to be exceeded, leading to a progressive decrease in strength. As a consequence, progressive failure is more marked in stiff-fissured clays than it is in intact clays.

Since the Fourth Rankine lecture presented by Skempton⁹⁶ on progressive failure and residual strength of soils, Bishop,^{12,14} Bjerrum,¹⁸

Kenney,⁴⁹ Peck,⁸² Skempton¹⁰⁰ and others discussed this problem and indicated that the use of peak strength in the slope stability analyses will be in error because the peak strength does not act along the entire failure surface. There are as yet no quantitative methods available for predicting the magnitude of the influence of progressive failure. However, limited information on the effect of progressive failure can be obtained by comparing the average mobilized shear strength, s_m (computed from stability analyses)^{*} with the average peak strength, s_f (computed based on corrected values of c and ϕ), in those cases where failure has occurred. For this purpose, six case records reported in the literature are analyzed. In these cases, the average effective stress, \bar{p} , was computed by using the "best estimate of pore pressures existing, when the slip took place." Laboratory measurements on c and ϕ were also reported. The corresponding overall mean corrective factors, \bar{N}_c and \bar{N}_ϕ , are computed based on the values obtained in the previous sections for the individual site under consideration. In order to compensate for the difference between the average peak strength and the average mobilized strength at failure, the corrective factor N_{s_f} is introduced such that

$$s_m = N_{s_f} s_f \quad (5.1)$$

The required information and the computed values of N_{s_f} for each of the six sites are given in Table 5.7. The values of N_{s_f} obtained from these limited number of failure cases imply the following points relative to

* For a failure case the safety factor must be equal to 1.0; therefore, the average mobilized shear strength at the time of slip, s_m , will be equal to the average shear stress. The latter can be computed from a knowledge of the overturning moment and arc length of the failure surface.

Table 5.7

Summary of Available Data for the Computation of N_{s_f}

Type of Slide	References	Site and Soil Type	s_m	\bar{p}'	\hat{c}	$\hat{\phi}$	\bar{N}_c	\bar{N}_ϕ	s_f	N_{s_f}
First-time	Skempton and Brown, ⁹⁴ Skempton, ⁹⁶ Skempton and Hutchinson ⁹⁹	Selset, boulder clay, intact	640 psf	760 psf	180 psf	32°	0.94	0.98	635 psf	1.0
First-time	Suklje and Vidmar, ¹⁰³ Skempton and Hutchinson ⁹⁹	Gradot Ridge, seat of the slip surface in stiff intact lacustrine clay	27 ton/m ²	80 ton/m ²	0	22°	--	0.95	30.4 ton/m ²	0.89
First-time	Skempton, ⁹⁶ Skempton and Hutchinson ⁹⁹	Northolt, London clay, stiff-fissured	380 psf	750 psf	320 psf	20°	0.70	0.89	466 psf	0.81
First-time	Skempton ⁹⁶	Kensal Green, London clay, stiff-fissured	380 psf	800 psf	320 psf	20°	0.70	0.89	482 psf	0.79
Slide on pre-existing slip surface	Henkel and Skempton, ³⁸ Skempton ⁹⁶	Jackfield, stiff-fissured clay	400 psf	1300 psf	220 psf	25°	0.70	0.89	684 psf	0.59
Slide on pre-existing slip surface	Skempton, ⁹⁶ Skempton and Hutchinson ⁹⁹	Sudbury Hill, London clay, stiff-fissured	160 psf	600 psf	320 psf	20°	0.67	0.86	400 psf	0.40

the effect of progressive failure on the soil strength:

1. For first-time slides in slopes of intact clays, s_m and s_f are in close agreement. In view of the two case records analyzed, N_{s_f} is estimated to range between 0.85 and 1.0.
2. For first-time slides in slopes of fissured clays, s_m is less than s_f . For the two failure cases analyzed involving London clay, N_{s_f} is calculated as 0.80. More case studies are needed in order to estimate the effect of progressive failure on first-time slides in slopes of fissured clays. The range of N_{s_f} corresponding to this condition is estimated approximately, based on the assumption that it should lie between the minimum value of N_{s_f} obtained from the first-time slides in intact clays and the maximum value of N_{s_f} obtained from the slides on pre-existing slip surfaces in stiff-fissured clays. From the results given in paragraphs (1) and (3) below, this range is estimated to be between 0.60 and 0.85.
3. For slides on pre-existing slip surfaces, the difference between s_m and s_f is large. For the two sites shown in Table 5.7, N_{s_f} is found to be between 0.40 and 0.60.

Residual Strength for the Analysis of Slopes on Pre-Existing Slip Surfaces

Studies (see for example Skempton^{96,100}) have demonstrated that after a slide has taken place, the strength on the slip surface is equal to the residual value. Therefore, it is desirable to analyze the stability of

slopes on pre-existing slip surfaces based on the average residual strength, s_r , along the potential failure surface. Let N_{s_r} be the corrective factor defined as

$$N_{s_r} = \frac{s_m}{s_r} \quad (5.2)$$

where s_r is the average residual strength measured in shear box tests without any correction for the effects of such factors as rate of shearing, anisotropy, etc. For example, for Jackfield $N_{s_r} = \frac{400 \text{ psf}}{447 \text{ psf}} = 0.90$ and for Sudbury $N_{s_r} = \frac{160 \text{ psf}}{161 \text{ psf}} = 0.99$. The closeness of the values for s_r and s_m in these two cases indicates that it is more appropriate to compute the stability of slopes on pre-existing slip surfaces based on the average residual strength. However, in practice ambiguities exist in the determination of residual strength.

In Table 5.8 the average values of the residual angle of shearing resistance, $\hat{\phi}_r$ (assuming the residual cohesion intercept, $\hat{c}_r = 0$), obtained from different methods of testing are given for Blue London clay, Brown London clay and Weald clay. These values are computed using the data summarized by Bishop et al.¹⁵ In the last column of Table 5.8, the ratio of $\hat{\phi}_r$ from any one of the test methods to that measured in the drained multiple reversal direct shear box test, $\hat{\phi}_{r_0}$, are shown. Examination of the values given shows that $\hat{\phi}_r$ obtained from different methods of testing could differ considerably from each other, with the multiple reversal direct shear box and the ring shear tests giving the highest and lowest values, respectively.

There is no common agreement among the investigators as to which method should be used to measure the actual residual strength of a soil in the laboratory and also as to the method that gives the best estimate of ϕ_r .

Table 5.8

Comparison of $\hat{\phi}_r$ Values from Different Testing Methods

Soil Type	Sample and Test Type	$\hat{\phi}_r$ (with $\hat{c}_r = 0$)	$\frac{\hat{\phi}_r}{\hat{\phi}_{r0}}$
Blue London clay	Drained multiple reversal direct shear box test. Undisturbed.	13.5°	1.0
	Drained ring shear test. Undisturbed.	9.3°	0.69
	Drained triaxial tests:		
	a. Presheared to large displacements. Undisturbed.	10.5°	0.78
b. Cut plane. Undisturbed.	13.7°	1.01	
Brown London clay	Drained multiple reversal direct shear box test. Undisturbed.	14.2°	1.0
	Drained ring shear test. Undisturbed.	10.1°	0.71
	Drained direct shear box tests:		
	a. Cut plane. Undisturbed.	12.3°	0.87
	b. Slip surface.	14.0°	0.99
	Drained triaxial tests:		
a. Cut plane. Undisturbed.	13.3°	0.94	
b. Slip surface.	13.7°	0.97	
Weald clay	Drained multiple reversal direct shear box test. Undisturbed.	13.3°	1.0
	Drained ring shear test. Undisturbed.	12.0°	0.90

in the field. Nevertheless, based on the discussions given by Skempton and Hutchinson⁹⁹ and by Bishop et al.,¹⁵ the average residual angle of shearing resistance in the field, ϕ_r , may be assumed to lie between the values obtained from the ring shear test and the multiple reversal direct shear box test. Hence, ϕ_r can be expressed as

$$\phi_r = N_{\phi_r} \hat{\phi}_{r0} \quad (5.3)$$

where N_{ϕ_r} is the corrective factor to account for the use of the multiple reversal direct shear box test results in estimating ϕ_r .

In view of the above discussion and the values given in the last column of Table 5.8, N_{ϕ_r} is assumed to lie between 0.70 and 1.0. A uniform distribution over this range gives $\bar{N}_{\phi_r} = 0.85$ and $\Delta_{\phi_r} = 0.10$.

The estimated ranges of the corrective factors needed to account for the effect of progressive failure under different conditions are summarized in Table 5.9. The corresponding values of \bar{N}_{s_f} , Δ_{s_f} and \bar{N}_{s_r} , Δ_{s_r} are also given. By comparing the soil and slope type at a particular site with the case records illustrated in Table 5.8, an engineer can choose the appropriate values of \bar{N}_{s_f} and Δ_{s_f} .

5.3 Uncertainty Associated with the Estimation of Pore Pressure Distribution

Pore pressures are usually measured directly from piezometers in the field, or estimated by drawing a flow net. For long-term stability of slopes, the pore pressure is controlled either by a static ground water condition or by a steady flow pattern. If there is no flow the value of u may be determined from the ground water level. On the other hand, for steady-state seepage, a flow net can be used to obtain the pore pressures at various

Table 5.9

Mean Corrections and Prediction Errors
Due to Progressive Failure

Type of Slide and Soil	Range of N_{s_f}	Assumed Distribution	\bar{N}_{s_f}	Δ_{s_f}
First-time. Intact	0.85-1.0	Un.	0.93	0.05
	0.85-1.0	TT2	0.95	0.04
	0.85-1.0	TT3	0.93	0.03
	0.85-1.0	TT1	0.90	0.04
First-time. Stiff-fissured	0.60-0.85	Un.	0.73	0.10
	0.60-0.85	TT2	0.77	0.08
	0.60-0.85	TT3	0.73	0.07
	0.60-0.85	TT1	0.68	0.09
Slides on pre-existing slip surfaces. Stiff-fissured	0.40-0.60	Un.	0.50	0.12
	<u>Range of N_{s_r}</u>		<u>\bar{N}_{s_r}</u>	<u>Δ_{s_r}</u>
Slides on pre-existing slip surfaces. Stiff-fissured	0.90-1.0	Un.	0.95	0.03

locations. Due to seasonal changes, the ground water level will fluctuate, thus affecting the value of u . The highest seasonal values will be more critical for the stability of a slope. If the records of water level over the years are available, then this data can be used to estimate the variability in u . Besides the seasonal variations, assumptions made in drawing flow nets, the probable errors in piezometric levels and the possible effects of future manmade structures could introduce additional uncertainties into the estimated pore pressures.

Scott,⁸⁷ in studying the slope failures in three soils, estimated that the maximum error in the assumed pore pressures at failure for the slopes he analyzed, would be ± 5 ft of head. The effects of this error on the safety factor for three different slopes were computed. The corresponding safety factors are given in Table 5.10 with F_0 , F_{-5} and F_{+5} designating the safety factors corresponding to the most likely u , to u decreased by 5' of head, and to u increased by 5' of head, respectively.

Bishop⁶ analyzed the variation of safety factor with pore pressure for a specific slope. Based on the data given, the changes in the factor of safety due to an estimated ± 10 percent change in the average pore pressure ratio, r_u^* , are computed (see Table 5.10). These results can be used to estimate the uncertainty in the resisting moment due to pore pressure variations. Let the corrective factor N_u be defined as

$$N_u = \frac{\mu_{M_R}(u)}{\bar{M}_R(\hat{u})} \quad (5.4)$$

where $\mu_{M_R}(u)$ and $\bar{M}_R(\hat{u})$ are the mean resisting moments computed from the actual

* r_u is defined as the ratio of pore pressure at a point to the weight of the overlying soil at the same point.

Table 5.10

Corrections to Estimated Pore Pressures for Different Sites

Reference	Soil Type and Location	F_0	$F_{-5'}$	$F_{+5'}$	Maximum Value of	Minimum Value of	Assumed Distribution	Statistical Parameters of N_u	
					$N_u (= \frac{F_{-5'}}{F_0})$	$N_u (= \frac{F_{+5'}}{F_0})$		\bar{N}_u	Δ_u
Scott ⁸⁷	Aftonian clay, Cut 31	1.37	1.53	1.27	1.12	0.93	Un.	1.025	0.05
	Yarmouth clay, Cut 3	1.27	1.40	1.14	1.10	0.90	Un.	1.000	0.06
	Kensan till, Cut 27	0.82	0.95	0.66	1.16	0.81	Un.	0.985	0.10
		F_0	$F_{-10\%}$	$F_{+10\%}$	$\frac{F_{-10\%}}{F_0}$	$\frac{F_{+10\%}}{F_0}$			
Bishop ⁶	Boulder clay fill	1.38	1.51	1.25	1.09	0.91	Un.	1.000	0.05

and best estimate of the pore pressure distributions along the failure surface, respectively. The value of $\mu_{M_R}(u)$ is not known, but the range of the mean resisting moment corresponding to possible changes in u is given in terms of the safety factors. These safety factors are tabulated in Table 5.10 and the range of N_u for each site is computed. Examination of these values (see Table 5.10) indicates that \bar{N}_u is about 1.0 and Δ_u varies between 0.05 to 0.10.

5.4 Uncertainty Due to the Method of Analysis (Model Uncertainty)

The assumption of neglecting the forces acting on the sides of slices in the Fellenius method of analysis is on the safe side, and the resisting moment obtained on this basis usually falls below the lower bound of M_R 's which satisfy statics (Whitman and Moore¹¹⁴). Bishop,⁶ and Whitman and Bailey¹¹⁵ have demonstrated that the error in the Fellenius method increases with increasing central angle of the failure arc and increasing pore pressure. In certain extreme cases (submerged slopes with large central angle of failure arc) this error could be quite high. However, it has been indicated (Turnbull and Hvorslev,¹¹¹ and Whitman and Bailey¹¹⁵) that the large error involved in the extreme cases could be reduced by using more refined versions of the Fellenius method.

In order to estimate N_f , which is the factor suggested to correct for the method of stability analysis and its associated uncertainty, the reported safety factors obtained from the Fellenius method (FM) are compared with those obtained from more rigorous methods (RM) in which side forces are taken into consideration and all the equilibrium conditions are satisfied

(see Table 5.11). The safety factors from the Fellenius and the rigorous methods may be expressed as (Lambe and Whitman⁵⁹),

$$F_{FM} = \frac{(\bar{M}_R)_{FM}}{\bar{M}_O} \quad (5.5)$$

$$F_{RM} = \frac{(\bar{M}_R)_{RM}}{\bar{M}_O} \quad (5.6)$$

Table 5.11
Available Data for N_f

Reference	Case Analyzed	Safety Factor by		N_f
		FM	RM	
Bishop ⁶	Boulder clay fill	1.38	1.60	1.16
	Moraine fill	1.53	1.92	1.25
Whitman and Moore ¹¹⁴	Example 4	1.38	1.52	1.10
	Example 6	1.57	1.88	1.20
Whitman and Bailey ¹¹⁵	Example 1	1.49	1.60	1.07
	Example 2	1.09	1.25	1.15
	Example 3	0.66	0.76	1.15
	Example 4	1.84	2.02	1.10
Wolfskill and Lambe ¹¹⁶	Siburua Dam			
	a. Stage 1	0.88	1.05	1.19
	b. Stage 2	0.83	1.00	1.20
	c. Stage 3	0.90	1.03	1.14

where $(\bar{M}_R)_{FM}$ and $(\bar{M}_R)_{RM}$ are the mean resisting moments determined with the Fellenius method and the rigorous method, respectively. \bar{M}_0 will have the same value in both methods. The two equations can be combined to give

$$(\bar{M}_R)_{RM} = \frac{F_{RM}}{F_{FM}} (\bar{M}_R)_{FM} \quad (5.7)$$

The ratio $\frac{F_{RM}}{F_{FM}}$ is by definition equal to N_f . In Table 5.11 the values of N_f computed for various cases are given. Based on these data the expected value and the standard deviation of N_f are found to be 1.16 and 0.051, respectively. Therefore, the basic variability in the resisting moment associated with the method of analysis will be

$$\delta_f = \frac{0.051}{1.16} = 0.044$$

whereas the prediction uncertainty in M_R due to the approximate Fellenius method, as given by the c.o.v. of \bar{N}_f , is

$$\Delta_f = \frac{\delta_f}{\sqrt{11}} = \frac{0.044}{3.32} = 0.013$$

However, the rigorous method will also involve an error in the prediction of the actual resisting moment. This error is estimated to be 0.10, assuming that it will be of the same order as that involved in the $\phi = 0$ analysis (see Section 4.3). Hence, the total uncertainty due to the Fellenius method of analysis is

$$\Omega_f = \sqrt{0.044^2 + 0.013^2 + 0.10^2} = 0.11$$

5.5 Analysis of Results

A general slope example is considered in order to estimate the total uncertainty and the required correction on M_R based on the results of the uncertainty analysis presented in this chapter. The potential failure surface is assumed to be located in a homogenous soil stratum with $\delta_c = 0.30$ and $\delta_\phi = 0.15$. n_s is taken as 25; therefore, $\Delta_o(c) = \frac{0.30}{\sqrt{25}} = 0.06$ and $\Delta_o(\phi) = \frac{0.15}{\sqrt{25}} = 0.03$. Since the total length of the potential failure surface is large, the number of equivalent specimens, n_e , will be very large for both c and ϕ . Accordingly, one can take $\delta_c = \delta_\phi \approx 0$.

The mean corrections and prediction errors for c and ϕ are computed from Eqs. 3.39, 3.41, 3.45 and 3.46 assuming the component corrective factors, $N_k(c)$'s and $N_k(\phi)$'s, $k = 1, 2, \dots, 6$, to be uniformly distributed. \bar{N}_{s_f} and Δ_{s_f} values for different soil types are obtained from Table 5.9, assuming a uniform distribution. Based on the results of Sections 5.3 and 5.4, values of $\bar{N}_u = 1.0$, $\Delta_u = 0.10$ and $\bar{N}_f = 1.16$, $\Omega_f = 0.11$ are assumed.

For this general example, the value of \bar{N}_{M_R} and Ω_{M_R} are computed for the three different conditions commonly encountered in practice. Ω_{M_R} is given by Eq. 3.56, and based on Eq. 2.15

$$\bar{N}_{M_R} = \frac{\mu_{M_R}}{\bar{M}_R} = \frac{\bar{N}_f \bar{N}_u \bar{N}_{s_f} [\bar{N}_c \bar{c} L + \tan(\bar{N}_\phi \bar{\phi}) \sum_{i=1}^m \bar{P}_i']}{\bar{c} L + \tan \bar{\phi} \sum_{i=1}^m \bar{P}_i'} \quad (5.8)$$

\bar{N}_{M_R} and Ω_{M_R} will vary depending on the relative magnitude of the resistance offered by the cohesive component to that offered by the frictional component.

Let η be the ratio of these two component resistances defined as

$$\eta = \frac{\bar{c} L}{\tan \bar{\phi} \sum_{i=1}^m \bar{p}_i'} \quad (5.9)$$

The statistical parameters of N_{M_R} , i.e., \bar{N}_{M_R} and Ω_{M_R} , are computed for two extreme cases: the cohesive component of the resisting moment is zero ($\eta = 0$), and the frictional component of the resisting moment is very small ($\eta \approx \infty$). Computations are also done for the case where the cohesive and frictional components of the resisting moment are equal ($\eta = 1$). The results are summarized in Table 5.12 for $\bar{\phi} = 5^\circ, 10^\circ, 20^\circ, 30^\circ$ and 40° . From Table 5.12 it is observed that:

1. For all types of slides, neither Ω_{M_R} nor \bar{N}_{M_R} is sensitive to changes in $\bar{\phi}$.
2. For first-time slides in intact clays, \bar{N}_{M_R} is close to 1.0, and Ω_{M_R} is about 0.24. The maximum value of \bar{N}_{M_R} (1.00) is attained when the cohesive component of M_R is very small compared to the frictional component ($\eta \approx 0$), whereas the minimum value (0.91) is obtained when the frictional component is negligible compared to the cohesive component ($\eta \approx \infty$).
3. For first-time slides in stiff-fissured clays, the mean resisting moment obtained using peak strength parameters without any correction, \bar{M}_R , overestimates the actual value of μ_{M_R} by 26 to 44 percent. This indicates that the effects of specimen size and progressive failure mechanism in stiff-fissured clays overrides the conservative results of the Fellenius method. Ω_{M_R} is found to be about 0.27 for first-time slides in stiff-fissured clays. The maximum (0.74) and the minimum (0.56) values of \bar{N}_{M_R} are obtained when $\eta \approx 0$ and $\eta \approx \infty$, respectively.

Table 5.12

Statistical Parameters of N_{M_R} for Different Soil Conditions
(With Minimum Soil Exploration)

Type of Slide and Soil	$\bar{\phi}$	$\bar{N}_f \bar{N}_u \bar{N}_{s_f}$	$\sqrt{\Omega_f^2 + \Delta_u^2 + \Delta_{s_f}^2}$	\bar{N}_c	Ω_c	\bar{N}_ϕ	Ω_ϕ	Statistical Parameters of N_{M_R}					
								$\eta = 0$		$\eta = 1.0$		$\eta = \infty$	
								\bar{N}_{M_R}	Ω_{M_R}	\bar{N}_{M_R}	Ω_{M_R}	\bar{N}_{M_R}	Ω_{M_R}
First-time slides in intact clays	5°	1.08	0.16	0.84	0.19	0.93	0.16	1.00	0.23	0.96	0.20	0.91	0.25
	10°	"	"	"	"	"	"	"	"	0.95	"	"	"
	20°	"	"	"	"	"	"	"	0.24	"	"	"	"
	30°	"	"	"	"	"	"	0.99	0.25	"	0.21	"	"
	40°	"	"	"	"	"	"	0.98	0.27	0.94	"	"	"
First-time slides in stiff- fissured clays	5°	0.85	0.18	0.66	0.21	0.87	0.17	0.74	0.25	0.65	0.23	0.56	0.28
	10°	"	"	"	"	"	"	"	"	"	"	"	"
	20°	"	"	"	"	"	"	0.73	0.26	0.64	"	"	"
	30°	"	"	"	"	"	"	0.72	0.27	"	"	"	"
	40°	"	"	"	"	"	"	0.70	0.29	0.63	0.24	"	"
Slides on pre- existing slip sur- faces in stiff- fissured clays	5°	0.58	0.19	0.66	0.21	0.87	0.17	0.50	0.26	0.44	0.23	0.38	0.28
	10°	"	"	"	"	"	"	"	"	"	"	"	"
	20°	"	"	"	"	"	"	"	0.27	"	0.24	"	"
	30°	"	"	"	"	"	"	0.49	0.28	"	"	"	"
	40°	"	"	"	"	"	"	0.48	0.29	0.43	0.25	"	"

4. For slides on pre-existing slip surfaces, a large difference between \bar{M}_R and μ_{M_R} ($\bar{N}_{M_R} = 0.38-0.49$) is found. This shows that the stability analysis of slopes on pre-existing slip surfaces using peak strength will be in significant error (see Fig. 5.7). For this case Ω_{M_R} is about 0.28.
5. In all three cases, the combined uncertainty arising from the method of analysis, pore pressure distribution and progressive failure is approximately equal to the combined uncertainty contributed by the effective stress parameters c and ϕ .

For all types of slides the overall mean correction is found to be different than 1.0. Therefore, the mean safety factor computed from the Fellenius method by using the \hat{c} and $\hat{\phi}$ values as measured in the laboratory will be different from the mean safety factor in the field. In Figs. 5.5 through 5.7 the failure probabilities corresponding to various mean safety factors are shown for the three different kinds of slides considered in this chapter. For first-time slides (see Figs. 5.5 and 5.6), Curve I corresponds to the case where the mean safety factor is based on the corrected value of the mean resisting moment. Curve II ($\eta = 0$) and Curve III ($\eta \approx \infty$) are based on mean safety factors computed using laboratory-measured parameters of the resisting moment. For example, a mean safety factor of 2.0 in a first-time slide in stiff-fissured clays corresponds to a risk level of 0.7×10^{-2} (from Curve I of Fig. 5.6) if the appropriate corrections are made. On the other hand, without any corrections, a mean safety factor of 2.0 will correspond to a failure probability between 0.1 (from Curve II of Fig. 5.6) to 0.40 (from Curve III of Fig. 5.6) depending on η .

In the case of slides on pre-existing slip surfaces (see Fig. 5.7), the risk levels corresponding to the "actual" and computed mean safety factors differ significantly. This indicates that the direct use of the peak strength parameters in analyzing the stability of slopes will give a false indication of reliability.

Evaluation of Risk

The minimum safety factor of 1.5 recommended in the current design of slopes under normal service conditions, may be considered to correspond to designs in which the lowest quartile value of the strength parameters are used (see Section 4.4.2). Assuming that C and ϕ are normally distributed with $\delta_C = 0.30$ and $\delta_\phi = 0.15$, the lowest quartile values of C and ϕ are computed to be 80 percent and 90 percent of the respective mean values. Therefore, the minimum value of the "actual" mean safety factor μ_F will be $\frac{1.5}{0.85} = 1.76$, where 0.85 is obtained assuming that the cohesive and frictional components of M_R are equal.

The total uncertainty in the resisting moment, Ω_{M_R} , is found to vary between 0.20 to 0.29 depending on the soil conditions and the value of η (see Table 5.12). These values of Ω_{M_R} are obtained assuming minimum soil exploration. However, if additional information is available for a specific site, the level of uncertainty will be smaller. In this latter case, it is estimated that the range of Ω_{M_R} will be between 0.16 to 0.22.

The failure probabilities corresponding to the minimum safety factor of 1.5 are tabulated for the three site conditions, assuming lognormal M_R . The Ω_{M_R} values given in Table 5.13 for the cases of minimum and extensive

soil exploration are the ones obtained by assuming that the cohesive and frictional components of M_R are equal. From Table 5.13 it is observed that for long-term stability, the recommended safety factor of 1.5 corresponds to failure probabilities ranging from 0.06 percent to 0.2 percent in the case of extensive soil exploration, whereas with minimum soil exploration the failure probability ranges from 0.48 percent to 1.6 percent. Again, this is in general

Table 5.13
Failure Probabilities of Slopes Designed with the
Current Safety Factor of 1.5

Type of Slide and Soil	F	μ_F	Minimum Soil Exploration*		Extensive Soil Exploration*	
			Ω_{M_R}	p_f	Ω_{M_R}	p_f
First-time, intact	1.5	1.76	0.21	0.0048	0.17	0.0006
First-time, stiff-fissured	1.5	1.76	0.24	0.013	0.18	0.0011
Slide on pre- existing slip surface, stiff- fissured	1.5	1.76	0.25	0.016	0.19	0.002

* Calculated assuming lognormal M_R .

agreement with Meyerhof's⁷¹ estimated frequency of failure of earth slopes (around 0.1 percent). In Fig. 5.8 the effect of the degree of soil exploration on the risk level is shown for first-time slides in stiff-fissured clays with $\eta = 1.0$. It is observed that for a given mean safety factor the risk level will be smaller in the case of extensive soil exploration compared to the case with only minimum soil exploration.

5.6 Recommended Safety Factors for Design

The recommended values of the computed mean safety factor corresponding to the three different cases discussed in the previous section are given in Table 5.14 considering both minimum and extensive soil explorations. The safety factors in the parentheses are for the extensive soil exploration. The conventional safety factors to be used with the lowest quartile values of the laboratory-measured peak strength parameters are also presented in Table 5.14. In designing slopes on pre-existing slip surfaces, the recommended values of the safety factors depend on whether the analysis will be based on the peak shear strength parameters or on the residual strength parameters (see Table 5.14). After a slide has taken place the strength on the slip surface is equal to the residual value (Skempton^{96,100}); hence a realistic analysis for this type of slopes requires the use of residual strength parameters. The recommended values of the mean safety factors (or the conventional safety factors) given in the last row of Table 5.14 correspond to the case where the average (or the lowest quartile) residual angle of shearing resistance ϕ_r , with $c_r = 0$, is to be obtained from drained multiple reversal direct shear box tests.

Table 5.14
Recommended Values of the Safety Factor for Design

Type of Slide and Soil	Cohesive Component of $M_R \ll$ Frictional Component of M_R						Cohesive Component of $M_R \gg$ Frictional Component of M_R					
	Mean Safety Factor (based on the average value of the soil parameters) Corresponding to $p_f =$			Conventional Safety Factor (based on the lowest quartile value of the soil parameters) Corresponding to $p_f =$			Mean Safety Factor (based on the average value of the soil parameters) Corresponding to $p_f =$			Conventional Safety Factor (based on the lowest quartile value of the soil parameters) Corresponding to $p_f =$		
	10^{-1}	10^{-2}	10^{-3}	10^{-1}	10^{-2}	10^{-3}	10^{-1}	10^{-2}	10^{-3}	10^{-1}	10^{-2}	10^{-3}
First-time slides in intact clays	1.43 [*] (1.30) ^{**}	1.86 (1.59)	2.25 (1.85)	1.29 (1.17)	1.67 (1.43)	2.03 (1.67)	1.56 (1.41)	2.02 (1.68)	2.45 (1.95)	1.25 (1.13)	1.62 (1.34)	1.96 (1.56)
First-time slides in stiff-fissured clays	2.07 (1.81)	2.77 (2.25)	3.43 (2.63)	1.86 (1.63)	2.49 (2.03)	3.09 (2.37)	2.65 (2.36)	3.54 (2.95)	4.40 (3.45)	2.12 (1.89)	2.83 (2.36)	3.52 (2.76)
Slides on pre-existing slip surfaces in stiff-fissured clays:												
Based on peak shear strength parameters	3.04 (2.71)	4.06 (3.39)	5.04 (3.96)	2.74 (2.44)	3.65 (3.05)	4.54 (3.56)	3.92 (3.50)	5.23 (4.37)	6.50 (5.10)	3.14 (2.80)	4.18 (3.50)	5.20 (4.08)
Based on residual shear strength parameter ϕ_r ($c_r = 0$)	1.17 (1.13)	1.44 (1.33)	1.65 (1.51)	1.05 (1.02)	1.30 (1.20)	1.49 (1.36)						

* With minimum soil exploration.

** With extensive soil exploration.

Chapter 6

APPLICATIONS TO ACTUAL FAILURE CASES

6.1 General Remarks

In designing earth slopes, the geometry of the slope is usually first chosen on the basis of experience, and then its stability is analyzed. Stability analyses are also made as an aid in the choice of remedial work whenever a slide has occurred, or when there is some reason to believe that slides might occur in the future. In any case, the geometry of the slope is defined by its actual or assumed dimensions.

In the conventional method of slope stability analysis, we search for the critical surface with the smallest safety factor. Similarly, in the present probabilistic procedure, we look for the surface with the largest failure probability (see Section 2.2.2). In the following sections, the failure probabilities for two slides, Congress Street Open Cut and Selset, are computed based on actual data. Also, in both cases the slopes are re-designed to meet a specified reliability level. These two slope failures are chosen for the analysis due to the availability of ample data from the sites.

6.2 An Example of Short-Term Slope Stability:
The Congress Street Open Cut in Chicago6.2.1 General Information

During the excavation of an open cut in Chicago for the Congress Street superhighway, a slide occurred, with the slope on the south side of

the cut failing for a length of about 200 ft. The failure took place principally in saturated glacial clay, and there was no time for any appreciable dissipation of pore water pressure. Therefore, the stability analysis will be based on the total stress method.

The failure was described as a rotational slide taking place on a more or less circular slip surface (Skempton and Hutchinson⁹⁹). The approximate position of the actual slip surface and the approximate dimensions of the slope at the time of failure are shown in Fig. 6.1. Detailed information about this slide has been reported by Ireland.⁴³

6.2.2 Inherent Variability and Error Due to Insufficient Sampling

The failure surface, whose depth is limited by a stiff underlying layer, is located mostly in a gritty blue clay which has been divided into three layers of different consistencies. The upper clay layer has been subjected to desiccation and contains some cracks and joints. Above the upper clay layer is a relatively thin layer of sand and silt, which is covered by fill (Fig. 6.1).

The undrained shear strength of the clays was measured by compression tests on triaxial specimens obtained from 8 borings. Sampling was done by 2 in. diameter Shelby tubes with the samples being at least 3 ft apart. The mean undrained strength and the coefficient of variation as computed from the reported laboratory results are given in Table 6.1 for each one of the clay layers. Assuming that the spatial correlation for the undrained strength within a layer is given by Eq. 3.8 with the spatial correlation parameter $v = 0.21$ (as obtained from Hooper and Butler's data⁴¹), the values of n_e are

Table 6.1

Data for the Undrained Strengths at Congress Street

Layers	\bar{s} (ksf)	σ_S (ksf)	δ_S	n_e	δ_s	n_s	$\Delta_o = \frac{\delta_S}{\sqrt{n_s}}$
Upper clay layer	1.06	0.54	0.51	28	0.096	38	0.083
Middle clay layer	0.62	0.16	0.26	54	0.035	55	0.035
Lower clay layer	0.78	0.25	0.32	125	0.029	33	0.056

taken from Fig. 3.2 as 28, 54, and 125 for the upper, middle and lower clay layers, respectively. The basic variability of the spatial average undrained strength, δ_s , computed for each layer are given in Table 6.1. In the same table, the uncertainty associated with insufficient sampling is also shown for each layer.

The estimates of the spatial average undrained strengths of these three cohesive layers are expected to be correlated among themselves. Data from the 8 boring holes about \hat{s} are given in Table 6.2. Based on these 8 sets of observations, the coefficient of correlation (using Eq. 2.11) between the upper and middle, upper and lower, and middle and lower clay layers are computed to be 0.66, 0.59 and 0.40, respectively.

Spatial Trend with Depth

In order to demonstrate the application of the procedure described

Table 6.2
Data for \hat{s} from Different Borings

Borings k	Upper clay layer	Middle clay layer	Lower clay layer
	\hat{s}_{1k} (ksf)	\hat{s}_{2k} (ksf)	\hat{s}_{3k} (ksf)
1	1.15	0.59	0.86
2	0.51	0.45	0.60
3	1.38	0.70	0.72
4	0.73	0.70	0.68
5	0.96	0.68	0.91
6	1.06	0.60	0.60
7	0.97	0.48	0.85
8	1.68	0.77	0.96

in Section 3.2.2, the variability in undrained strength with depth is analyzed for each layer. For this purpose the layers are divided into segments as shown in Fig. 6.2. Within a layer the lengths of the segments are taken to be equal. Linear regression analysis is carried out through the use of computer, and the results are presented in Table 6.3. The values computed for the segments and the resulting equivalent statistical parameters of s for each layer are also shown in Table 6.3. Since the variability in the undrained strength exhibits a different trend in the different layers (see Fig. 6.3), it is not possible to lump the three layers into one common regression line. Computations for the first layer are illustrated in Appendix F.

The c.o.v.'s obtained for each layer based on the regression analysis may be interpreted as describing the combined uncertainty associated with the

Table 6.3

Statistical Parameters of s Based on Regression Analysis

Layers	Results of Regression Analysis for Each Layer				Segment	Computations for the Segments				Equivalent Statistical Parameters for the Spatial Average Undrained Strength of Layers		
	\hat{S} (ksf)	σ_S (ksf)	\bar{z} (ft)	σ_z (ft)		\bar{z}_i (ft)	\bar{s}_i (ksf)	VAR (ksf) ²	COV (ksf) ²	σ_s (ksf)	\bar{s} (ksf)	c.o.v.
Upper clay layer	-0.051z +1.77	0.51	14.0	3.67	I	9.5	1.29	1.71x10 ⁻²	0.12x10 ⁻² (I,II)	0.086	1.11	0.077
					II	16.5	0.93	1.00x10 ⁻²	0.12x10 ⁻² (II,I)			
Middle clay layer	0.00084z +0.59	0.163	30.1	5.87	I	25.0	0.61	8.45x10 ⁻⁴	1.30x10 ⁻⁴ (I,II)	0.022	0.62	0.036
					II	35.0	0.62	8.21x10 ⁻⁴	1.30x10 ⁻⁴ (II,I)			
Lower clay layer	0.039z -0.97	0.22	45.3	3.14	I	44.0	0.75	0.17x10 ⁻²	0.1x10 ⁻² (I,II) 0.17x10 ⁻² (I,III)	0.039	0.81	0.047
					II	48.0	0.90	0.26x10 ⁻²	0.1x10 ⁻² (II,I) 0.12x10 ⁻² (II,III)			
					III	44.5	0.77	0.16x10 ⁻²	0.17x10 ⁻² (III,I) 0.12x10 ⁻² (III,II)			

inherent variability and insufficient sampling (i.e., $\sqrt{\delta_s^2 + \Delta_0^2}$). In Table 6.4, the results of the regression analysis are compared with those obtained from Table 6.1. Except for the upper clay layer, the values calculated from the regression analysis are in close agreement with those obtained assuming no spatial trend. It should be pointed out that the values given in Table 6.1 for the inherent variability in s_i are computed assuming that the spatial correlation between two points is an exponentially decaying function of the distance separating them. On the other hand, in the regression analysis the spatial correlation between two points is expressed only as a function of depth. In cases where the variation of soil strength indicates a marked spatial trend with depth, the use of regression analysis will be a better choice.

Table 6.4
Comparison of the Statistical Parameters of s as
Obtained from Two Different Methods

Layers	Based on the Values Given in Table 6.1		Based on Regression Analysis	
	\bar{s} (ksf)	$\sqrt{\delta_s^2 + \Delta_0^2}$	\bar{s} (ksf)	$\sqrt{\delta_s^2 + \Delta_0^2}$
Upper clay layer	1.06	0.127	1.11	0.077
Middle clay layer	0.62	0.050	0.62	0.036
Lower clay layer	0.78	0.063	0.78	0.047

For this case study, the subsequent computations will be based on the values given in Table 6.1, where the inherent variability and the uncertainty associated with insufficient sampling are quantified separately.

6.2.3 Discrepancies Between Laboratory and In Situ Strengths

Among the various factors that contribute to the discrepancy between the laboratory-determined average undrained strength and the in situ average strength acting along the failure surface, the most important is the effect of mechanical disturbance during tube sampling. The suggested values given in Table 4.5 are combined with the additional data reported by Peck⁷⁹ to obtain the updated mean and coefficient of variation of $N_2(s)$, yielding $\bar{N}_2(s) = 1.38$ and $\Delta_2(s) = 0.024$ (see Section 2.3.2 for computations).

The Chicago clays have a medium sensitivity ($S_t \approx 4$). Hence, the value of \bar{N}_1 and Δ_1 are estimated to be 1.05 and 0.02, respectively (see Table 4.2).

The clays in the middle and lower layers are intact, whereas due to desiccation there exist some cracks and joints in the upper layer. Based on the values given in Table 4.8, it is estimated that for the fissured upper clay layer $\bar{N}_3 = 0.75$ and $\Delta_3 = 0.09$, and for the other two intact clay layers $\bar{N}_3 = 0.93$ and $\Delta_3 = 0.05$.

The slide at the Congress Street Open Cut occurred during excavation, and therefore failure was not delayed; still, the rate of shearing could have been much slower than that in laboratory tests. There is no information available on the effects of rate of shearing on the undrained shear strength of Chicago clays. Nevertheless, if the sensitivity to rate of shearing of the clays in the three layers is assumed to lie between slightly sensitive to

sensitive, then from Table 4.10 the range of $N_4(s)$ could be taken as 0.6 to 1.0. A uniform distribution over this range gives $\bar{N}_4 = 0.80$ and $\Delta_4 = 0.14$.

Skempton and Hutchinson,⁹⁹ in connection with their analysis of this failure, have indicated that Chicago clays probably show little variation in strength resulting from anisotropy. Therefore, from Table 4.12, assuming the isotropic case, one gets $\bar{N}_5 = 1.0$ and $\Delta_5 = 0.03$.

For the effect of plane strain, the mean correction and error for the three layers are taken to be $\bar{N}_6 = 1.05$ and $\Delta_6 = 0.03$ (see Section 4.2.6).

As far as the effect of progressive failure is concerned some reduction in the undrained strength could be expected. Based on the results of Section 4.2.7, it is assumed that $\bar{N}_7 = 0.93$ and $\Delta_7 = 0.03$ for the stiff upper clay layer, and $\bar{N}_7 = 0.97$ and $\Delta_7 = 0.03$ for the middle and lower clay layers.

Observe that \bar{N}_j 's and Δ_j 's, $j = 1, 2, 4, 5, 6$, are taken to be the same for all of the three layers, since all these layers consist of the same gritty blue clay. However, the upper clay layer differs from the middle and lower clay layers due to the presence of cracks and joints. Accordingly, different values of \bar{N}_j 's and Δ_j 's $j = 3, 7$, are taken for the upper clay layer from those of the middle and lower clay layers.

Based on these values, the mean correction and error are computed for each of the clay layers, including the uncertainty due to insufficient sampling. For the upper clay layer, Eq. 2.13 yields

$$\bar{N}_s = (1.05)(1.38)(0.75)(0.80)(1.0)(1.05)(0.93) = 0.85$$

and from Eq. 3.12

$$\begin{aligned}\Delta_s &= \sqrt{0.083^2 + 0.02^2 + 0.024^2 + 0.09^2 + 0.14^2 + 0.03^2 + 0.03^2 + 0.03^2} \\ &= 0.20\end{aligned}$$

Similarly, it is found that $\bar{N}_s = 1.10$ and $\Delta_s = 0.16$ for the middle clay layer, whereas $\bar{N}_s = 1.10$ and $\Delta_s = 0.17$ for the lower clay layer. Because of the additional information on the discrepancies between the in situ and laboratory undrained strengths, the total uncertainty for this site is smaller than those (0.21 to 0.24) for the general case considered in Section 4.4.

The resultant c.o.v. of the corrective factors that are the same for both the upper and middle clay layers is found to be $\Delta_{12}(s) = 0.15$, whereas $\Delta_{13}(s) = 0.15$ and $\Delta_{23}(s) = 0.16$. The subscripts 1, 2 and 3 refer respectively to the upper, middle and lower clay layers.

6.2.4 Consideration of the Cohesionless Layer

The resistance contributed by the layer of cohesionless material (sand and miscellaneous fill) is small compared to the total resistance of the other three cohesive layers. However, in order to have a complete analysis of this slide, the effect of the cohesionless layer will be taken into consideration. In Appendix G, the mean and c.o.v. of the resisting moment contributed by this layer are derived as (see Appendix G for the explanation of notations)

$$\mu_{M_{R_0}} \approx 1/2 \bar{N}_{P_0} \gamma_0 h_0^2 \bar{K}_0 \frac{1}{\cos(\beta_0 + \bar{\phi}_0)} \sin \bar{\phi}_0 r \quad (6.1)$$

$$\Omega_{M_{R_0}}^2 \approx \Omega_{P_0}^2 + \Omega_{K_0}^2 + [\cot \bar{\phi}_0 + \tan \alpha_0]^2 \bar{\phi}_0^2 \Omega_{\bar{\phi}_0}^2 \quad (6.2)$$

Based on a study for a similar case (Tang et al.¹⁰⁵), \bar{N}_p and Ω_p are estimated to be 0.80 and 0.20, respectively. The value of $\bar{\phi}_0$ is given as 30° (Ireland⁴³), and Ω_{ϕ_0} is estimated to be 0.05. Sowers and Sowers¹⁰² suggested that $K_0 = 0.6$ for loose sand and $K_0 = 0.4$ for dense sand. According to Terzaghi and Peck,¹⁰⁸ K_0 ranges from about 0.40 for dense sand to 0.50 for loose sand. Assuming a TT3 distribution between 0.4 to 0.6, $\bar{K}_0 = 0.5$ and $\Omega_{K_0} = 0.08$. The uncertainties associated with γ_0 and the dimensions describing the geometry of the slope and the failure surface (β_0 , h_0 , r) are small relative to the other variables in the analysis and are assumed to be negligible.

It will be assumed that there is no correlation between the soil parameters of the cohesionless layer and the soil parameters of the cohesive layers. Within the cohesionless layer, K_0 and ϕ_0 are assumed to be statistically independent. In reality, these are correlated because both ϕ_0 and K_0 depend on the relative density of the sand (Terzaghi and Peck¹⁰⁸).

6.2.5 Computation of Failure Probability

From Eqs. 3.14 and 6.1 the resultant mean resisting moment is expressed as

$$\mu_{M_R} = \bar{N}_f r \sum_{i=1}^3 \lambda_i \bar{N}_{s_i} \bar{s}_i + 1/2 \bar{N}_{p_0} \gamma_0 h_0^2 \bar{K}_0 \frac{1}{\cos(\beta_0 + \bar{\phi}_0)} \sin \bar{\phi}_0 r \quad (6.3)$$

where the first term consists of the total resistance from the three cohesive layers, and the second term denotes the resistance from the cohesionless layer.

Substitution of the respective values obtained earlier into Eq. 6.3 gives

$$\begin{aligned} \mu_{M_R} &= 902 + 1281 + 3804 + 125 \\ &= 5987 + 125 = 6112 \text{ kip-ft/ft} \end{aligned}$$

with only 2 percent of the resisting moment contributed by the cohesionless layer. The total uncertainty in M_R is obtained by combining Eqs. 3.17 and 6.2, giving $\Omega_{M_R} = 0.18$, where a resistance model uncertainty of 0.08 is assumed. Approximately 40 percent of $\Omega_{M_R}^2$ is contributed by the correlation among the cohesive layers, whereas the contribution by the uncertainty in the cohesionless layer is negligible (less than 0.1 percent of $\Omega_{M_R}^2$).

The overturning moment is due to the weight of the soil mass above the failure surface. The expected value of M_O is computed from Eq. 3.20a as 5164 kip-ft/ft. The uncertainty in density is assumed to be negligible compared to the other random variables in the analysis; hence, $\Omega_{M_O} = 0$.

The probability of failure for the estimated actual slip surface, therefore, becomes (assuming lognormal M_R)

$$\begin{aligned} p_f &= 1 - \Phi \left[\frac{\ln\left(\frac{6112}{5164}\right) - \frac{1}{2} 0.18^2}{0.18} \right] = 1 - \Phi(0.84) \\ &= 1 - 0.80 = 0.20 \end{aligned}$$

The failure probabilities for twelve other potential failure surfaces are also computed and given in the second column of Table 6.5. The failure probabilities are all high. In Fig. 6.4 it is observed that the most critical failure surface (No. 13) is not the same as the estimated actual slip surface (No. 1). This is not unexpected since $\phi = 0$ analysis generally will not lead

to a correct prediction of the actual shear surface (Skempton⁹²). Therefore, consistent with the $\phi = 0$ analysis, the failure probability for the slope is found to be 0.82 considering the most critical failure surface. This value is very high and agrees with the fact that the slope has actually failed.

Table 6.5
Failure Probabilities Computed from the
Original and New Slope Profiles

Potential Failure Surface Number (1)	P_f (Original Profile) (2)	P_f (New Profile) (3)
1	0.20	0.15×10^{-3}
2	0.42	0.11×10^{-2}
3	0.72	0.55×10^{-2}
4	0.60	0.12×10^{-2}
5	0.77	0.14×10^{-1}
6	0.71	0.24×10^{-2}
7	0.69	0.39×10^{-2}
8	0.70	0.22×10^{-2}
9	0.76	0.14×10^{-1}
10	0.11	0.12×10^{-5}
11	0.77	0.50×10^{-1}
12	0.68	0.11×10^{-1}
13	0.82	0.17×10^{-1}

6.2.6 Risk-Based Design

Suppose the probability of failure of the slope is desired to be

5 percent;^{*} this implies that none of the potential failure surfaces should have a probability of failure greater than 5 percent. A new slope profile is chosen (see Fig. 6.4), and the corresponding failure probabilities for each one of the potential failure surfaces are computed (see third column of Table 6.5). For the most critical failure surface (No. 11), $p_f = 5$ percent. Since this value is not greater than the specified risk level of 5 percent, the new profile is acceptable.

6.2.7 Design Using Recommended Mean Safety Factors

If there had been no detailed information available from the site, with the exception of the description of the soil, the slope could be designed by using the mean safety factors suggested in Table 4.18. In this slope, the clay is stiff-fissured in the upper layer and intact in the middle and lower layers; thus, according to Table 4.18, the recommended value of \bar{F} will be between 1.72 and 2.49 if a 99 percent reliability (i.e., $p_f = 10^{-2}$) is desired. A representative value of \bar{F} can be obtained from Eq. 4.2. Hence,

$$\begin{aligned}\bar{F} &= \left(\frac{1496}{8715}\right) 2.49 + \left(\frac{1681 + 5403}{8715}\right) 1.72 + \left(\frac{135}{8715}\right) 1.72 \\ &= 1.85\end{aligned}$$

where \bar{F} is taken to be 1.72 for the cohesionless layer. A design profile in this case should be chosen so that the value of \bar{F} for the most critical potential failure surface will be greater than 1.85. For example, if the new profile obtained in Section 6.2.6 is chosen (see Fig. 6.4), then the resisting and overturning moments for the most critical potential failure

^{*} This is approximately equivalent to requiring the minimum "actual" mean safety factor to be greater than 1.37 from Eq. 2.20. Considering that the design of this temporary slope will be based on the results of a failure analysis, this low value of the safety factor is acceptable.

surface (No. 11) of this profile are computed as 8715 kip-ft/ft and 6736 kip-ft/ft, respectively. Thus,

$$\bar{F} = \frac{8715}{6736} = 1.29 < 1.85$$

Therefore, this profile is not acceptable at a 99 percent reliability ($p_f = 10^{-2}$), and another slope profile with a smaller angle of inclination should be chosen.

By using the same procedure it is found that the new profile is not acceptable at a 95 percent reliability level either. It should be observed, however, that the analysis given in Section 6.2.6 with appropriate corrections for the method of analysis and local soil conditions indicates that the same profile is safe at a 95 percent reliability level (see third column of Table 6.5).

6.3 An Example of Long-Term Slope Stability: Landslide at Selset

6.3.1 General Information

Details of this slide have been published by Skempton and Brown.⁹⁴ The slide was a rotational landslide and the long-term conditions existed (Skempton⁹⁶). The slip was entirely within a deposit of heavily over-consolidated boulder clay, which was very uniform with no fissures and joints. The landslide took place in the south slope of the River Lune valley, which was 42 ft high with an inclination of 28°. The length of the slip was about 180 ft. Based on the six profiles of the slope, an average section through the slip was given by Skempton and Brown.⁹⁴ The exact location of the slip surface was not determined by the investigators; for this purpose, various

possible slip circles were examined. The average section of the slope and the most critical potential failure surface as given by Skempton and Brown⁹⁴ are shown in Fig. 6.5.

6.3.2 Inherent Variability and Error Due to Insufficient Sampling

Eight samples were taken at different locations of the slope. From each sample at least three specimens (1-1/2 in. diam. x 3 in.) were prepared, and the peak effective stress parameters were measured in slow drained triaxial tests on these specimens. Owing to the presence of occasional large stones, it was sometimes necessary to form the specimens by packing the material into brass tubes, without change in water content and with zero air voids. The values of the peak effective stress parameters obtained from these specimens and from the ones that are cut from the undisturbed cores are given in Table 6.6.

Table 6.6
Summary of Test Results at Selset

Sample	Depth (ft)	Bulk Density (lb/cu ft)	Drained Shear Strength Parameters \hat{c} (ksf) $\hat{\phi}$		Undisturbed or Remoulded
a	3	140	0.17	34°	Remoulded
b	9	135	0.20	32°	Undisturbed
c	25	141	0.08	34°	Remoulded
d	42	134	0.19	29°	"
e	12	141	0.27	33°	Undisturbed
f	6	139	0.12	32°	"
g	10	140	0.26	30°	Remoulded
h	9	141	0.16	32°	"

Based on these data, the specimens cut from the undisturbed cores yield

$$\bar{c} = 0.197 \text{ ksf}$$

$$\sigma_c = 0.0613 \text{ ksf}$$

$$\bar{\phi} = 32.3^\circ$$

$$\sigma_\phi = 0.6^\circ$$

whereas from the remoulded specimens

$$\bar{c} = 0.172 \text{ ksf}$$

$$\sigma_c = 0.058 \text{ ksf}$$

$$\bar{\phi} = 31.8^\circ$$

$$\sigma_\phi = 2.0^\circ$$

To check whether there is a significant difference between the two sets of data, the differences in the sample means of the strength parameters are tested at a 5 percent significance level. No significant difference is found between the two sample means of c and ϕ at a 5 percent significance level. Thus, the two sets of data are combined and the following values are obtained for the entire stratum of the boulder clay:

$$\bar{c} = 0.181 \text{ ksf}$$

$$\bar{\phi} = 32^\circ$$

$$\sigma_c = 0.060 \text{ ksf}$$

$$\sigma_\phi = 1.7^\circ$$

$$\delta_c = 0.33$$

$$\delta_\phi = 0.05$$

The average unit weight of the boulder clay is computed to be 0.139 kip/cu ft with a c.o.v. of 0.02.

If the spatial correlation for C and ϕ are given by Eq. 3.8, then the value of n_e obtained from Fig. 3.2 corresponding to $L = 104$ ft will be very large compared to $n_s = 8$ (for example, $n_e = 72$ for $v = 0.10$ and $n_e = 315$ for $v = 0.30$). Therefore, δ_c and δ_ϕ may be neglected in computing Ω_c and Ω_ϕ .

The uncertainties associated with insufficient sampling are computed to be

$$\Delta_0(c) = \frac{0.33}{\sqrt{8}} = 0.117$$

$$\Delta_0(\phi) = \frac{0.05}{\sqrt{8}} = 0.018$$

$$\Delta_0(\gamma) = \frac{0.02}{\sqrt{8}} = 0.007$$

6.3.3 Discrepancies Between Laboratory and In Situ Strengths

For this site Skempton and Brown⁹⁴ indicated that the effect of disturbance due to sampling is not significant. The comparison of the strength parameters (c and ϕ) obtained from remoulded specimens and undisturbed cores also shows that this effect is rather small. Based on the results of Section 5.2.1, it is estimated that $\bar{N}_1(c) = \bar{N}_1(\phi) = 1.0$, $\bar{N}_2(\phi) = 1.10$, $\bar{N}_2(c) = 1.15$ and $\Delta_1(c) = \Delta_1(\phi) = 0$, $\Delta_2(\phi) = 0.05$, $\Delta_2(c) = 0.08$.

The boulder clay at Selsset was intact; therefore, from Table 5.2 $\bar{N}_3(c) = 0.93$, $\Delta_3(c) = 0.05$ and $\bar{N}_3(\phi) = 1.0$, $\Delta_3(\phi) = 0$. Skempton and Hutchinson,⁹⁹ in studying this landslide have reported that "the strength of this type of clay would presumably be little influenced by the rate of shearing, and anisotropy may well be insignificant." Thus, based on the results given in Section 5.2.3 and 5.2.4 it is estimated that $\bar{N}_4(c) = \bar{N}_4(\phi) = 0.87$, $\Delta_4(c) = \Delta_4(\phi) = 0.11$, and $\bar{N}_5(c) = \bar{N}_5(\phi) = 0.98$, $\Delta_5(c) = \Delta_5(\phi) = 0.04$. For the effect of plane strain, the following values are taken (see Section 5.2.5): $\bar{N}_6(c) = 1.0$, $\Delta_6(c) = 0.04$ and $\bar{N}_6(\phi) = 1.08$, $\Delta_6(\phi) = 0.04$.

Using these values in Eqs. 3.39, 3.41, 3.45 and 3.46 gives $\bar{N}_c = 0.91$, $\Delta_c = 0.17$ and $\bar{N}_\phi = 1.01$, $\Delta_\phi = 0.14$. Hence, from Eqs. 3.40a and 3.44a

$$\Omega_c \approx \Delta_c = 0.17$$

$$\Omega_\phi \approx \Delta_\phi = 0.14$$

In this intact, non-fissured clay, the reduction of the peak strength due to the influence of progressive failure is expected to be small. From Table 5.9, for this first-time slide, \bar{N}_{s_f} is taken as 0.95 and Δ_{s_f} as 0.04.

6.3.4 Uncertainty Associated with Pore Pressure Distribution

Based on shallow piezometers and open boreholes, the free water surface was well defined. The water level was practically at the ground surface, except at the top of the slope. Field observations at this site indicated that the rock was more permeable than the boulder clay. Since the available information was not sufficient to construct an accurate flow net, two flow

net patterns corresponding to two extreme conditions were suggested by Skempton and Brown⁹⁴ (see Fig. 6.6):

- a. Rock is of the same permeability as the boulder clay (Flow net A),
- b. Rock is infinitely permeable as compared with the boulder clay (Flow net B).

These two assumptions do not cause great differences in the pore pressures in the region of slope failure, since the flow nets in this area are controlled mainly by the free water surface which coincides with the ground surface in the lower two-thirds of the slope. In addition to the two flow nets, two other simple ground water conditions have also been analyzed as indicated by Skempton and Brown:⁹⁴

- c. Horizontal flow,
- d. Flow parallel to the slope, which leads to an extreme upper limit for stability.

The failure probability of the slope will be computed using the flow net B, which gives $\bar{M}_R(\hat{u}) = 61.9r$ kip-ft/ft. The mean resisting moments corresponding to the other three different pore pressure distributions are given in Table 6.7. The correction for pore pressure, N_u , as computed from Eq. 5.4 ranges from 0.91 to 1.10 (see Table 6.7). A uniform distribution over this range gives $\bar{N}_u = 1.005$ and $\Delta_u = 0.06$.

6.3.5 Computation of the Failure Probability

The mean resisting moment based on flow net B is computed from Eq. 3.50 as

Table 6.7

Mean Resisting Moments Corresponding to Different
Pore Pressure Distributions

Assumed Pore Pressure Distribution	$\mu_{M_R}(u)$ (kip-ft/ft)	$N_u = \frac{\mu_{M_R}(u)}{M_R(\hat{u})}$
Flow net A (Case a)	65.3r	1.05
Horizontal flow (Case c)	56.5r	0.91
Flow parallel to slope (Case d)	68.1r	1.10

$$\begin{aligned}
 \mu_{M_R} &= (1.16)(1.005)(0.95)r[0.91 \times 0.181 \times 104' \\
 &\quad + \tan(1.01 \times 32^\circ) \times 62.19] \\
 &= 1.108r(17.1 + 39.2) = (1.108)(56.3r) \\
 &= 62.4r \text{ kip-ft/ft}
 \end{aligned}$$

and the total uncertainty from Eq. 3.56 is

$$\begin{aligned}
 \Omega_{M_R}^2 &= 0.11^2 + 0.06^2 + 0.04^2 + \frac{r^2}{(56.3r)^2} [17.1^2 \times 0.17^2 \\
 &\quad + 49.1^2 \times 0.14^2] \\
 &= 0.0173 + \frac{1}{56.3^2} (8.45 + 47.25) = 0.0173 + 0.0175 \\
 &= 0.0348
 \end{aligned}$$

$$\Omega_{M_R} \approx 0.19$$

The expected value of M_0 is computed from Eq. 3.57, yielding 61.21r kip-ft/ft, whereas $\Omega_{M_0} = \Omega_Y = 0.007$ is negligible. The depth of the tension crack is given as 4.5 ft. Only a very small portion of the crack is below the free water surface and, therefore, the moment due to the force of the water pressure in the crack ($=0.005r$ kip-ft/ft) is negligible compared to the overturning moment due to the weight of the soil.

The failure probability for the most critical sliding surface, from Eq. 2.19, is

$$p_f = 1 - \Phi \left[\frac{\ln \left(\frac{62.4r}{61.21r} \right) - \frac{1}{2} 0.19^2}{0.19} \right]$$

$$= 1 - \Phi(0.001) = 0.50$$

The failure probability above is quite high, and since the slide has actually failed, we can say that this result is consistent with the observation; in other words, with such a high failure probability, failure should be expected.

6.3.6 Risk-Based Design

Suppose this slope is to be designed for a risk of 1 percent. In this case the desired reliability level of 0.99 may be attained by reducing the neutral stresses through adequate drainage. The corresponding intensity of the pore pressure can be computed by using the same corrected data as follows:

From Eq. 2.20, the required mean resisting moment is

$$\begin{aligned}
\mu_{M_R} &= 61.21r \exp [\phi^{-1}(1.0 - 0.01)0.19 + \frac{1}{2} \times 0.19^2] \\
&= 61.21r \exp (0.458) = 61.21r \times 1.58 \\
&= 97r \text{ kip-ft/ft}
\end{aligned} \tag{6.4}$$

but, from Eq. 3.50

$$\mu_{M_R} = 1.108r [17.1 + \tan (32.3^\circ) (\sum_{i=1}^9 \bar{w}_i \cos \theta_i - \sum_{i=1}^9 \bar{u}_i \ell_i)] \tag{6.5}$$

From Eqs. 6.4 and 6.5

$$97r = 1.108r [17.1 + 0.630 (130.1 - \sum_{i=1}^9 \bar{u}_i)]$$

$$\sum_{i=1}^9 \bar{u}_i = 18.4 \text{ kip/ft}$$

In the case of no drainage, from flow net B,

$$\sum_{i=1}^9 \bar{u}_i = 67.9 \text{ kip/ft}$$

Therefore, a 72 percent reduction in the intensity of pore pressure is necessary for a reliability of 0.99. Well systems and horizontal drains could be used to control the ground water and seepage conditions within the slope, and thus achieve the required reduction in the pore pressure. For more information about slope stabilization with drainage, the reader is referred to Cedergren.²¹

6.3.7 Design Using Recommended Mean Safety Factors

For this site, $\eta = 0.48$; thus, the recommended computed mean safety

factor corresponding to $p_f = 10^{-2}$ is about 1.59 (see Table 5.14). The required intensity of pore pressure for $\bar{F} = 1.59$ can be obtained from

$$\bar{F} = 1.59 = \frac{[\bar{c}L + \tan \bar{\phi} (\sum_{i=1}^9 \bar{W}_i \cos \theta_i - \sum_{i=1}^9 \bar{U}_i)]r}{\bar{M}_0}$$

The substitution of the respective values indicates that a 91 percent (versus 72 percent obtained in Section 6.3.6 where the required corrections were made based on a detailed evaluation of the available data) reduction in the intensity of pore pressure is necessary for a reliability of 0.99.

Chapter 7

SUMMARY AND CONCLUSIONS

Probabilistic and statistical methods are used to develop a procedure by which the risk of failure may be systematically analyzed and incorporated into the practical design of slopes. The proposed probabilistic procedure provides a consistent method for the modeling, analysis and updating of uncertainties that are involved in the stability analysis of earth slopes. The available data and reported research results, together with experience, supply valuable information for determining realistic measures of uncertainties.

The safety of a particular slope is found to depend not only on the inherent variability of the shear strength parameters, but also on the uncertainties in the assessment of their in situ values along the potential failure surface and any simplifying assumptions used in the slope stability analysis.

On the basis of the results of the preceding chapters, the following conclusions can be made:

1. In the short-term stability of slopes, the uncertainties are due mainly to the incomplete knowledge of the in situ value of the average undrained shear strength along the potential failure surface. The total uncertainty in the spatial average undrained strength, measured in terms of the c.o.v. Ω_s , is estimated to be between 0.14 to 0.25, depending on the degree of soil exploration.
2. The safety of long-term stability of slopes should consider also the errors associated with the approximations in the method of analysis and the inaccuracies in the estimation of the pore

pressure distribution. The total uncertainty in the resisting moment M_R is estimated to be between 0.17 to 0.29 for first-time slides and is about 0.19 to 0.29 for slopes on pre-existing slides depending on the degree of soil exploration.

3. For slopes in stiff-fissured clays, it is observed that the resisting moment, computed on the basis of the peak shear strength parameters without any corrections for the systematic biases in the design variables and equations, significantly overestimates the actual resistance that can be mobilized in the field. For first-time slides this difference is about 26 to 44 percent, whereas for slopes on pre-existing slides it is about 55 percent. Due to the compensating effect of various factors, this discrepancy is somewhat smaller for first-time slides in intact clays.
4. For slopes in which the weight of the soil mass above the sliding surface is the only external load, the uncertainty in the overturning moment is small relative to that in the resisting moment; thus, the overturning moment M_O may be treated as a deterministic quantity in the reliability analysis.
5. The risk level of present slope design (with recommended minimum safety factors of 1.3 to 1.5 defined in terms of the lowest quartile values of the strength parameters) is found to vary between 0.006 percent to 4 percent for short-term stability, whereas with the safety factor of 1.5 the failure probabilities for long-term stability range between 0.06 percent to 1.6 percent. These failure probabilities are obtained assuming that the various

corrections required in the estimation of the resisting moment have been considered. If these corrections are not considered, designs using simply the laboratory-measured strength parameters may yield much higher failure probabilities.

6. If laboratory-measured average values are to be used directly in design, mean safety factors between 1.4 to 4.5 will be required to achieve a reliability of 99.9 percent.

LIST OF REFERENCES

1. Ang, A. H.-S. and B. R. Ellingwood, "Critical Analysis of Reliability Principles Relative to Design," Proceedings, International Conference on Application of Statistics and Probability to Soil and Structural Engineering, Hong Kong, September 1971.
2. Ang, A. H.-S., "Probabilistic Bases of Safety, Performance, and Design," Proceedings, Speciality Conference on Safety and Reliability of Metal Structures, ASCE, Pittsburgh, Pennsylvania, November 1972.
3. Ang, A. H.-S., "Engineering Risk Analysis and Risk-Based Design," Proceedings, Journal of the Structural Division, ASCE (to be published).
4. Benjamin, J. R. and C. A. Cornell, Probability, Statistics, and Decision for Civil Engineers, McGraw-Hill, New York, 1970.
5. Biernatowski, K., "Stability of Slopes in Probabilistic Solution," Proceedings, Seventh International Conference on Soil Mechanics and Foundation Engineering, Mexico City, Vol. 2, 1969.
6. Bishop, A. W., "The Use of the Slip Circle in the Stability Analysis of Slopes," Geotechnique, Vol. 5, No. 1, 1955.
7. Bishop, A. W., "Discussion on the Soil Properties and Their Measurements," Proceedings, Fourth International Conference on Soil Mechanics and Foundation Engineering, London, Vol. 3, 1957.
8. Bishop, A. W. and L. Bjerrum, "The Relevance of the Triaxial Test to the Solution of the Stability Problems," Proceedings, Research Conference on Shear Strength of Cohesive Soils, ASCE, Boulder, Colorado, June 1960.
9. Bishop, A. W. and D. J. Henkel, The Measurement of Soil Properties in the Triaxial Test, Edward Arnold Ltd., London, 1962.
10. Bishop A. W., D. L. Webb and P. I. Lewin, "Undisturbed Samples of London Clay from the Ashford Common Shaft: Strength-Effective Stress Relationships," Geotechnique, Vol. 15, No. 1, 1965.
11. Bishop, A. W., "The Strength of Soils as Engineering Materials," Sixth Rankine Lecture, Geotechnique, Vol. 16, No. 2, 1966.
12. Bishop, A. W., "Progressive Failure with Special Reference to the Mechanism Causing It," Proceedings, Geotechnical Conference, Oslo, Vol. 2, 1967.
13. Bishop, A. W. and A. L. Little, "The Influence of Size and Orientation of the Sample on the Apparent Strength of the London Clay at Maldon, Essex," Proceedings, Geotechnical Conference, Oslo, Vol. 1, 1967.

14. Bishop, A. W., "The Influence of Progressive Failure on the Choice of the Method of Stability Analysis," Geotechnique, Vol. 21, No. 2, 1971.
15. Bishop A. W., G. E. Green, V. K. Garga, A. Andresen and J. D. Brown, "A New Ring Shear Apparatus and Its Application to the Measurement of Residual Strength," Geotechnique, Vol. 21, No. 4, 1971.
16. Bjerrum, L. and B. Kjaernsli, "Analysis of the Stability of Some Norwegian Natural Clay Slopes," Geotechnique, Vol. 7, No. 1, 1957.
17. Bjerrum, L., N. Simons and I. Torblaa, "The Effect of Time on the Shear Strength of a Soft Marine Clay," Proceedings, Conference on Earth Pressure Problems, Brussels, Vol. 1, 1958.
18. Bjerrum, L., "Progressive Failure in Slopes of Over-Consolidated Plastic Clay and Clay Shales," Proceedings, Journal of Soil Mechanics and Foundations Division, ASCE, Vol. 93, No. SM5, 1967.
19. Cadling, L. and S. Odenstad, "The Vane Borer," Proceedings, Royal Swedish Geotechnical Institute, No. 2, 1950.
20. Casagrande, A. and S. D. Wilson, "Effect of Rate of Loading on the Strength of Clays and Shales at Constant Water Content," Geotechnique, Vol. 2, No. 3, 1951.
21. Cedergren, H. R., Seepage, Drainage, and Flow Nets, John Wiley and Sons Inc., New York, 1968.
22. Cornell, C. A., "First-Order Uncertainty Analysis of Soils Deformation and Stability," Proceedings, International Conference on Application of Statistics and Probability to Soil and Structural Engineering, Hong Kong, September 1971.
23. Costello, J. F. and J. G. Laguros, "Probability and Economical Foundations," Proceedings, International Conference on Application of Statistics and Probability to Soil and Structural Engineering, Hong Kong, September 1971.
24. Cozzolini, E.V.M., "Statistical Forecasting of Compression Index," Proceedings, Fifth International Conference on Soil Mechanics and Foundation Engineering, Paris, Vol. 1, 1961.
25. Crawford, C. B. and W. J. Eden, "Stability of Natural Slopes in Sensitive Clay," Proceedings, Journal of the Soil Mechanics and Foundations Division, ASCE, Vol. 93, No. SM4, 1967.
26. Dickey, J. W., C. C. Ladd and J. J. Rixner, "A Plane Strain Shear Device for Testing Clays," C. R. No. 3-101, U.S. Army Engineer Waterways Experiment Station, Vicksburg, Mississippi, January 1968.

27. Duncan, J. M. and H. B. Seed, "Anisotropy and Stress Reorientation in Clays," Proceedings, Journal of the Soil Mechanics and Foundations Division, ASCE, Vol. 92, No. SM5, 1966.
28. Duncan, J. M. and H. B. Seed, "Strength Variation Along Failure Surfaces in Clay," Proceedings, Journal of the Soil Mechanics and Foundations Division, ASCE, Vol. 92, No. SM6, 1966.
29. Duncan, J. M., "Undrained Strength and Pore-Water Pressures in Anisotropic Clays," Proceedings, Fifth Australia-New Zealand Conference on Soil Mechanics and Foundation Engineering, University of Auckland, New Zealand, 1967.
30. Duncan, J. M. and P. Dunlop, "Slopes in Stiff-Fissured Clays and Shales," C. R. No. S-68-4, U.S. Army Engineer Waterways Experiment Station, Vicksburg, Mississippi, June 1968.
31. Dunlop, P. and J. M. Duncan, "Development of Failure Around Excavated Slopes," Proceedings, Journal of Soil Mechanics and Foundations Division, ASCE, Vol. 96, No. SM2, 1970.
32. Ellingwood, B. R. and A. H.-S. Ang, "A Probabilistic Study of Safety Criteria for Design," Civil Engineering Studies, SRS No. 387, University of Illinois, Urbana, June 1972.
33. Esu, F., "Influence of Weathering on Behaviour of Stiff Clays; Structure of Clays; with Special Reference to Experience with Italian Clays," Panel Discussion, Session 2, Proceedings, Geotechnical Conference, Oslo, Vol. 2, 1967.
34. Feld, J., "The Factor of Safety in Soil and Rock Mechanics," Proceedings, Sixth International Conference on Soil Mechanics and Foundation Engineering, Montreal, Vol. 3, 1965.
35. Flaate, K. S., "Stresses and Movements in Connection with Braced Cuts in Sand and Clay," Ph.D. Thesis, Department of Civil Engineering, University of Illinois, Urbana, 1966.
36. Folayan, J. I., K. Höeg and J. R. Benjamin, "Decision Theory Applied to Settlement Predictions," Proceedings, Journal of the Soil Mechanics and Foundations Division, ASCE, Vol. 96, No. SM4, 1970.
37. Gibson, R. E. and D. J. Henkel, "The Influence of Duration of Tests at Constant Rate of Strain on Measured 'Drained' Strength," Geotechnique, Vol. 4, No. 1, 1954.
38. Henkel, D. J. and A. W. Skempton, "A Land-Slide at Jackfield, Shropshire, in a Heavily Over-Consolidated Clay," Geotechnique, Vol. 5, No. 2, 1955.
39. Henkel, D. J. and N. H. Wade, "Plane Strain Tests on a Saturated Remolded Clay," Proceedings, Journal of the Soil Mechanics and Foundations Division, ASCE, Vol. 92, No. SM6, 1966.

40. Holtz, R. D. and R. J. Krizek, "Statistical Evaluation of Soils Test Data," Proceedings, International Conference on Application of Statistics and Probability to Soil and Structural Engineering, Hong Kong, September 1971.
41. Hooper, J. A. and F. G. Butler, "Some Numerical Results Concerning the Shear Strength of London Clay," Geotechnique, Vol. 16, No. 4, 1966.
42. Hvorslev, M. J., "Physical Components of the Shear Strength of Saturated Clays," Proceedings, Research Conference on Shear Strength of Cohesive Soils, ASCE, Boulder, Colorado, June 1960.
43. Ireland, H. O., "Stability Analysis of the Congress Street Open Cut in Chicago," Geotechnique, Vol. 4, No. 4, 1954.
44. Jacobsen, M., "The Undrained Shear Strength of Preconsolidated Boulder Clay," Proceedings, Geotechnical Conference, Oslo, Vol. 1, 1967.
45. Jakobson, B., "The Landslide at Surte on the Göta River," Proceedings, Royal Swedish Geotechnical Institute, No. 5, 1952.
46. Jakobson, B., "Isotropy of Clays," Geotechnique, Vol. 5, No. 1, 1955.
47. Jumikis, A. R., "Factor of Safety in Foundation Engineering," HRB, Highway Research Record, No. 156, 1967.
48. Kay, J. N. and R. J. Krizek, "Estimation of the Mean for Soil Properties," Proceedings, International Conference on Application of Statistics and Probability to Soil and Structural Engineering, Hong Kong, September 1971.
49. Kenney, T. C., "The Influence of Mineral Composition on the Residual Strength of Natural Soils," Proceedings, Geotechnical Conference, Oslo, Vol. 1, 1967.
50. Kenney, T. C., "Shear Strength of Soft Clay," Proceedings, Geotechnical Conference, Oslo, Vol. 2, 1967.
51. Kinner, E. B. and C. C. Ladd, "Load-Deformation Behavior of Saturated Clays During Undrained Shear," C. R. No. 3-101, U.S. Army Engineer Waterways Experiment Station, Vicksburg, Mississippi, May 1970.
52. Kjaernsli, B. and N. Simons, "Stability Investigations of the North Bank of the Drammen River," Geotechnique, Vol. 12, No. 2, 1962.
53. Klein, G. K. and V. N. Karavaev, "Statistical Approach to the Selection of the Optimum Dimensions of Retaining Walls," Soil Mechanics and Foundation Engineering, Vol. 8, No. 1, August 1971.
54. Ladd, C. C. and T. W. Lambe, "The Strength of 'Undisturbed' Clay Determined from Undrained Tests," Proceedings, Symposium on Laboratory Shear Testing of Soils, ASTM Special Technical Publication No. 361, Ottawa, 1963.

55. Ladd, C. C., R. B. Bovee, L. Edgers and J. J. Rixner, "Consolidated-Undrained Plane Strain Shear Tests on Boston Blue Clay," C. R. No. 3-101, U.S. Army Engineer Waterways Experiment Station, Vicksburg, Mississippi, March 1971.
56. Ladd, C. C., Za-C. Moh and D. G. Gifford, "Statistical Analysis of Undrained Strength of Soft Bangkok Clay," Proceedings, International Conference on Application of Statistics and Probability to Soil and Structural Engineering, Hong Kong, September 1971.
57. La Gatta, D. P., "Residual Strength of Clays and Clay-Shales by Rotation Shear Tests," Harvard Soil Mechanics Series No. 86, Cambridge, Massachusetts, July 1970.
58. La Gatta, D. P., "The Effect of Rate of Displacement on Measuring the Residual Strength of Clays," C. R. No. S-71-5, U.S. Army Engineer Waterways Experiment Station, Vicksburg, Mississippi, August 1971.
59. Lambe, T. W. and R. V. Whitman, Soil Mechanics, John Wiley and Sons Inc., New York, 1969.
60. Langejan, A., "Some Aspects of the Safety Factor Considered as a Problem of Probability," Proceedings, Sixth International Conference on Soil Mechanics and Foundation Engineering, Montreal, Vol. 2, 1965.
61. Lo, K. Y., "Stability of Slopes in Anisotropic Soils," Proceedings, Journal of the Soil Mechanics and Foundations Division, ASCE, Vol. 91, No. SM4, Part 1, 1965.
62. Lo, K. Y., Closure of "Stability of Slopes in Anisotropic Soils," Proceedings, Journal of the Soil Mechanics and Foundations Division, ASCE, Vol. 92, No. SM4, 1966.
63. Lo, K. Y., "The Operational Strength of Fissured Clays," Geotechnique, Vol. 20, No. 1, 1970.
64. Lumb, P., "The Variability of Natural Soils," Canadian Geotechnical Journal, Vol. 3, No. 2, 1966.
65. Lumb, P., "Statistical Methods in Soil Investigations," Proceedings, Fifth Australia-New Zealand Conference on Soil Mechanics and Foundation Engineering, University of Auckland, New Zealand, 1967.
66. Lumb, P., "Safety Factors and Probability Distributions of Soil Strength," Canadian Geotechnical Journal, Vol. 7, No. 3, 1970.
67. Lumb, P., "Precision and Accuracy of Soil Tests," Proceedings, International Conference on Application of Statistics and Probability to Soil and Structural Engineering, Hong Kong, September 1971.

68. Lytton, R. L., "Risk Design of Stiffened Mats on Clay," Proceedings, International Conference on Application of Statistics and Probability to Soil and Structural Engineering, Hong Kong, September 1971.
69. Marsland, A., "Panel Discussion," Session 2, Proceedings, Geotechnical Conference, Oslo, Vol. 2, 1967.
70. Marsland, A. and M. E. Butler, "Strength Measurements on Stiff Fissured Barton Clay from Fawley (Hampshire)," Proceedings, Geotechnical Conference, Oslo, Vol. 1, 1967.
71. Meyerhof, G. G., "Safety Factors in Soil Mechanics," Canadian Geotechnical Journal, Vol. 7, No. 4, 1970.
72. Mood, A. M. and F. A. Graybill, Introduction to the Theory of Statistics, McGraw-Hill, Tokyo, 1963.
73. Morgenstern, N. R. and V. E. Price, "The Analysis of the Stability of General Slip Surfaces," Geotechnique, Vol. 15, No. 1, 1965.
74. Morgenstern, N. R., "Shear Strength of Stiff Clay," Proceedings, Geotechnical Conference, Oslo, Vol. 2, 1967.
75. Morse, R. K., "The Importance of Proper Soil Units for Statistical Analysis," Proceedings, International Conference on Application of Statistics and Probability to Soil and Structural Engineering, Hong Kong, September 1971.
76. Nelson, J. D., E. W. Brand and Ze-C. Moh, "A Probabilistic Approach to the Correction of Soil Strength," Proceedings, International Conference on Application of Statistics and Probability to Soil and Structural Engineering, Hong Kong, September 1971.
77. Nishida, Y., S. Wakamatsu and N. Oda, "Probability of Safety for Pile Foundations," Proceedings, International Conference on Application of Statistics and Probability to Soil and Structural Engineering, Hong Kong, September 1971.
78. Noorany, I. and H. B. Seed, "In-Situ Strength Characteristics of Soft Clays," Proceedings, Journal of the Soil Mechanics and Foundations Division, ASCE, Vol. 91, No. SM2, 1965.
79. Peck, R. B., "Sampling Methods and Laboratory Tests for Chicago Subway Soils," Proceedings, Purdue Conference on Soil Mechanics and Its Applications, Lafayette, Indiana, 1940.
80. Peck, R. B., "Earth Pressure Measurements in Open Cuts, Chicago Subway," Transactions, ASCE, Vol. 108, 1943.
81. Peck, R. B., "Bearing Capacity and Settlement: Certainties and Uncertainties," Proceedings, Symposium on Bearing Capacity and Settlement of Foundations, Duke University, North Carolina, 1967.

82. Peck, R. B., "Stability of Natural Slopes," Proceedings, Journal of the Soil Mechanics and Foundations Division, ASCE, Vol. 93, No. SM4, 1967.
83. Ranganatham, B. V., A. C. Sani and V. Sreenivasulu, "Strength Anisotropy on Slope Stability and Bearing Capacity of Clays," Proceedings, Seventh International Conference on Soil Mechanics and Foundation Engineering, Mexico City, Vol. 2, 1969.
84. Resendiz, D. and I. Herrera, "A Probabilistic Formulation of Settlement-Controlled Design," Proceedings, Seventh International Conference on Soil Mechanics and Foundation Engineering, Mexico City, Vol. 2, 1969.
85. Rosenblueth, E., "Discussions," Proceedings, Seventh International Conference on Soil Mechanics and Foundation Engineering, Mexico City, Vol. 3, Session 2, 1969.
86. Schultze, E., "Frequency Distributions and Correlations of Soil Properties," Proceedings, International Conference on Application of Statistics and Probability to Soil and Structural Engineering, Hong Kong, September 1971.
87. Scott, J. D., "Slope Failures in Over-Consolidated Fissured Clays in Southwestern Iowa," Ph.D. Thesis, University of Illinois, Champaign-Urbana, 1964.
88. Sevaldson, R. A., "The Slide at Lodalen, October 6th, 1954," Geotechnique, Vol. 6, No. 4, 1956.
89. Shuk, T., "Optimization of Footings in Compressible Soils," Proceedings, Seventh International Conference on Soil Mechanics and Foundation Engineering, Mexico City, Vol. 2, 1969.
90. Simons, N. E., "Discussions," Proceedings, Geotechnical Conference, Oslo, Vol. 2, 1967.
91. Singh, A., "How Reliable is the Factor of Safety in Foundation Engineering," Proceedings, International Conference on Application of Statistics and Probability to Soil and Structural Engineering, Hong Kong, September 1971.
92. Skempton, A. W., "The $\phi = 0$ Analysis of Stability and Its Theoretical Basis," Proceedings, Second International Conference on Soil Mechanics and Foundation Engineering Rotterdam, Vol. 1, 1948.
93. Skempton, A. W. and H. Q. Golder, "Practical Examples of the $\phi = 0$ Analysis of the Stability of Clays," Proceedings, Second International Conference on Soil Mechanics and Foundation Engineering, Rotterdam, Vol. 2, 1948.
94. Skempton, A. W. and J. D. Brown, "A Land-Slide in Boulder Clay at Selset, Yorkshire," Geotechnique, Vol. 11, No. 4, 1961.

95. Skempton, A. W. and V. A. Sowa, "The Behaviour of Saturated Clays During Sampling and Testing," Geotechnique, Vol. 13, No. 4, 1963.
96. Skempton, A. W., "Long-Term Stability of Clay Slopes," Geotechnique, Vol. 14, No. 2, 1964.
97. Skempton, A. W. and P. La Rochelle, "The Bradwell Slip: A Short-Term Failure in London Clay," Geotechnique, Vol. 15, No. 3, 1965.
98. Skempton, A. W., R. L. Schuster and D. J. Petley, "Joints and Fissures in the London Clay at Wraysbury and Edgware," Geotechnique, Vol. 19, No. 2, 1969.
99. Skempton, A. W. and J. N. Hutchinson, "Stability of Natural Slopes and Embankment Foundations," Proceedings, Seventh International Conference on Soil Mechanics and Foundation Engineering, Mexico City, State-of-the-Art Volume, 1969.
100. Skempton, A. W., "First-Time Slides in Over-Consolidated Clays," Geotechnique, Vol. 20, No. 3, 1970.
101. Sowers, G. F., "The Safety Factor in Excavations and Foundations," Paper sponsored by Ad Hoc Committee on Factors of Safety in Soil Engineering and presented at the 48th Annual Meeting, 1969.
102. Sowers, G. B. and G. F. Sowers, Introductory Soil Mechanics and Foundations, The MacMillan Co., New York, 1970.
103. Suklje, L. and S. Vidmar, "A Landslide Due to Long-Term Creep," Proceedings, Fifth International Conference on Soil Mechanics and Foundation Engineering, Paris, Vol. 2, 1961.
104. Tang, W. H., "A Bayesian Evaluation of Information for Foundation Engineering Design," Proceedings, International Conference on Application of Statistics and Probability to Soil and Structural Engineering, Hong Kong, September 1971.
105. Tang, W. H., M. S. Yucemen and A. H.-S. Ang, "Reliability Analysis and Design of Braced Excavation Systems," Proceedings, International Conference on Application of Statistics and Probability to Soil and Structural Engineering, Hong Kong, September 1971.
106. Tang, W. H. and A. H.-S. Ang, "Modeling, Analysis and Updating of Uncertainties," Preprint, ASCE National Structural Engineering Meeting, San Francisco, April 1973.
107. Taylor, D. W., Fundamentals of Soil Mechanics, John Wiley, New York, 1948.
108. Terzaghi, K. and R. B. Peck, Soil Mechanics in Engineering Practice, John Wiley, New York, 1968.

109. Turkstra, C. J., Theory of Structural Design Decisions, Solid Mechanics Division Study No. 2, University of Waterloo, Waterloo, Ontario, Canada, 1970.
110. Turkstra, C. J., "Applications of Bayesian Decision Theory," Structural Reliability and Codified Design, Solid Mechanics Division Study No. 3, University of Waterloo, Waterloo, Ontario, Canada, 1970.
111. Turnbull, W. J. and M. J. Hvorslev, "Special Problems in Slope Stability," Proceedings, Journal of the Soil Mechanics and Foundations Division, ASCE, Vol. 93, No. SM4, 1967.
112. Ward, W. H., S. G. Samuels and M. E. Butler, "Further Studies of the Properties of London Clay," Geotechnique, Vol. 9, No. 2, 1959.
113. Ward, W. H., A. Marsland and S. G. Samuels, "Properties of the London Clay at the Ashford Common Shaft: In-Situ and Undrained Strength Tests," Geotechnique, Vol. 15, No. 4, 1965.
114. Whitman, R. V. and P. J. Moore, "Thoughts Concerning the Mechanics of Slope Stability Analysis," Proceedings, Second Pan-American Conference on Soil Mechanics and Foundation Engineering, Brazil, Vol. 1, 1963.
115. Whitman, R. V. and W. A. Bailey, "Use of Computers for Slope Stability Analysis," Proceedings, Journal of the Soil Mechanics and Foundations Division, ASCE, Vol. 93, No. SM4, 1967.
116. Wolfskill, L. A. and T. W. Lambe, "Slide in the Siburua Dam," Proceedings, Journal of the Soil Mechanics and Foundations Division, ASCE, Vol. 93, No. SM4, 1967.
117. Wright, S. G. and J. M. Duncan, "Analyses of Waco Dam Slide," Proceedings, Journal of the Soil Mechanics and Foundations Division, ASCE, Vol. 98, No. SM9, 1972.
118. Wu, T. H. and L. M. Kraft, "Probability of Foundation Safety," Proceedings, Journal of the Soil Mechanics and Foundations Division, ASCE, Vol. 93, NO. SM5, 1967.
119. Wu, T. H. and L. M. Kraft, "Safety Analysis of Slopes," Proceedings, Journal of the Soil Mechanics and Foundations Division, ASCE, Vol. 96, No. SM2, 1970.
120. Wu, T. H. and L. M. Kraft, "Seismic Safety of Earth Dams," Proceedings, Journal of the Soil Mechanics and Foundations Division, ASCE, Vol. 96, No. SM6, 1970.

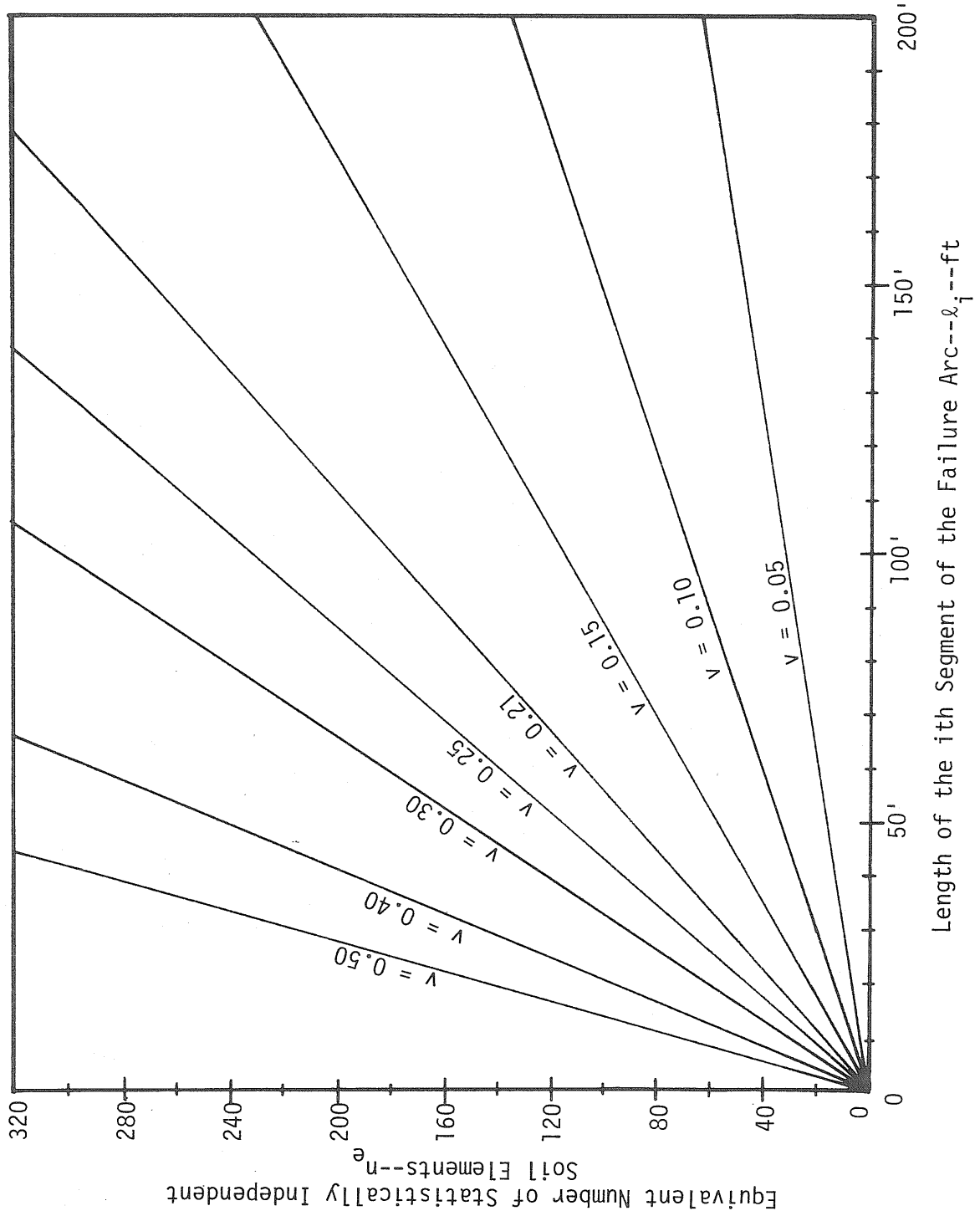


Fig. 3.2 Equivalent Number of Statistically Independent Soil Elements

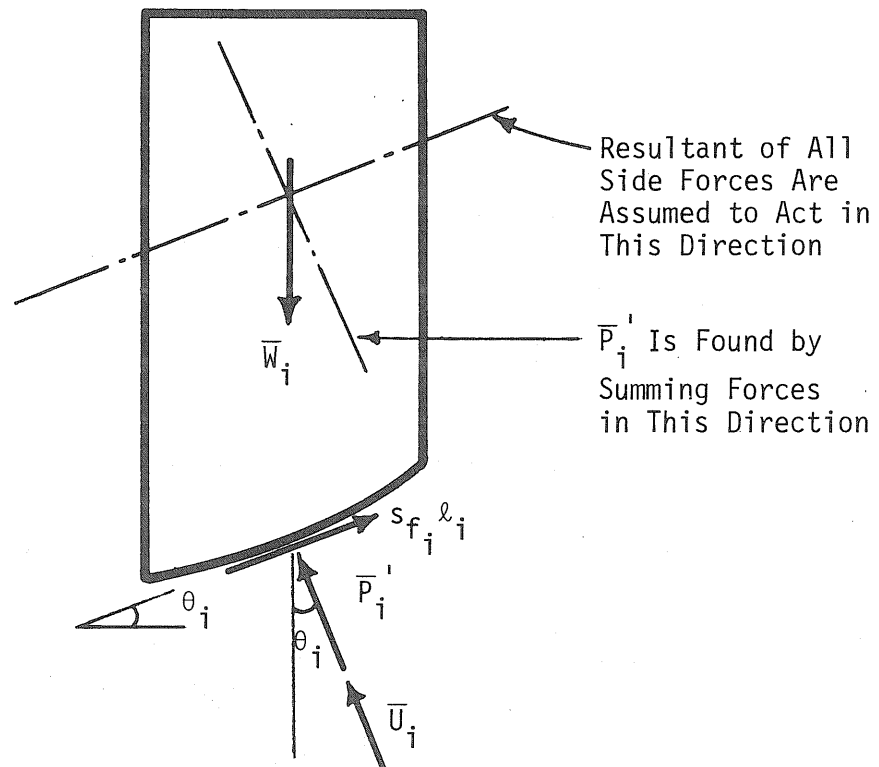


Fig. 3.3 Forces Considered in the Fellenius Method of Slices

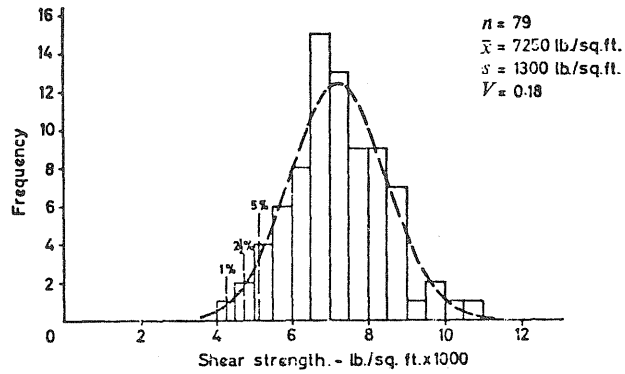


Fig. 4.1 A Typical Histogram for the Undrained Shear Strength of London Clay (From Hooper and Butler, Ref. 41)

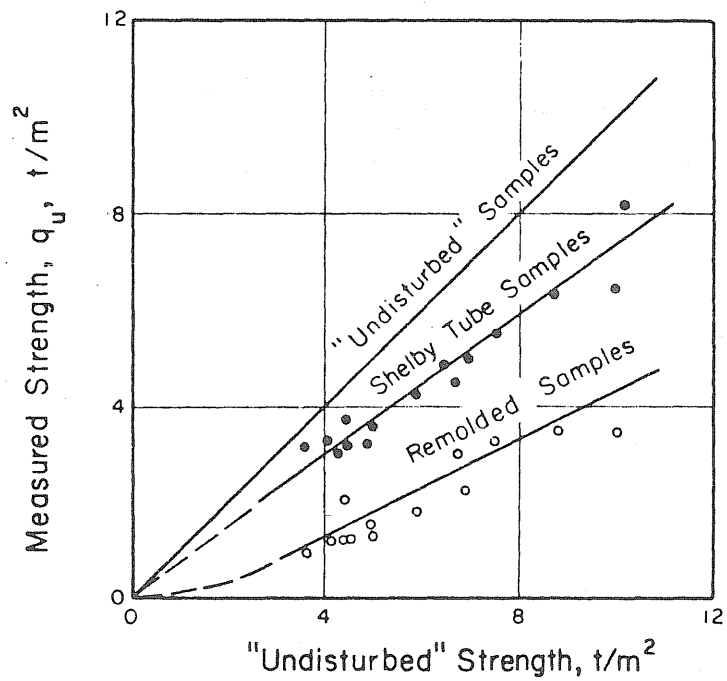


Fig. 4.2 Unconfined Compression Tests from Chicago Subway (Flaate, Ref. 35)

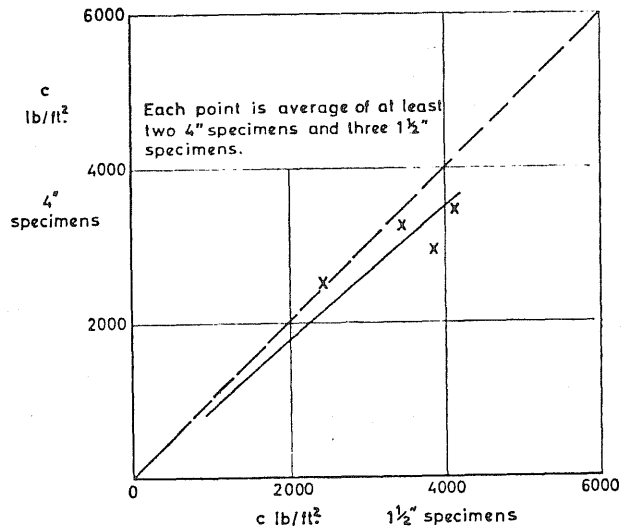


Fig. 4.3 Relation Between Undrained Strengths Measured on 4 in. x 8 in. and 1-1/2 in. x 3 in. Specimens for Brown London Clay at Kensal Green (From Skempton and La Rochelle, Ref. 97)

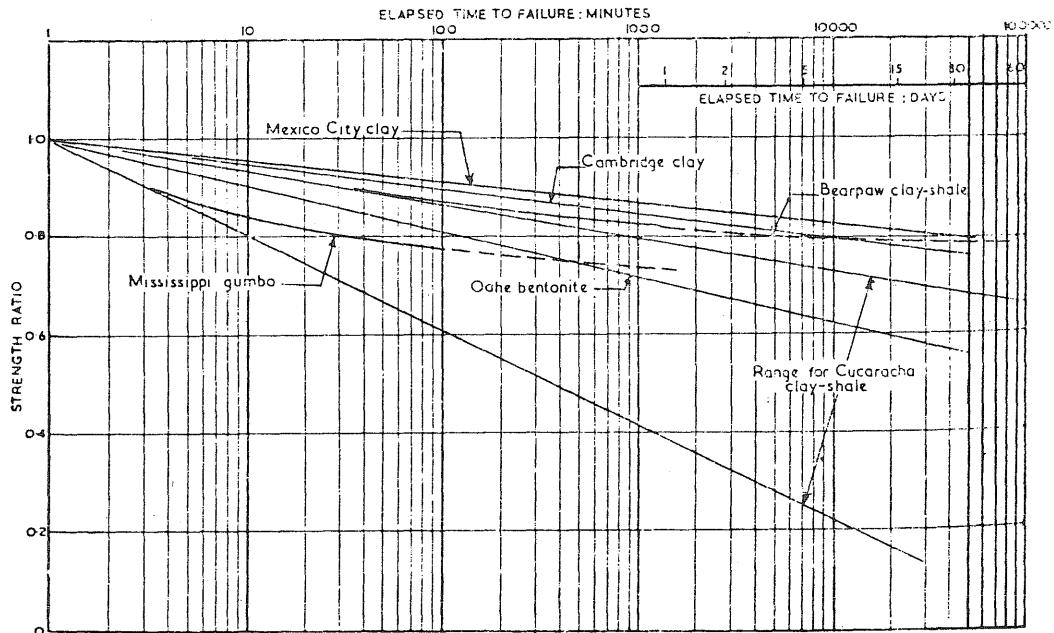


Fig. 4.4 Strength Ratio Versus Elapsed Time to Failure (From Casagrande and Wilson, Ref. 20)

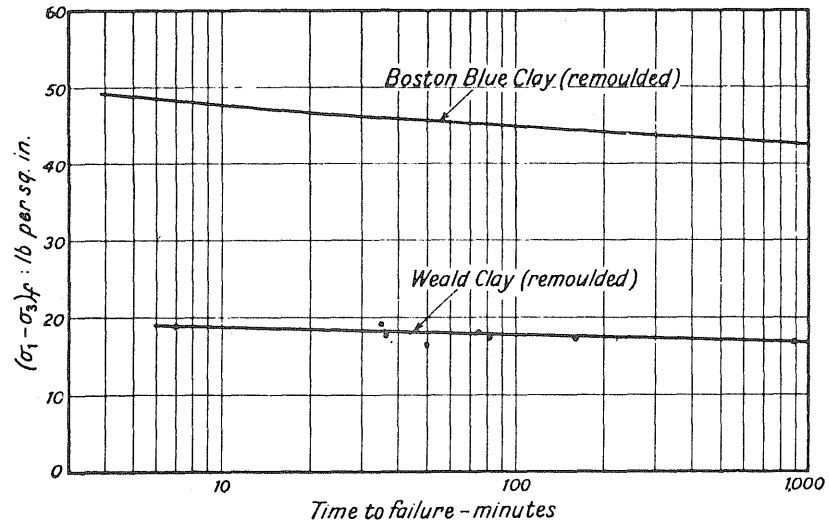
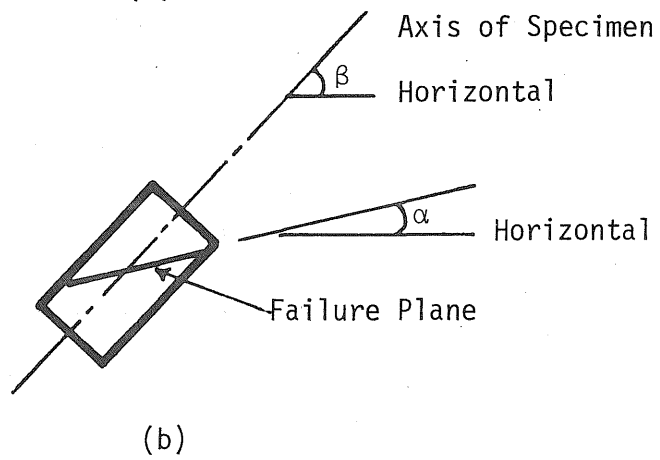
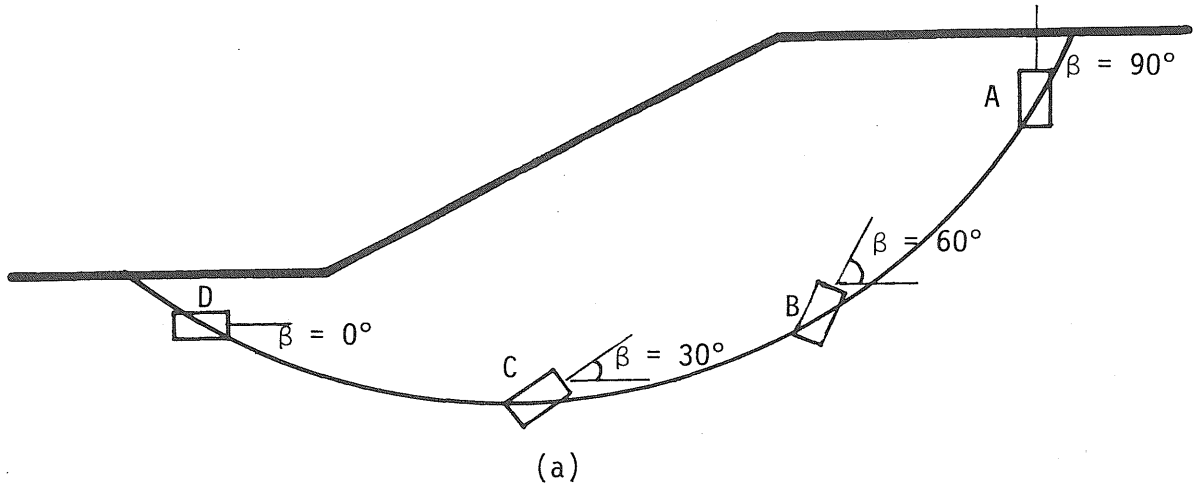


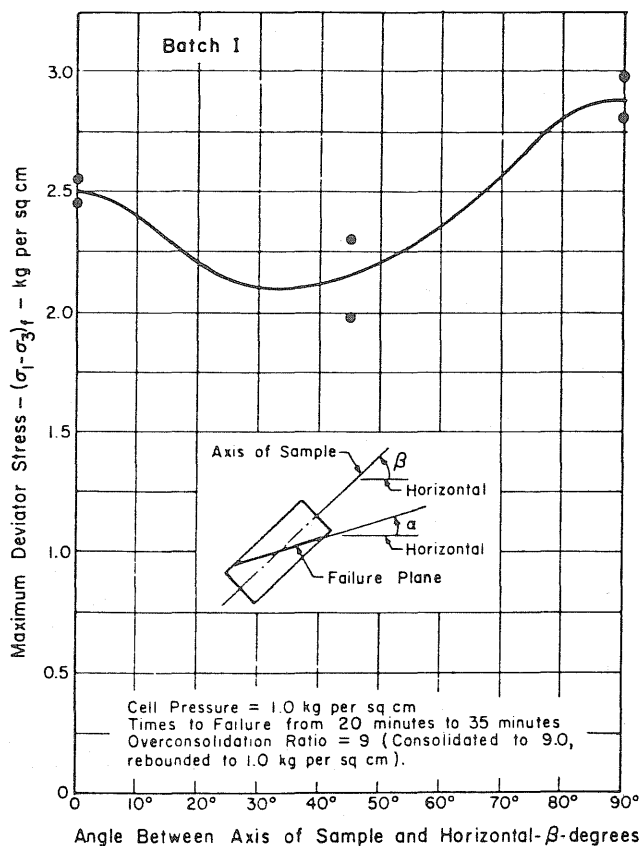
Fig. 4.5 The Variation in Strength with Time to Failure for Undrained Tests on Weald Clay and Boston Blue Clay (From Bishop and Henkel, Ref. 9)



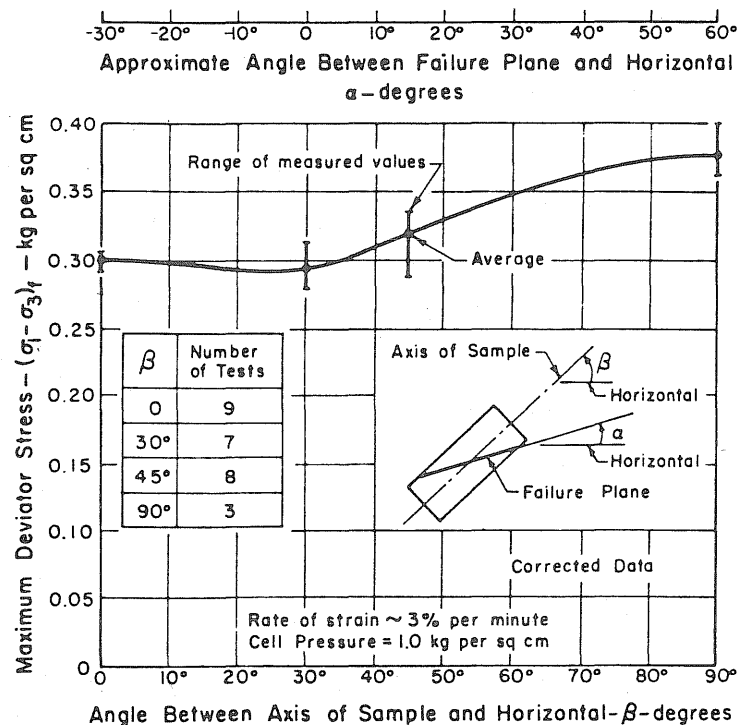
Location of Soil Element on the Failure Surface	α	β
A (top)	60°	90°
B	30°	60°
C	0°	30°
D (toe)	-30°	0°

(c)

Fig. 4.6 (a) Orientation of Specimens at Various Locations of the Failure Surface, (b) Definition of Geometric Parameters Related to the Orientation of Specimens, (c) Variation of α and β for a Typical Slip Circle



(a)



(b)

Fig. 4.7 Variation of Maximum Deviator Stress with Orientation of Failure Plane in UU Triaxial Tests: (a) for Over-Consolidated Kaolinite Clay (From Duncan and Seed, Ref. 27); (b) for Normally Consolidated San Francisco Bay Mud (From Duncan and Seed, Ref. 28)

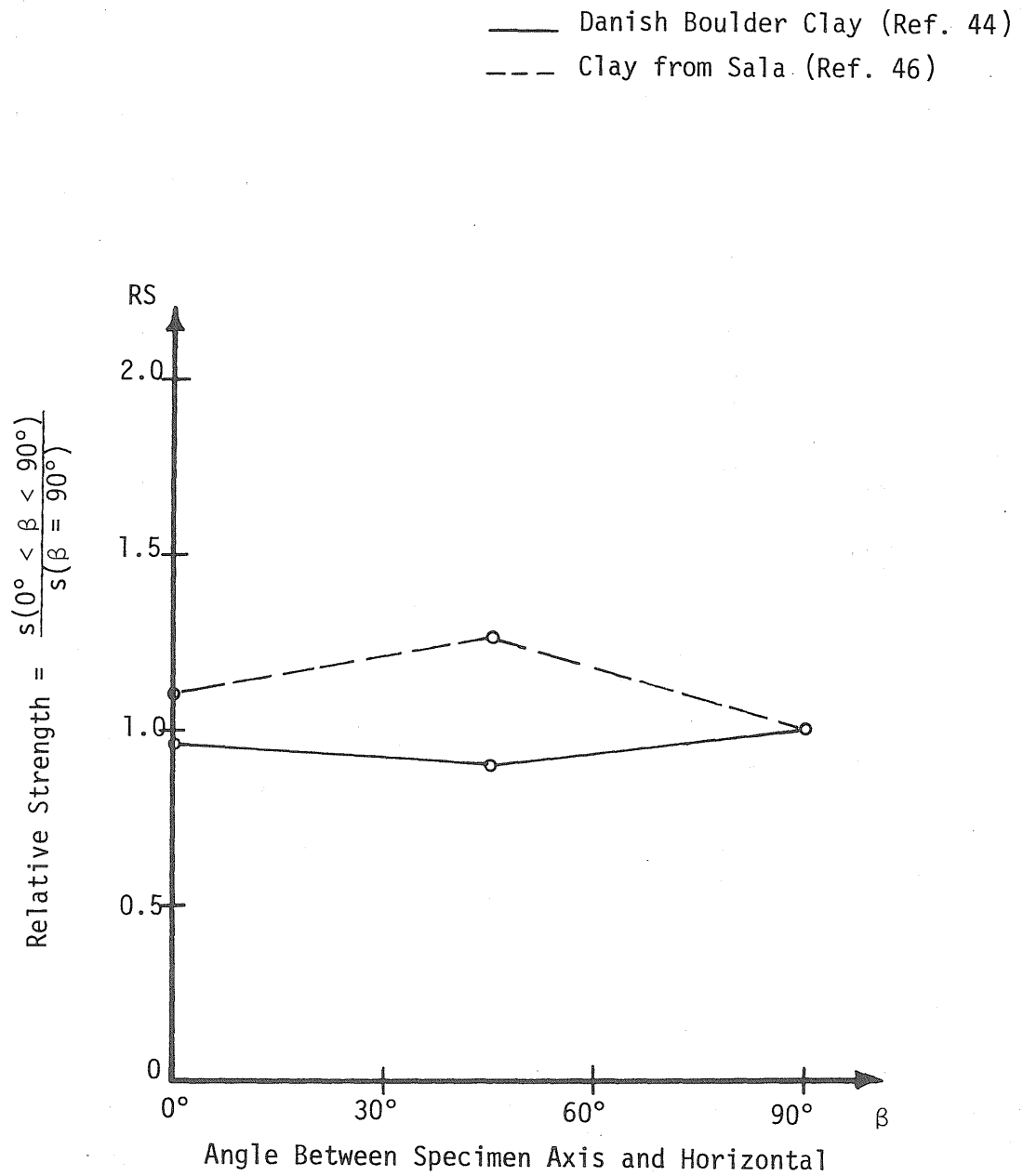


Fig. 4.8 Variation of Undrained Strength with Specimen Orientation (Isotropic Clays)

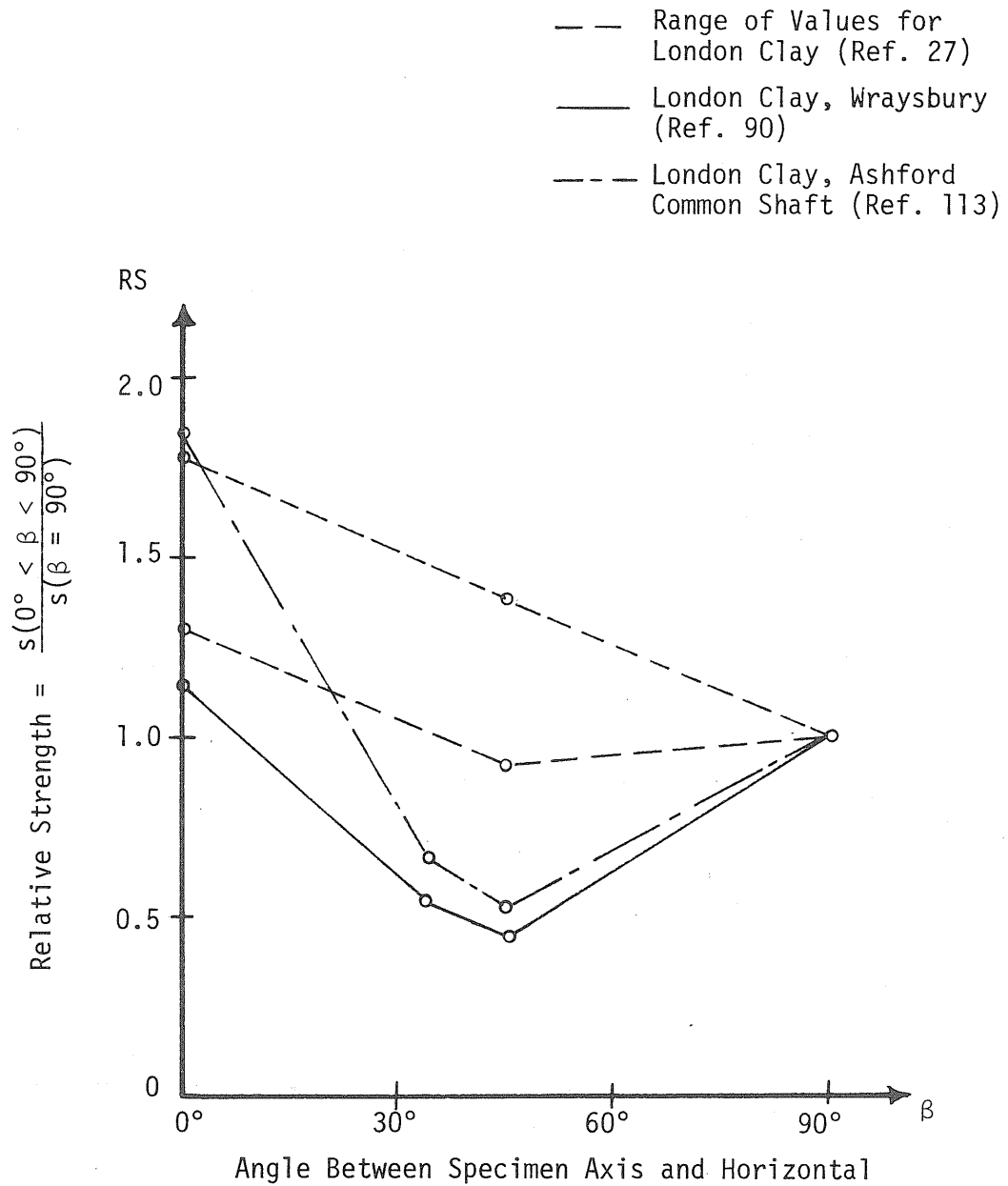


Fig. 4.9 Variation of Undrained Strength with Specimen Orientation (Clays with C-Anisotropy)

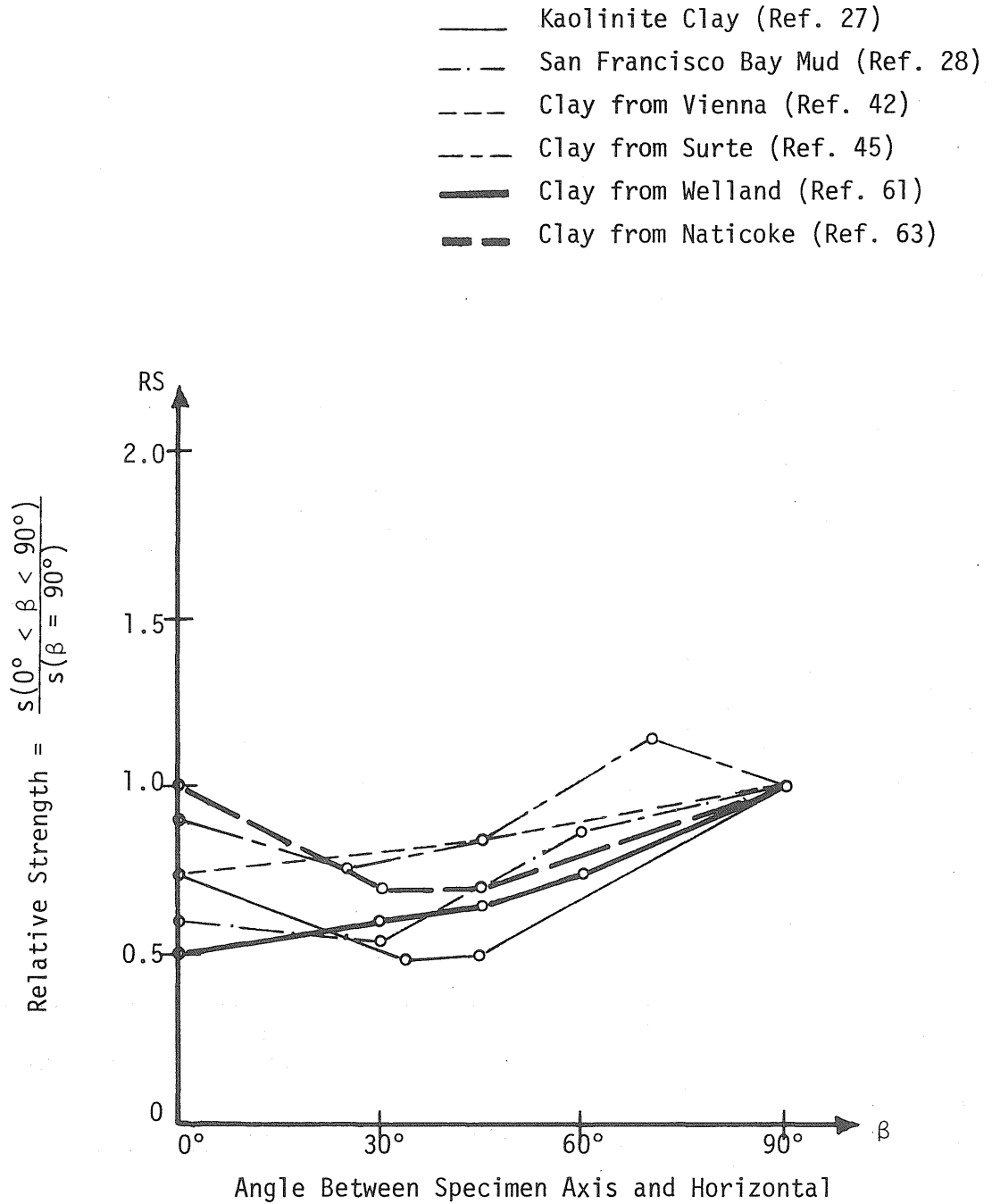


Fig. 4.10 Variation of Undrained Strength with Specimen Orientation (Clays with M-Anisotropy)

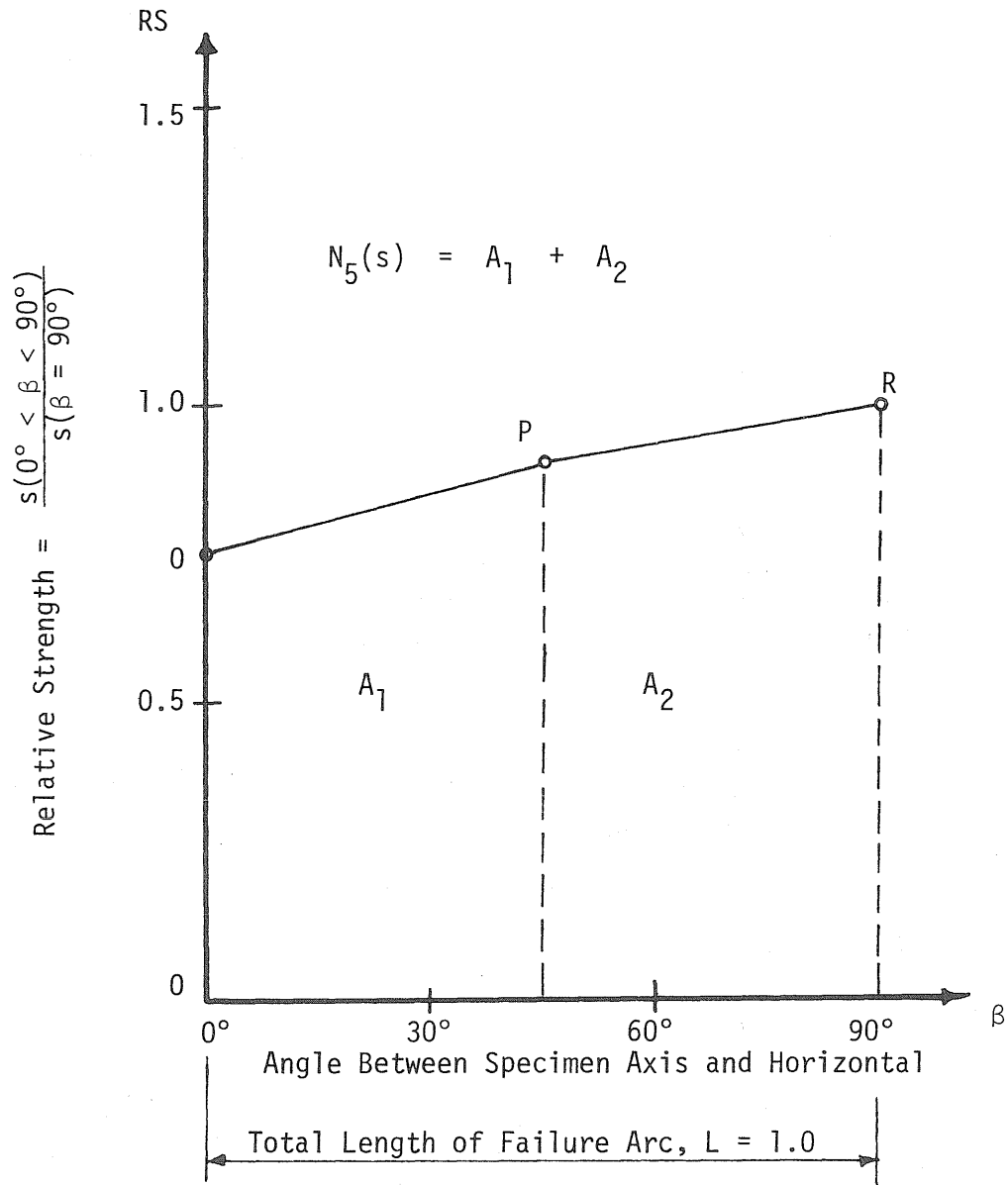
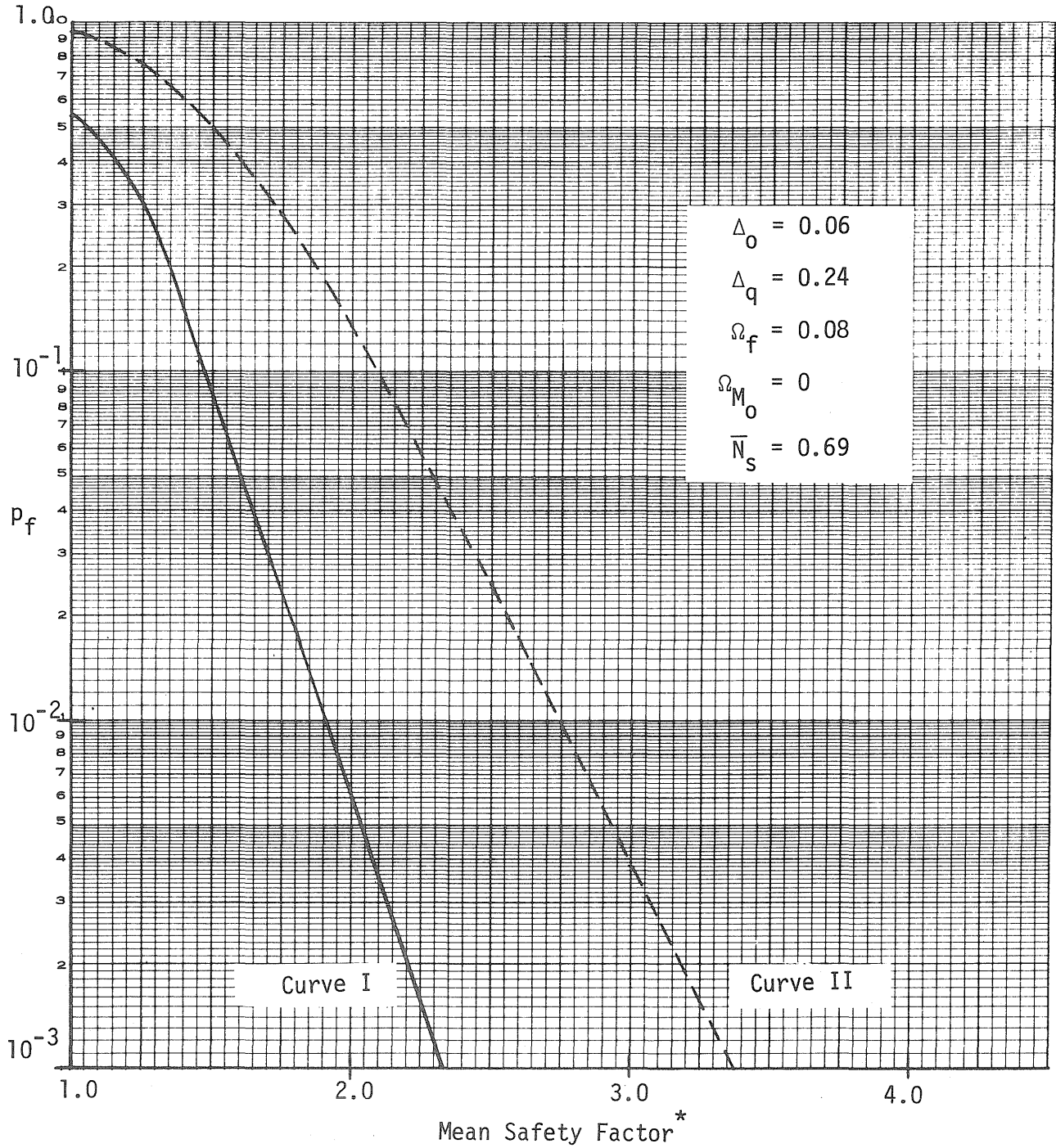


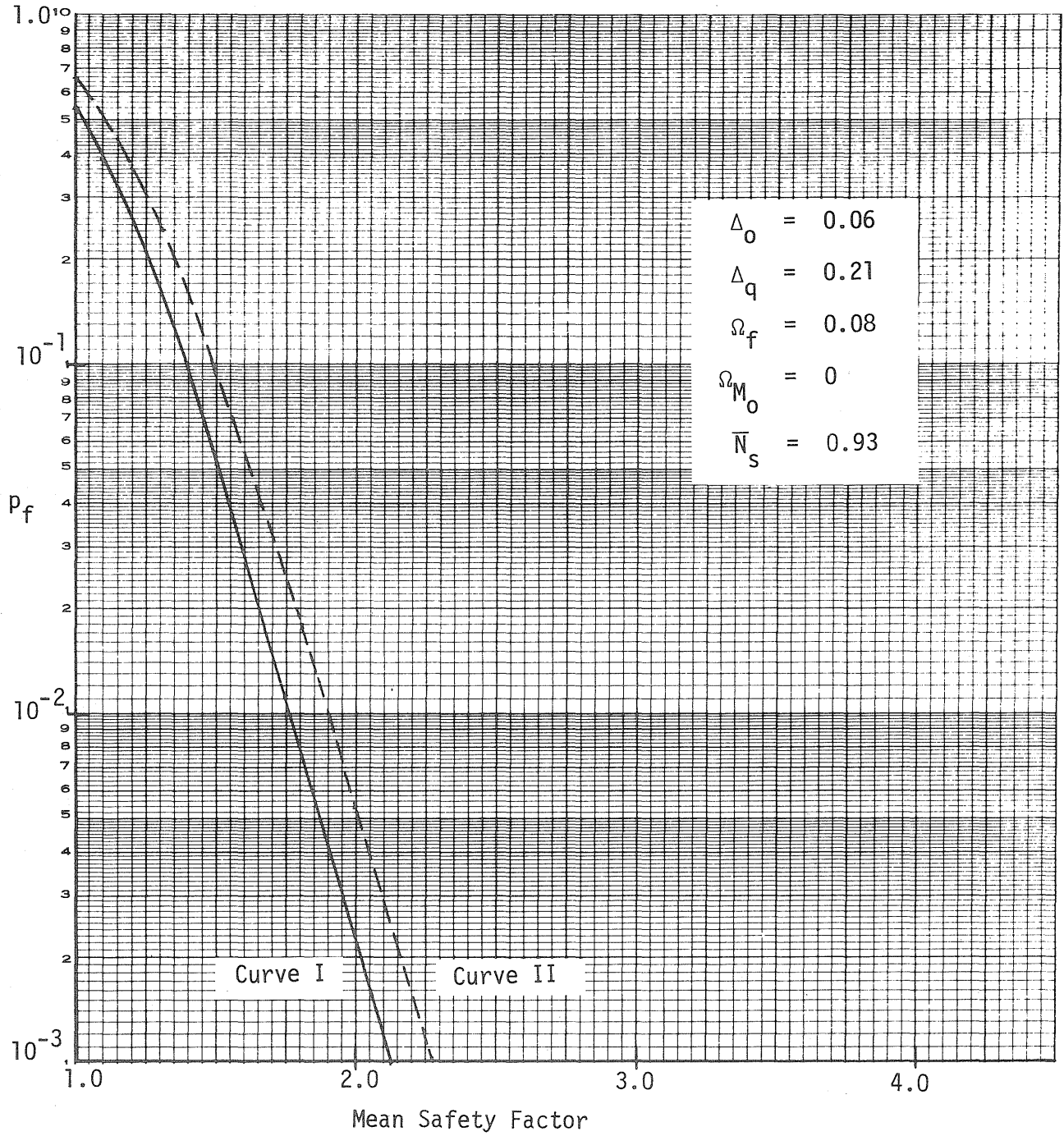
Fig. 4.11 Example to Illustrate the Computation of $N_5(s)$



Curve I - Based on the corrected mean value of undrained strength
 Curve II - Based on the laboratory-measured mean value of undrained strength

Fig. 4.12 Variation of p_f with Mean Safety Factor for Stiff-Fissured Clays (with Minimum Soil Exploration)

*Based on the average value of soil parameters



(see Fig. 4.12 for identification of curves)

Fig. 4.13 Variation of p_f with Mean Safety Factor for Intact Clays
(with Minimum Soil Exploration)

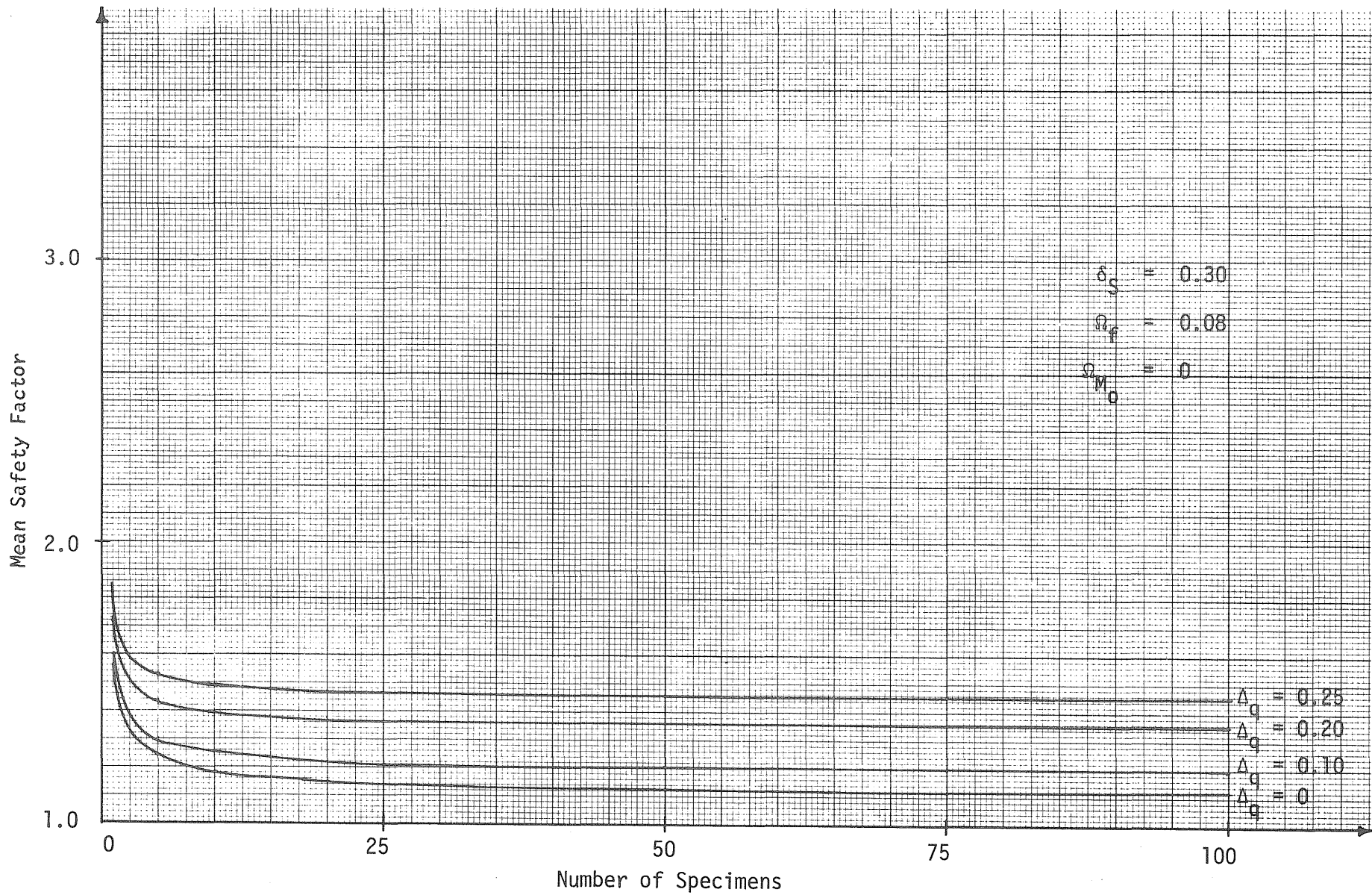


Fig. 4.14a Variation of Mean Safety Factor with Number of Specimens ($p_f = 10^{-1}$)

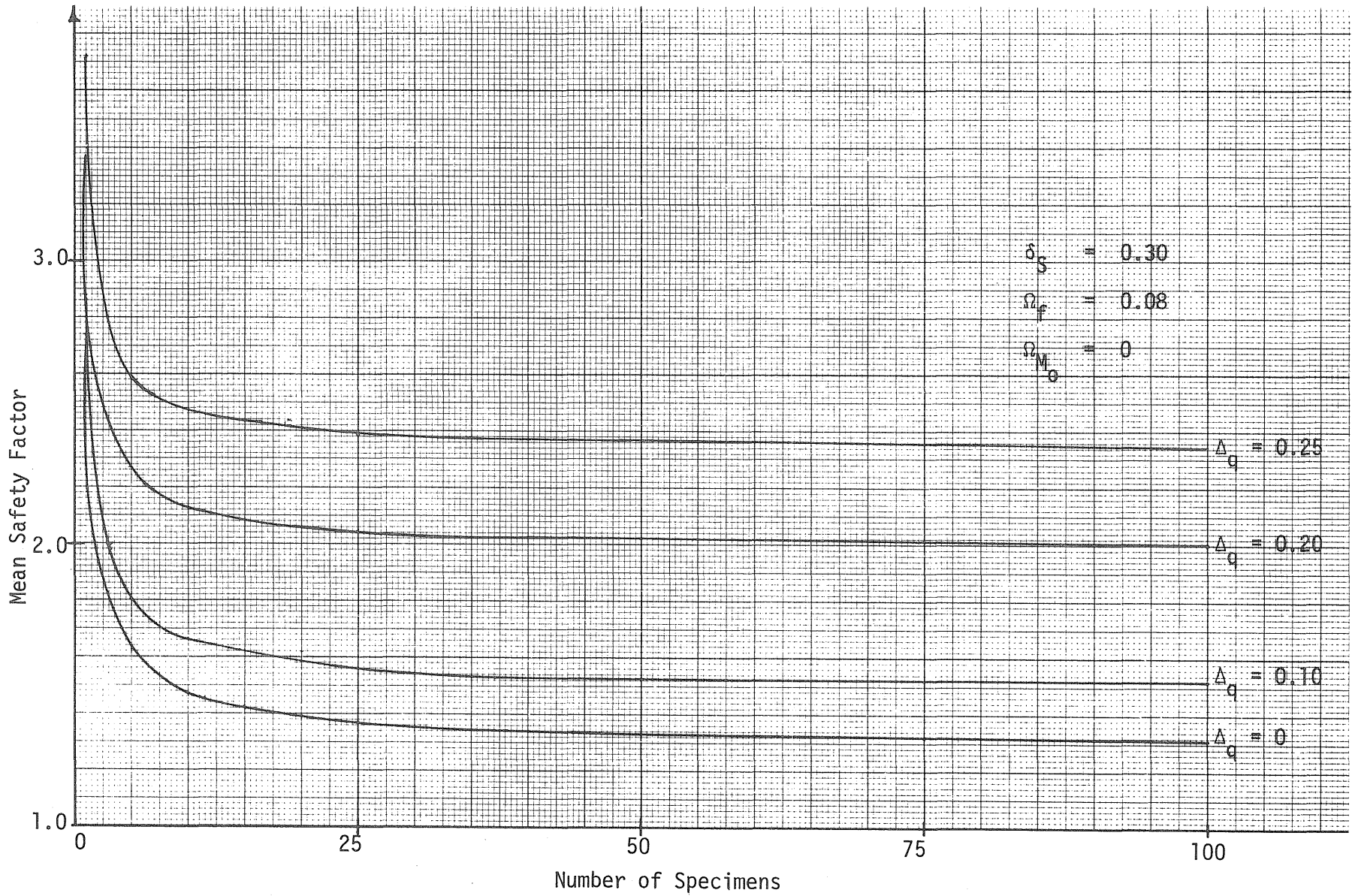


Fig. 4.14b Variation of Mean Safety Factor with Number of Specimens ($p_f = 10^{-3}$)

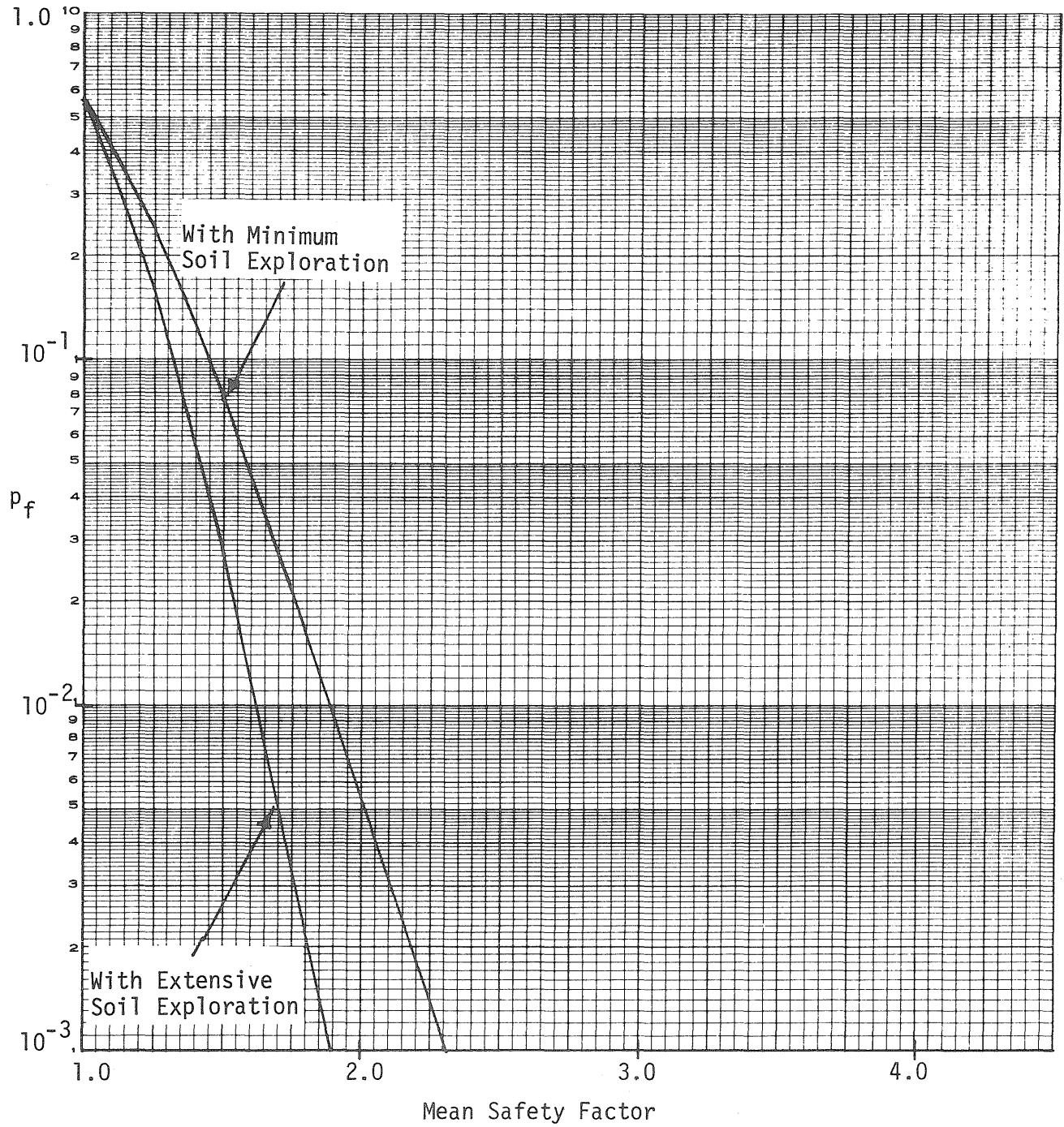


Fig. 4.15 Variation of p_f with Mean Safety Factor Considering the Degree of Soil Exploration (Stiff-Fissured Clays)

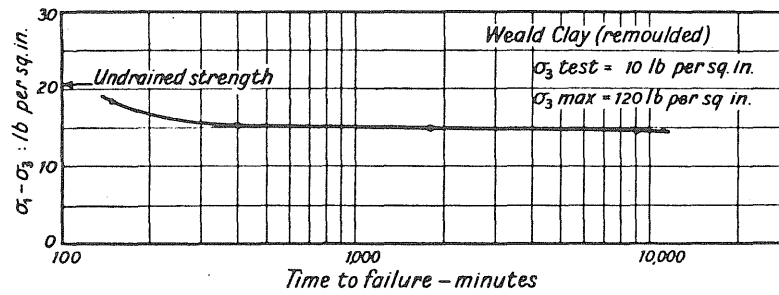


Fig. 5.1 Variation in Strength with Time to Failure in Drained Compression Tests on Remoulded Weald Clay (From Bishop and Henkel, Ref. 9)

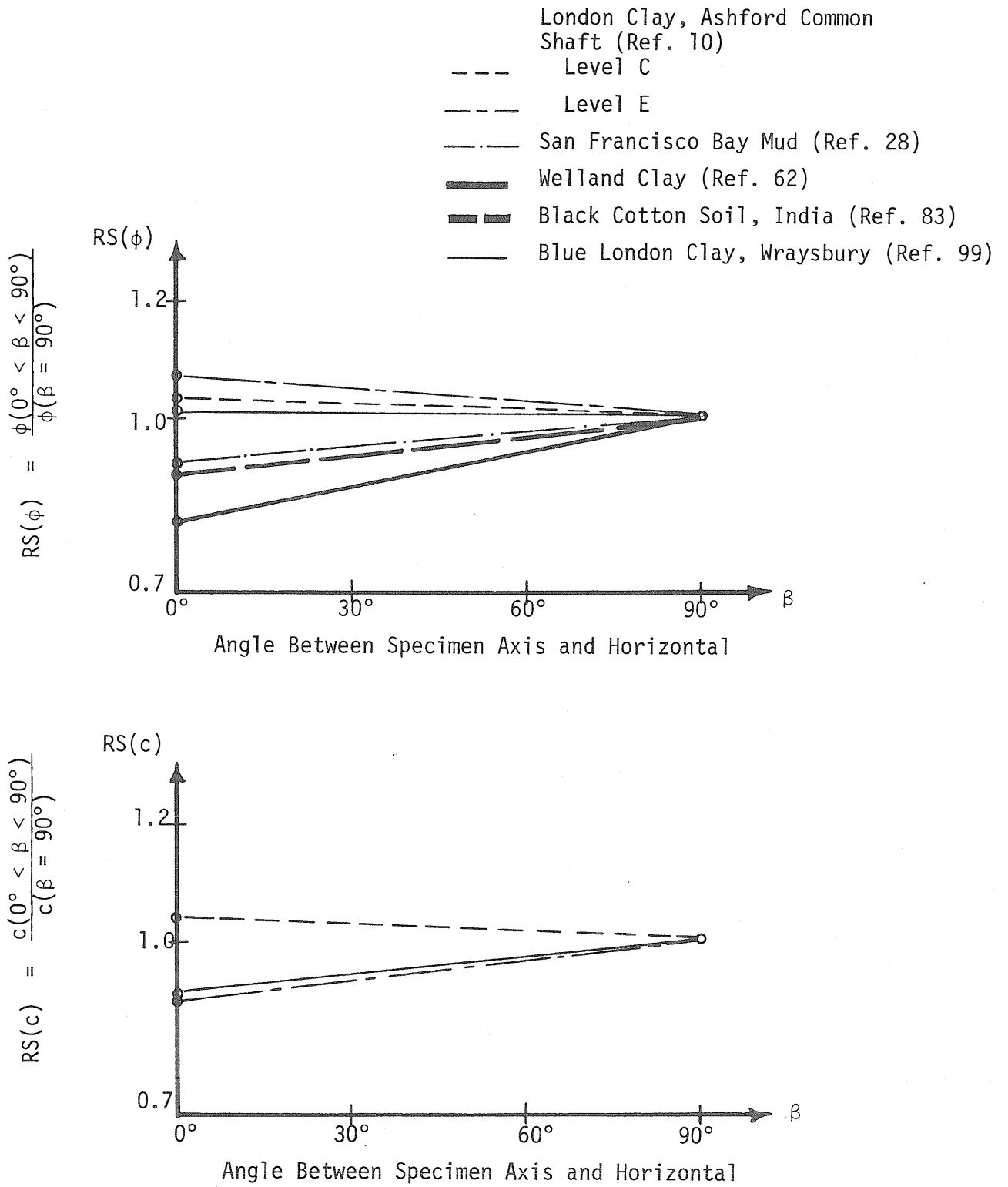


Fig. 5.2 Variation of ϕ and c with Specimen Orientation

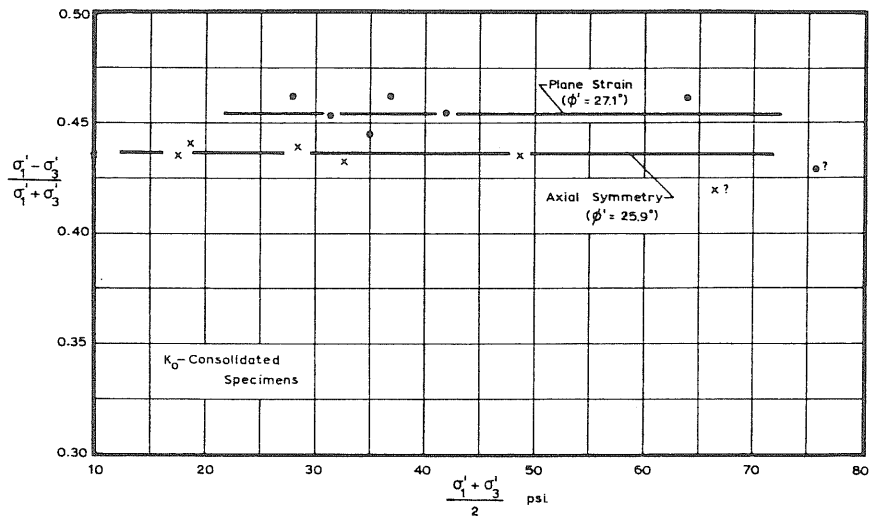


Fig. 5.3 Comparison of Strengths for Plane Strain and Triaxial Specimens in Terms of Effective Stresses for Remoulded Weald Clay (From Henkel and Wade, Ref. 39)

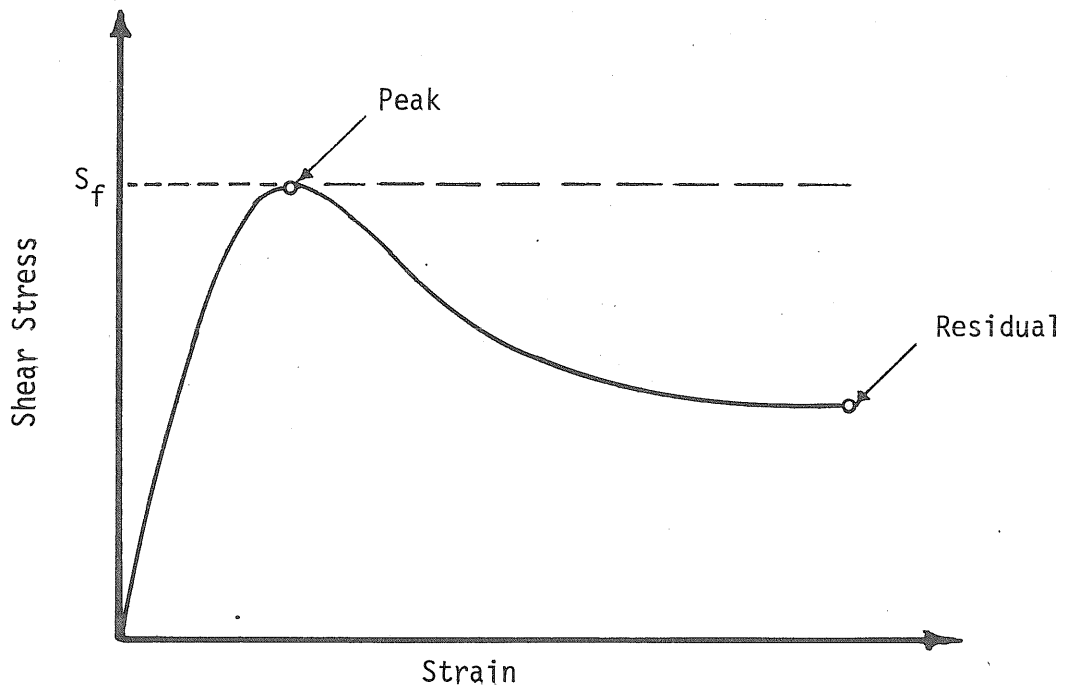
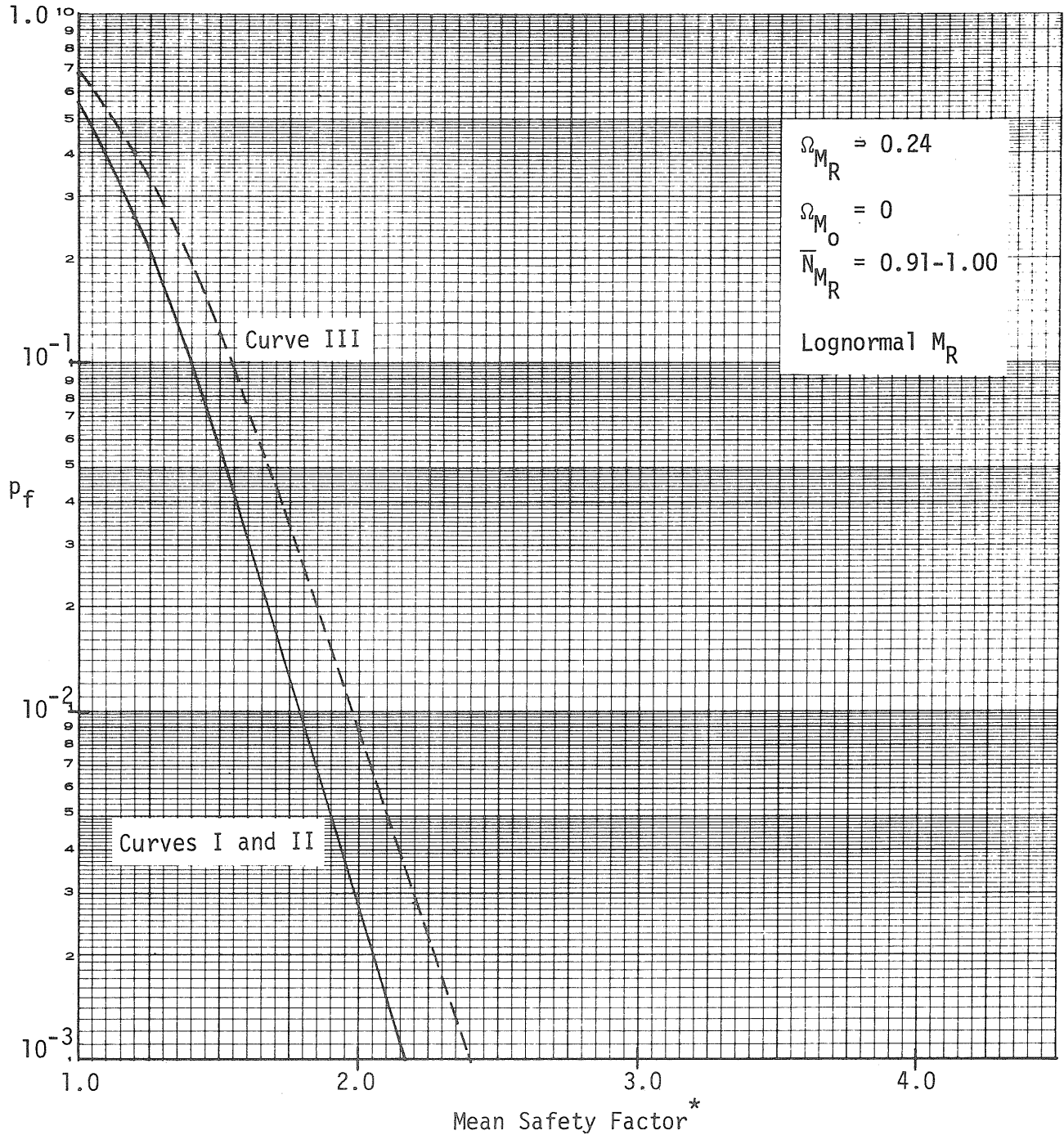


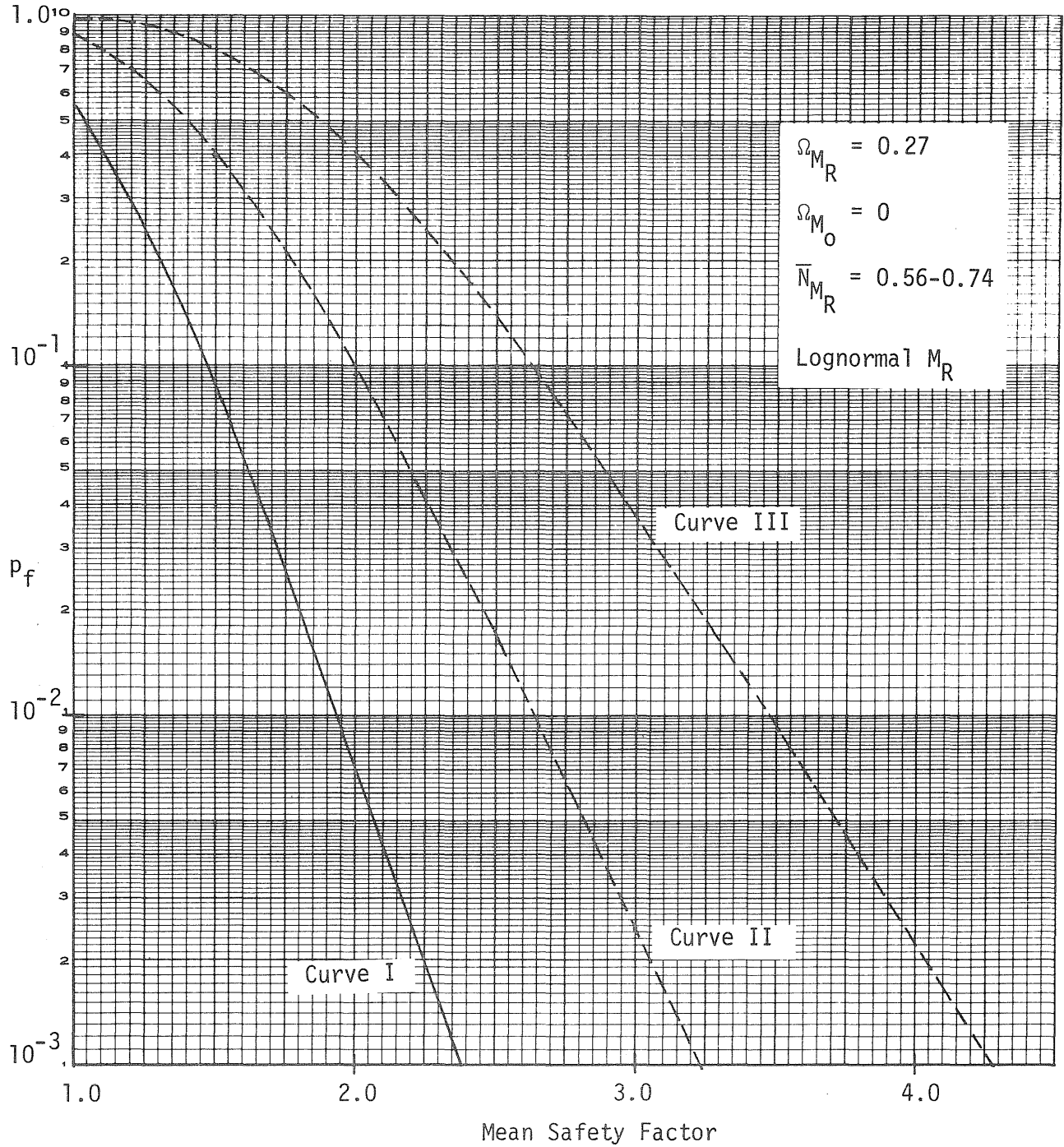
Fig. 5.4 Stress Strain Curve Considering Large Displacements



- Curve I - Based on corrected mean design variables and design method
- Curve II - Based on mean laboratory-measured peak strength parameters and without any corrections for the design method (Cohesive component of $M_R \ll$ Frictional component of M_R)
- Curve III - Based on mean laboratory-measured peak strength parameters and without any corrections for the design method. (Cohesive component of $M_R \gg$ Frictional component of M_R)

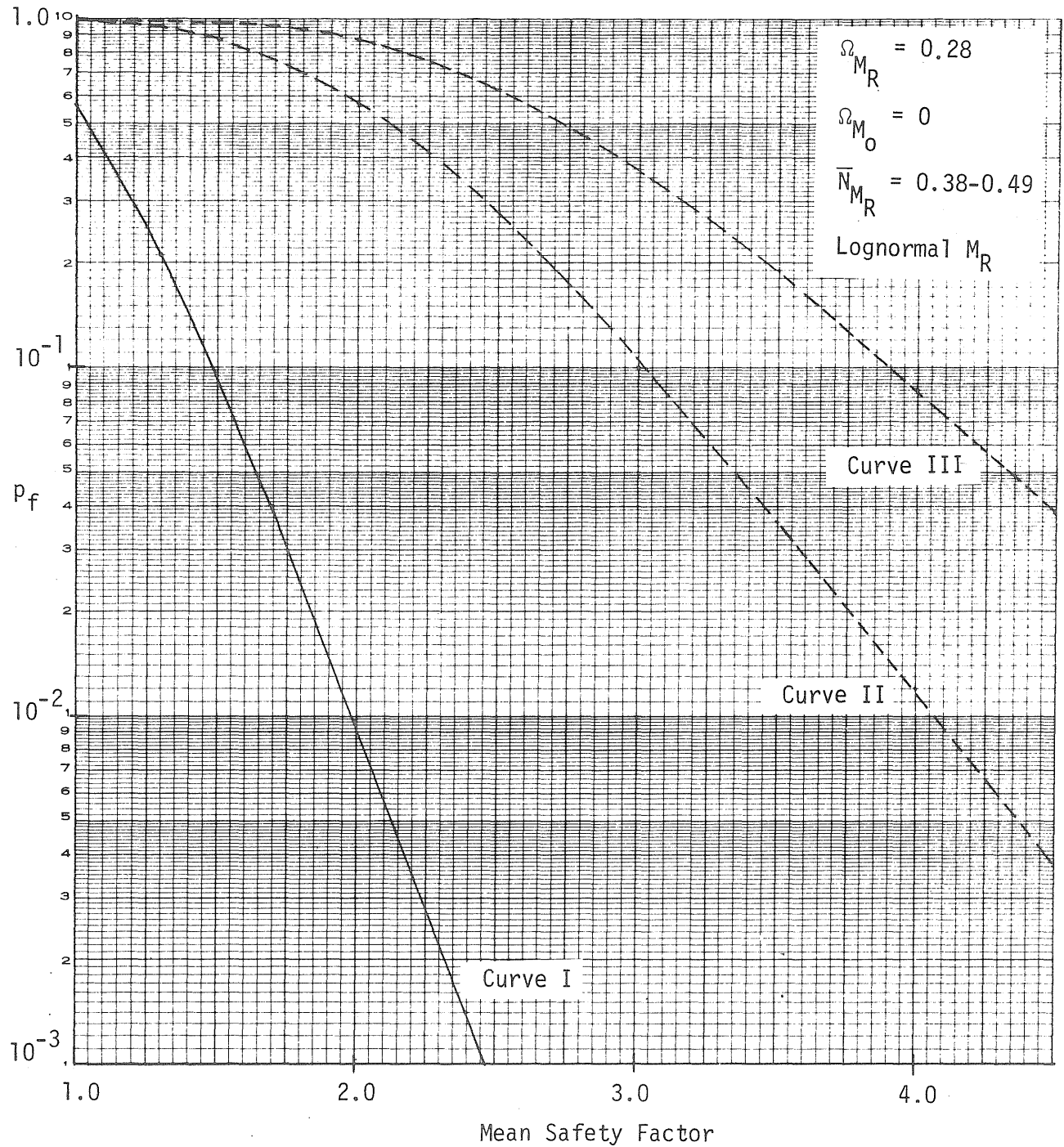
Fig. 5.5 Variation of p_f with Mean Safety Factor for First-Time Slides in Intact Clays (with Minimum Soil Exploration)

*Based on the average value of soil parameters.



(See Fig. 5.5 for identification of curves)

Fig. 5.6 Variation of p_f with Mean Safety Factor for First-Time Slides in Stiff-Fissured Clays (with Minimum Soil Exploration)



(See Fig. 5.5 for identification of curves)

Fig. 5.7 Variation of p_f with Mean Safety Factor for Slides on Pre-Existing Slip Surfaces in Stiff-Fissured Clays (with Minimum Soil Exploration)

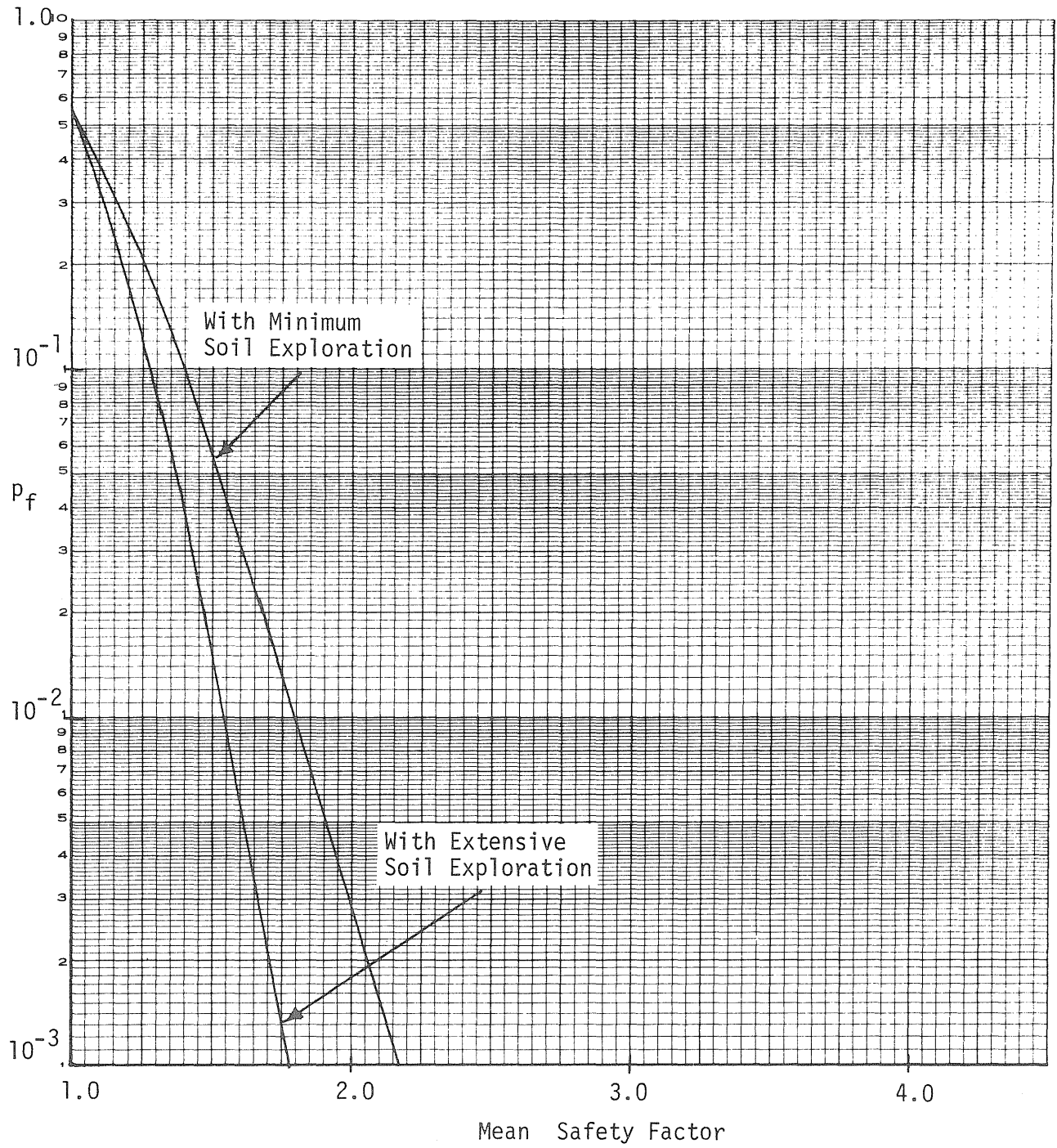


Fig. 5.8 Variation of p_f with Mean Safety Factor Considering the Degree of Soil Exploration (First-Time Slides in Stiff-Fissured Clays)

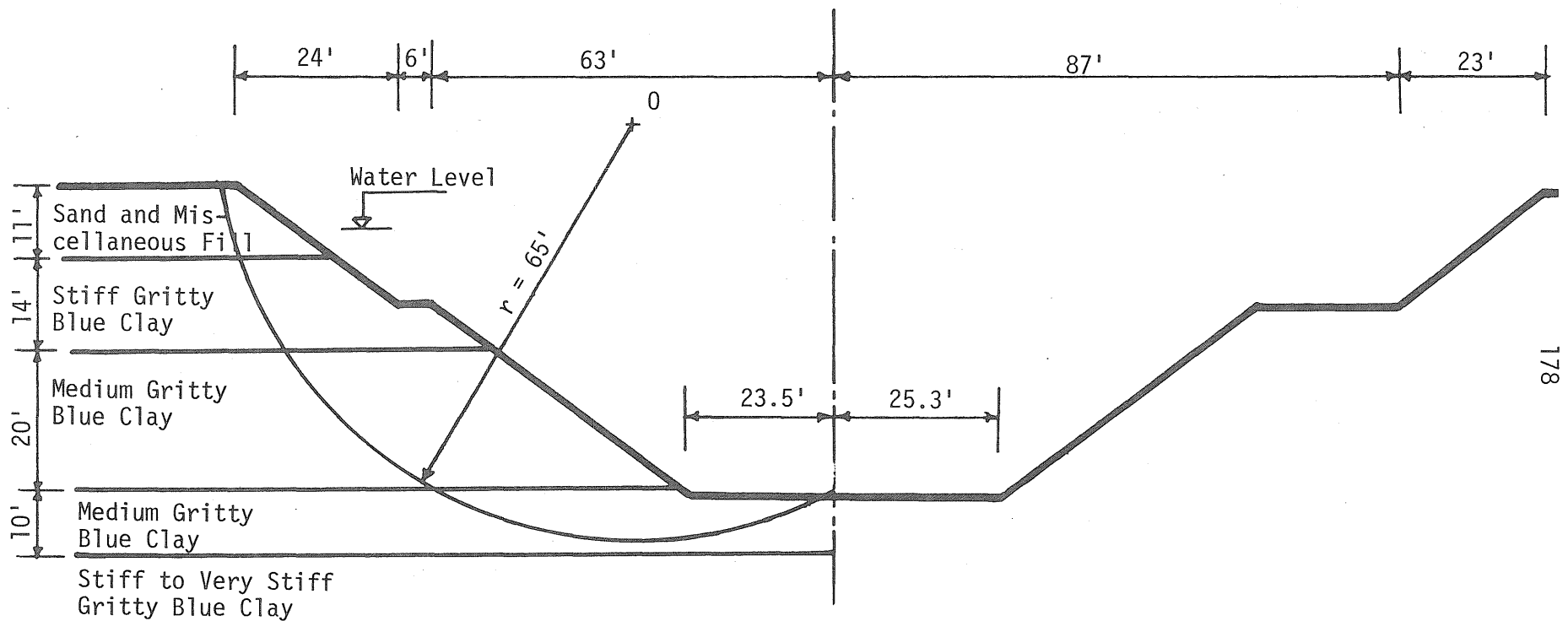


Fig. 6.1 Approximate Cross Section of the Cut and the Approximate Position of the Actual Slip Surface at Congress Street Open Cut

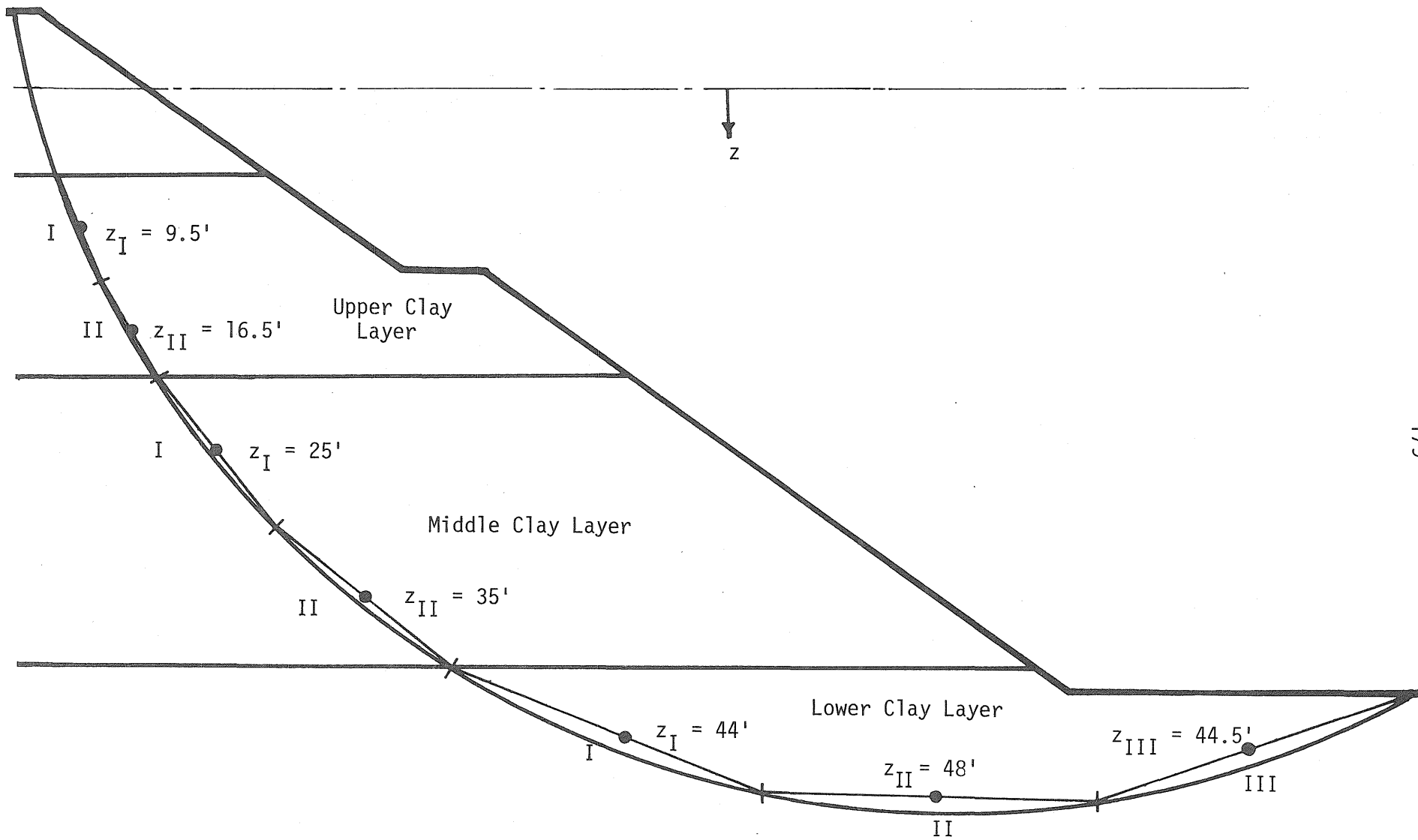


Fig. 6.2 Segments Along the Failure Surface

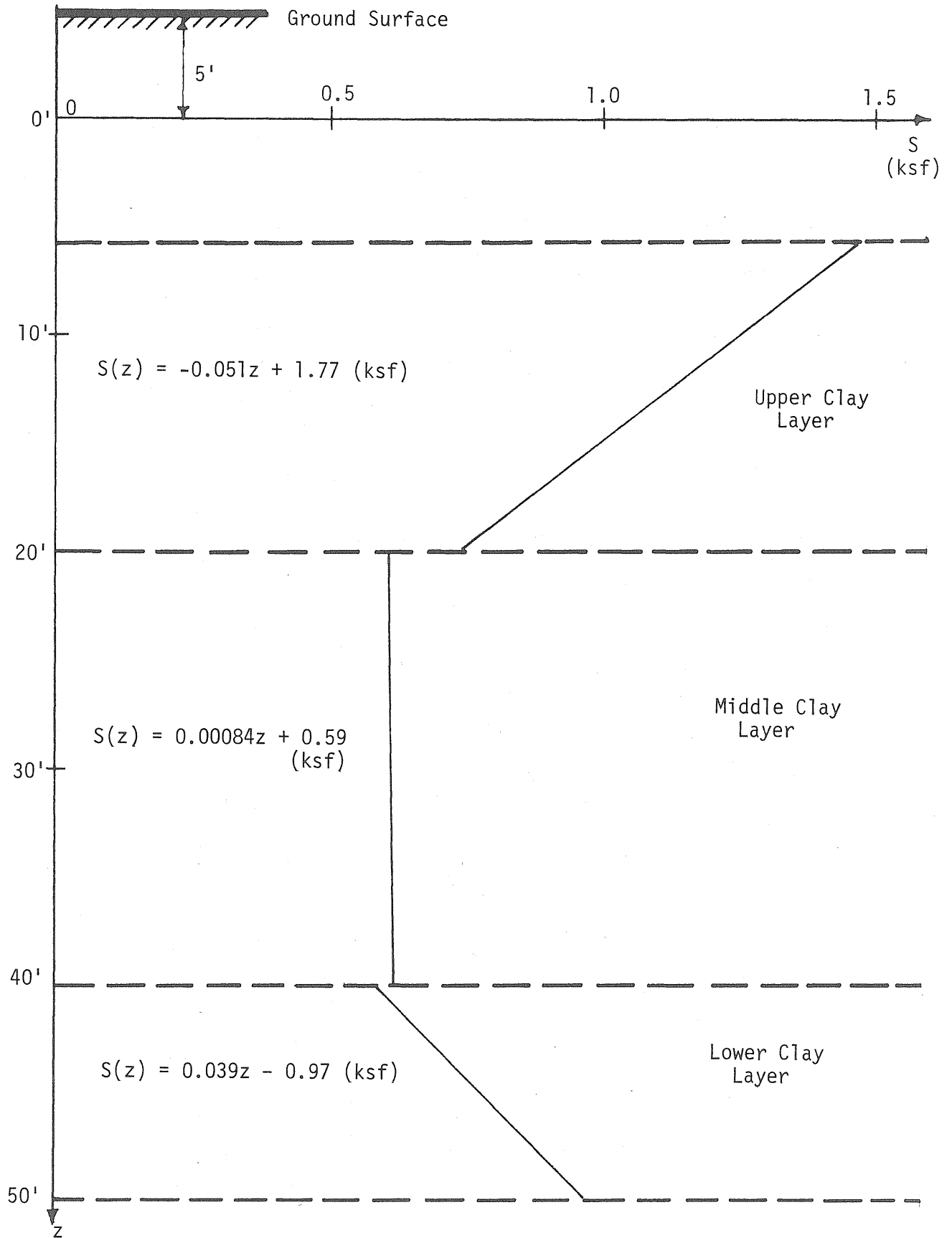


Fig. 6.3 Undrained Shear Strength Versus Depth

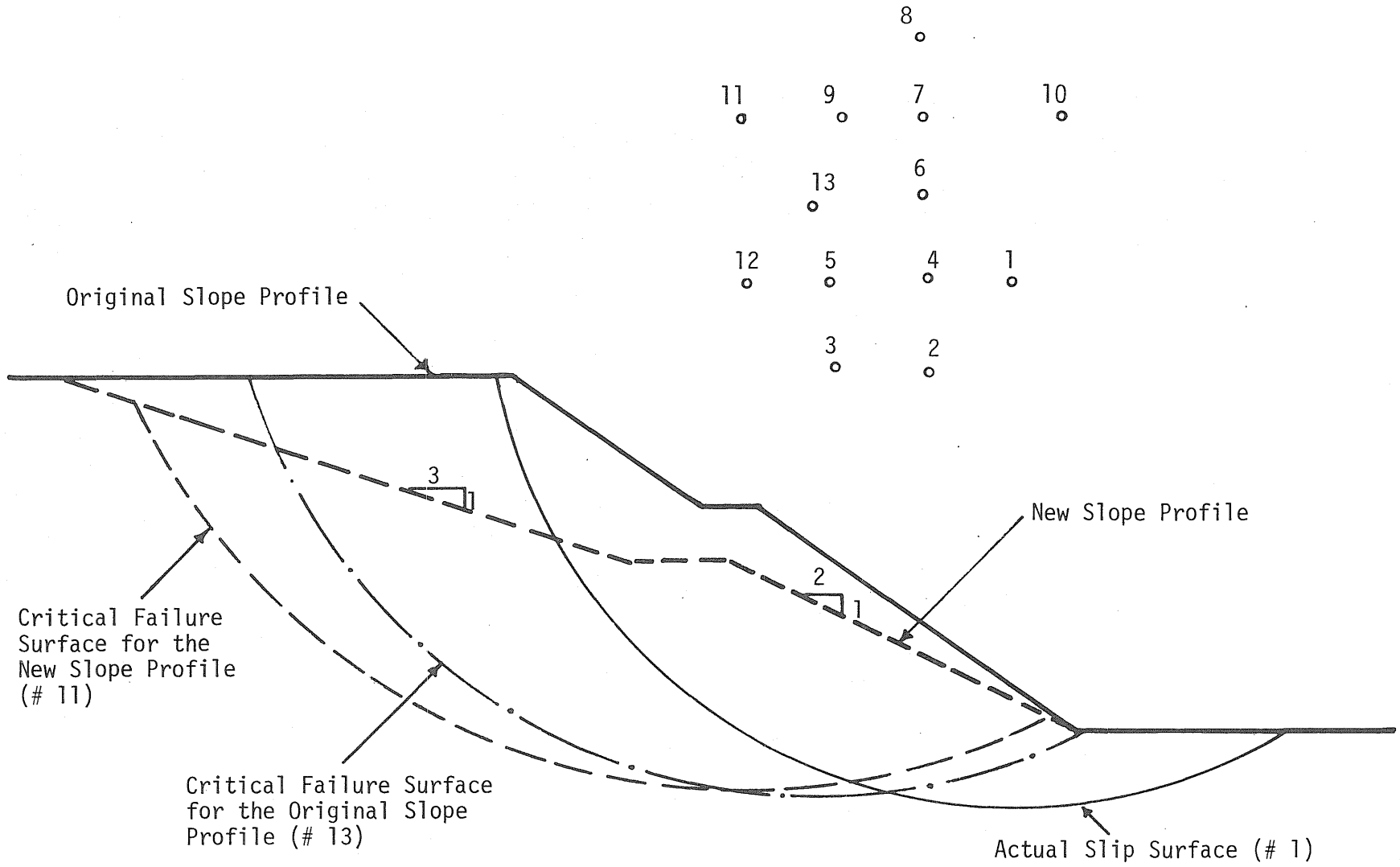
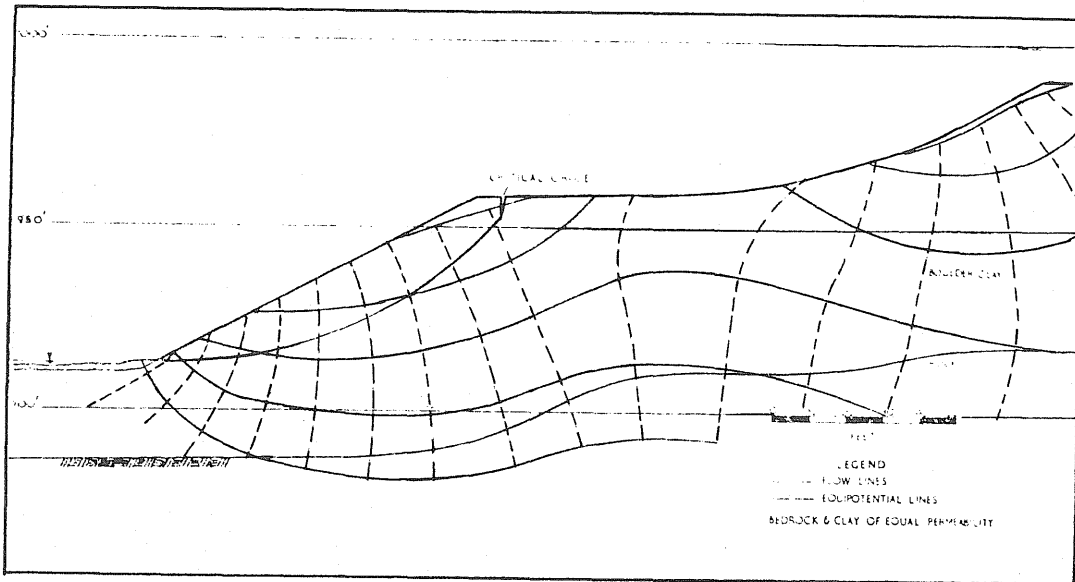
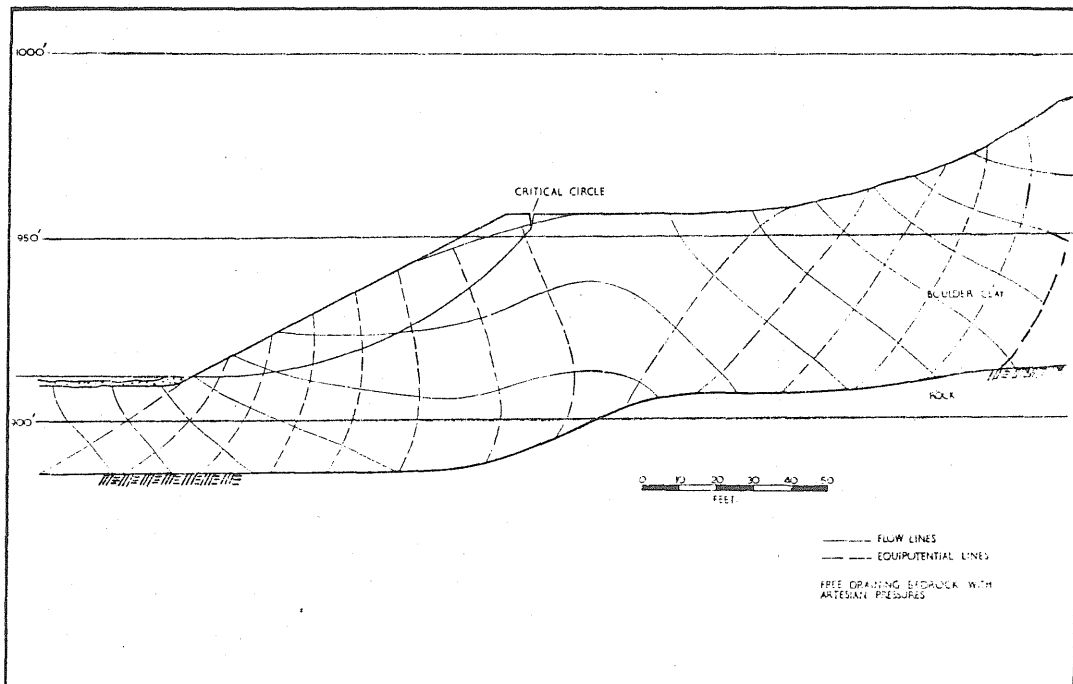


Fig. 6.4 Original and New Slope Profiles, the Location of the Rotation Centers and the Position of the Actual and Critical Slip Surfaces (Congress Street)



Flow Net A



Flow Net B

Fig. 6.6 Flow Nets A and B (From Skempton and Brown, Ref. 94)

APPENDIX A

COMPUTATION OF \bar{N}_2'' AND Δ_2'' FOR s FROM PECK'S DATA

The data given by Peck⁷⁹ is shown in Table A.1. From this data $\bar{N}_2''(s)$ and $\Delta_2''(s)$ are computed as follows:

Let $N_2''(S)$ be the corrective factor for the individual soil specimen to account for the effect of mechanical disturbance. For the i th specimen it is given as

$$N_2''(S_i) = \frac{S_i}{\hat{S}_i} \quad (\text{A.1})$$

where S_i and \hat{S}_i are the undrained strengths measured from block specimens (undisturbed) and tube specimens (disturbed), respectively, at the same (i th) location. By definition

$$s = \frac{1}{n} \sum_{i=1}^n S_i \quad (\text{A.2})$$

$$\hat{s} = \frac{1}{n} \sum_{i=1}^n \hat{S}_i \quad (\text{A.3})$$

$$s = N_2''(s) \hat{s} \quad (\text{A.4})$$

From Eq. A.4

$$N_2''(s) = \frac{s}{\hat{s}}$$

However, based on the first-order analysis

Table A.1

Comparison of Shear Strengths of Undisturbed and
Shelby Tube Samples at Chicago Subway

Measurement Number:	S_i (ksf)	\hat{S}_i (ksf)	$N_2(S_i)$
1	0.35	0.31	1.13
2	0.40	0.32	1.25
3	0.41	0.28	1.46
4	0.42	0.35	1.20
5	0.43	0.30	1.43
6	0.48	0.32	1.50
7	0.49	0.34	1.44
8	0.58	0.40	1.45
9	0.68	0.43	1.58
10	0.70	0.50	1.40
11	0.75	0.56	1.34
12	0.87	0.63	1.38
13	0.96	0.65	1.48

$$N_2''(s) \approx \frac{E(s)}{E(\hat{s})} \quad (\text{A.5})$$

From Eqs. A.1 and A.2

$$s = \frac{1}{n} \sum_{i=1}^n N_2''(S_i) \hat{S}_i \quad (\text{A.6})$$

Hence, using Eqs. A.3, A.5 and A.6

$$\begin{aligned}
 N_2''(s) &\approx \frac{E \left[\frac{1}{n} \sum_{i=1}^n N_2''(S_i) \hat{S}_i \right]}{E \left[\frac{1}{n} \sum_{i=1}^n \hat{S}_i \right]} \\
 &= \frac{\frac{1}{n} n \bar{N}_2''(S) E(\hat{S})}{\frac{1}{n} n E(\hat{S})} = \bar{N}_2''(S)
 \end{aligned}$$

Thus,

$$\bar{N}_2''(s) = E[\bar{N}_2''(S)] = \bar{N}_2''(S) = \frac{1}{n_s} \sum_{i=1}^{n_s} N_2''(S_i)$$

and

$$\text{VAR}(N_2''(s)) \approx \text{VAR}(\bar{N}_2''(S)) = \frac{\text{VAR}(N_2''(S))}{n_s}$$

or in terms of c.o.v.'s

$$\Delta_2''(s) = \frac{\Delta_2''(S)}{\sqrt{n_s}}$$

where n_s is the number of specimens tested. From the given data one computes

$$\bar{N}_2''(s) = \bar{N}_2''(S) = 1.39$$

and

$$\Delta_2''(s) = \frac{0.09}{\sqrt{13}} = 0.025$$

APPENDIX B

COMPUTATION OF THE SPATIAL CORRELATION PARAMETER
v FROM HOOPER AND BUTLER'S DATA

Let $\rho(\lambda)$ be the coefficient of correlation for the undrained strength values measured at two points within the same segment of the potential failure surface that are λ distance apart. The spatial correlation between these two measurements are assumed to be a function of λ . Cornell²² suggested that a reasonable choice for this function could be $e^{-v\lambda}$ or $e^{-v\lambda^2}$ for describing correlation with distance. If $e^{-v\lambda}$ is chosen, then

$$\rho(\lambda) = e^{-v\lambda} \quad (B.1)$$

where v is a spatial correlation parameter to be estimated from data. To estimate the value of v , data reported by Hooper and Butler⁴¹ about the shear strength of London clay is used. A large number of undrained triaxial tests were performed on specimens that are 1-1/2 in. in diameter and 3 in. high. Samples were obtained either by using 4 in. diameter open-drive sampling equipment (U4) or by using hydraulically pushed 1-1/2 in. diameter and 18 in. long sample tubes (U1-1/2). Three specimens were extruded from each of these samples and tested at the same lateral pressure in the triaxial cell. The means, standard deviations, and coefficients of variation corresponding to sets of three U4 and U1-1/2 samples for various sites are given in Table B.1. In the same table the means, standard deviations, and coefficients of variation obtained by considering each specimen separately (group size 1) are also shown.

Let m_1 be the number of U4 samples and n_1 be the total number of specimens prepared from the U4 samples. Since from each sample three specimens were prepared

Table B.1

Summary of Shear Strength Data
(from Hooper and Butler, Ref. 41)

Region	Average Depth (ft)	n_s	Mean (psf)	Standard Deviation (psf)	c.o.v.	Sample Type	Group Size
Block 1	87	47	7000	2000	0.29	U4	3
		139	7000	2250	0.32	U4	1
		27	7250	900	0.12	U1-1/2	3
		79	7250	1300	0.18	U1-1/2	1
Block 11	64	74	5200	1400	0.27	U4	3
		212	5200	1700	0.33	U4	1
Railway	60	82	6450	1050	0.16	U1-1/2	3
		246	6450	1350	0.21	U1-1/2	1
Block 3	73	31	7000	1000	0.14	U1-1/2	3
		92	7000	1200	0.17	U1-1/2	1

$$n_1 = 3m_1 \quad (B.2)$$

Based on data on samples (group size 3), with the distance between two samples being large enough so that the spatial correlation is negligible, one gets

$$\sigma_s^2 = \frac{\sigma_{m_1}^2}{m_1} = \frac{\sigma_{m_1}^2}{\frac{n_1}{3}} \quad (B.3)$$

where σ_{m_1} is the standard deviation of the undrained strength computed from the data on U4 samples (group size 3).

If the data obtained by considering each specimen separately (group size 1) is used, then the correlation among the three specimens extracted from the same sample should be taken into account, whereas specimens from different samples are assumed to be uncorrelated. Correlation coefficient will be the

same among the specimens since, the three specimens are all equidistant from each other with $\lambda \approx 1.75$ in. (see Fig. B.1). Therefore,

$$\rho_{12} = \rho_{13} = \rho_{23} = \rho(1.75 \text{ in.})$$

and

$$\sigma_s^2 = \frac{\sigma_{n_1}^2}{n_1} + \frac{2}{n_1^2} m_1 \sum_{i=1}^3 \sum_{j=i+1}^3 \rho_{ij} \sigma_{S_i}^2 \sigma_{S_j}^2$$

with $\sigma_{S_i} = \sigma_{S_j} = \sigma_{n_1}$,

$$\begin{aligned} \sigma_s^2 &= \frac{\sigma_{n_1}^2}{n_1} + \frac{2}{n_1^2} \frac{n_1}{3} 3\rho(1.75 \text{ in.}) \sigma_{n_1}^2 \\ &= \frac{\sigma_{n_1}^2}{n_1} + \frac{\sigma_{n_1}^2}{n_1} 2\rho(1.75 \text{ in.}) \\ &= \frac{\sigma_{n_1}^2}{n_1} (1 + 2\rho(1.75 \text{ in.})) \end{aligned} \quad (\text{B.4})$$

where σ_{n_1} is the standard deviation of the undrained strength obtained by considering each specimen separately (group size 1) in U4 sampling. Equating Eqs. B.3 and B.4 and simplifying

$$\rho(1.75 \text{ in.}) = 1.5 \left(\frac{\sigma_{m_1}}{\sigma_{n_1}} \right)^2 - 0.5 \quad (\text{B.5})$$

Similarly, if m_2 is the number of U1-1/2 samples and n_2 is the total number of specimens prepared from the U1-1/2 samples, based on data on samples (group size 3)

$$\sigma_s^2 = \frac{\sigma_{m_2}^2}{m_2} = \frac{\sigma_{m_2}^2}{\frac{n_2}{3}} \quad (\text{B.6})$$

where σ_{m_2} is the standard deviation of the undrained strength computed from the data on U1-1/2 samples (group size 3).

In using the data obtained by considering each specimen separately (group size 1), it is again assumed that only the specimens from the same sample are correlated. However, due to different distances between specimens (see Fig. B.2) the correlation coefficients will be

$$\rho_{12} = \rho_{23} = \rho(\lambda) = \rho(6 \text{ in.})$$

$$\rho_{13} = \rho(2\lambda) = \rho(12 \text{ in.})$$

From Eq. B.1

$$\begin{aligned} \rho(6 \text{ in.}) &= e^{-6v} \\ \rho(12 \text{ in.}) &= e^{-12v} = [\rho(6 \text{ in.})]^2 \end{aligned} \quad (\text{B.7})$$

Therefore, for group size 1

$$\begin{aligned} \sigma_s^2 &= \frac{\sigma_{n_2}^2}{n_2} + \frac{2}{n_2} m_2 \sum_{i=1}^3 \sum_{j=i+1}^3 \rho_{ij} \sigma_{n_2}^2 \\ &= \frac{\sigma_{n_2}^2}{n_2} \left\{ 1 + \frac{2}{3} [2 \rho(6 \text{ in.}) + \rho^2(6 \text{ in.})] \right\} \\ &= \frac{\sigma_{n_2}^2}{n_2} \left[1 + \frac{4}{3} \rho(6 \text{ in.}) + \frac{2}{3} \rho^2(6 \text{ in.}) \right] \end{aligned} \quad (\text{B.8})$$

where σ_{n_2} is the standard deviation of the undrained strength obtained by considering each specimen separately (group size 1) in U1-1/2 sampling. Equating Eqs. B.6 and B.8 and simplifying

$$\rho^2(6 \text{ in.}) + 2\rho(6 \text{ in.}) + 1.5 - 4.5 \left(\frac{\sigma_{m_2}}{\sigma_{n_2}} \right)^2 = 0$$

Solving for $\rho(6 \text{ in.})$

$$\rho(6 \text{ in.}) = -1 + \sqrt{4.5 \left(\frac{\sigma_{m_2}}{\sigma_{n_2}} \right)^2 - 0.5} \quad (\text{B.9})$$

Substitution of the data given in Table B.1 into Eqs. B.5 and B.9 gives the values of $\rho(\lambda)$ as shown in Table B.2. From Table B.2, $\bar{\rho}(1.75 \text{ in.})$ and $\bar{\rho}(6 \text{ in.})$ are computed as 0.61 and 0.47. Corresponding to these values, Eq. B.1 gives $v = 0.28$ and $v = 0.13$, the average of which is 0.21. Only for

Table B.2
Values of $\rho(\lambda)$

Region	Sample Type	$\rho(1.75 \text{ in.})$	$\rho(6.0 \text{ in.})$
Block 1	U4	0.69	--
	U1-1/2	--	0.29
Block 11	U4	0.52	--
Railway	U1-1/2	--	0.49
Block 3	U1-1/2	--	0.62

one site (Block 1) data exists for both $\rho(1.75 \text{ in.})$ and $\rho(6 \text{ in.})$, and both of them give $v = 0.21$. Based on Hooper and Butler's data v is taken as 0.21, and the spatial correlation as expressed by Eq. B.1 becomes

$$\rho(\lambda) = e^{-0.21\lambda} \quad (\text{B.10})$$

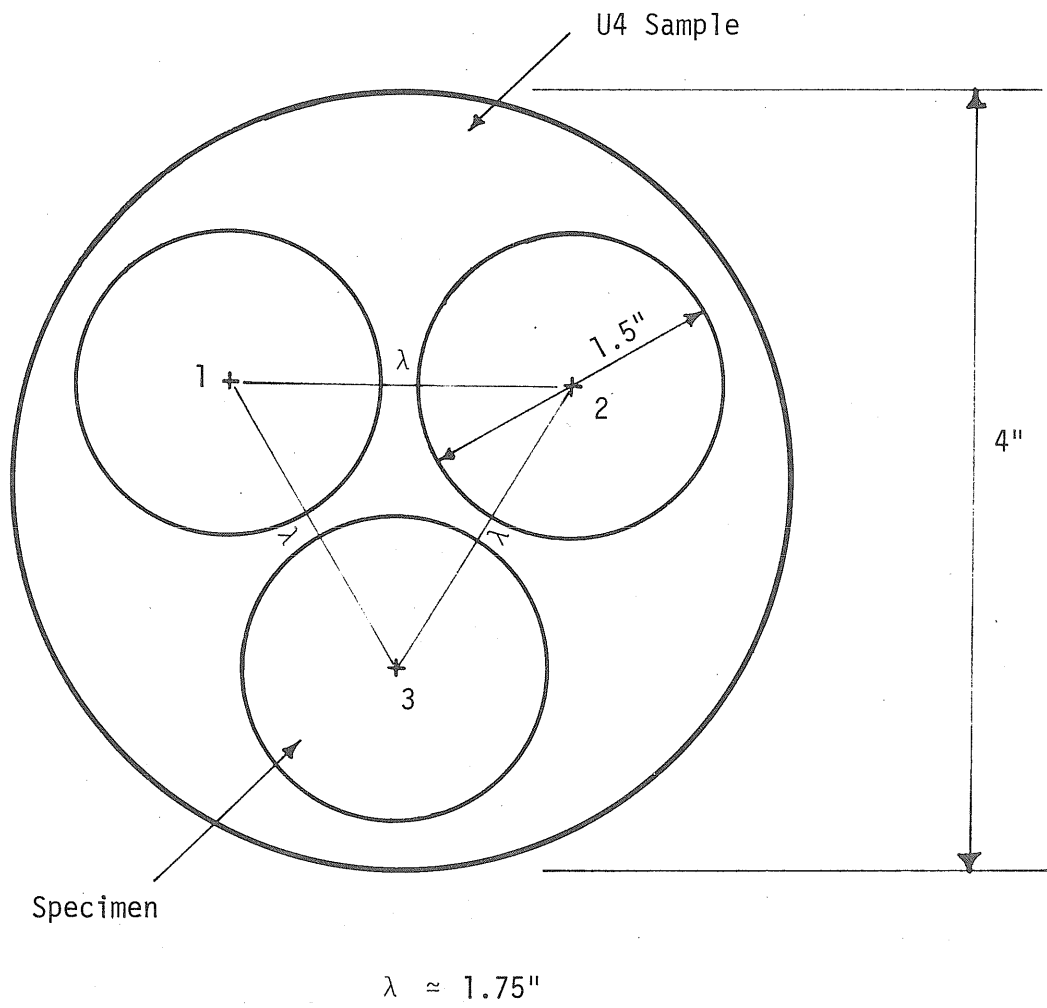


Fig. B.1 U4 Sampling

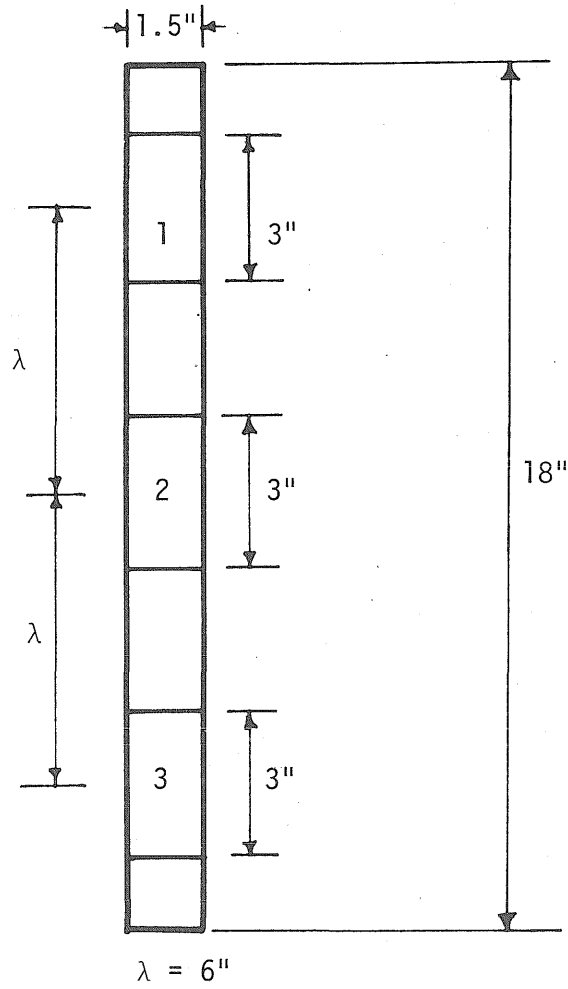


Fig. B.2 U1-1/2 Sampling

APPENDIX C

DERIVATION OF AN APPROXIMATE EXPRESSION FOR $\rho_{N_i N_j}$

The correlation between N_{s_i} and N_{s_j} will be due to those factors that are the same for both s_i and s_j . Using Eq. 2.12 one can write

$$N_{s_i} = \prod_{k=0}^{n_0} N_k(s_i) \quad (C.1)$$

$$N_{s_j} = \prod_{k=0}^{n_0} N_k(s_j) \quad (C.2)$$

For simplicity in notation and in order to get a general expression, consider two random variables Z_1 and Z_2 given as

$$Z_1 = X_1 \cdot X_2 \cdot \dots \cdot X_n = \prod_{k=1}^n X_k \quad (C.3)$$

$$Z_2 = Y_1 \cdot Y_2 \cdot \dots \cdot Y_n = \prod_{k=1}^n Y_k \quad (C.4)$$

$\rho_{Z_1 Z_2}$, the coefficient of correlation between Z_1 and Z_2 , is

$$\rho_{Z_1 Z_2} = \frac{E \left[\left(\prod_{k=1}^n X_k \right) \left(\prod_{k=1}^n Y_k \right) \right] - E \left(\prod_{k=1}^n X_k \right) E \left(\prod_{k=1}^n Y_k \right)}{\sqrt{\text{VAR} \left(\prod_{k=1}^n X_k \right)} \sqrt{\text{VAR} \left(\prod_{k=1}^n Y_k \right)}} \quad (C.5)$$

It is assumed that only X_k and Y_k , $k = 1, 2, \dots, n$, may be

correlated, with the corresponding correlation coefficients denoted by ρ_k , $k = 1, 2, \dots, n$. The following expressions are obtained based on the Taylor series expansion about the mean values and assuming that terms involving third and higher degrees of the c.o.v.'s are negligible.

$$E\left(\prod_{k=1}^n X_k\right) = \prod_{k=1}^n \bar{X}_k$$

$$E\left(\prod_{k=1}^n Y_k\right) = \prod_{k=1}^n \bar{Y}_k$$

$$\begin{aligned} E\left[\left(\prod_{k=1}^n X_k\right)\left(\prod_{k=1}^n Y_k\right)\right] &= \left(\prod_{k=1}^n \bar{X}_k\right)\left(\prod_{k=1}^n \bar{Y}_k\right) \\ &\quad + \frac{1}{2} \sum_{k=1}^n \left(\frac{\partial Z_1}{\partial X_k}\right)_0 \left(\frac{\partial Z_2}{\partial Y_k}\right)_0 \text{COV}(X_k, Y_k) \\ &= \left(\prod_{k=1}^n \bar{X}_k\right)\left(\prod_{k=1}^n \bar{Y}_k\right) \left[1 + \sum_{k=1}^n \rho_k \Delta_k(X) \Delta_k(Y)\right] \end{aligned}$$

$$\text{VAR}\left(\prod_{k=1}^n X_k\right) \approx \left(\prod_{k=1}^n \bar{X}_k\right)^2 \left[\sum_{k=1}^n \Delta_k^2(X)\right] = \left(\prod_{k=1}^n \bar{X}_k\right)^2 \Delta_X^2$$

$$\text{VAR}\left(\prod_{k=1}^n Y_k\right) \approx \left(\prod_{k=1}^n \bar{Y}_k\right)^2 \left[\sum_{k=1}^n \Delta_k^2(Y)\right] = \left(\prod_{k=1}^n \bar{Y}_k\right)^2 \Delta_Y^2$$

where $\Delta_k(X)$ and $\Delta_k(Y)$ are the c.o.v.'s of X_k and Y_k , respectively. Substituting these equations into Eq. C.5 and simplifying, one gets

$$\rho_{Z_1 Z_2} \approx \frac{\sum_{k=1}^n \rho_k \Delta_k(X) \Delta_k(Y)}{\Delta_X \Delta_Y} \quad (C.6)$$

From Eq. C.6, the correlation between N_{s_i} and N_{s_j} can be expressed as

$$\rho_{N_i N_j} \approx \frac{\sum_{k=0}^{n_0} \rho_k \Delta_k(s_i) \Delta_k(s_j)}{\Delta_{s_i} \Delta_{s_j}} \quad (C.7)$$

In this study it is assumed that $\rho_k = 1.0$ for those corrective factors that are the same for both s_i and s_j , and $\rho_k = 0$ otherwise. For example, if the same kind of mechanical disturbance during sampling occurs in two layers, then the same corrective factor would be used, and $N_2(s_i)$ and $N_2(s_j)$ would be perfectly correlated (i.e., $\rho_2 = 1.0$). Thus, if $\{n_c\}$ denotes those corrective factors for which $\rho_k = 1.0$, then

$$\rho_{N_i N_j} = \frac{\sum_{\{n_c\}} \Delta_k(s_i) \Delta_k(s_j)}{\Delta_{s_i} \Delta_{s_j}} \quad (C.8)$$

but, $\Delta_k(s_i) = \Delta_k(s_j) = \Delta_k(s)$; therefore,

$$\rho_{N_i N_j} = \frac{\sum_{\{n_c\}} \Delta_k^2(s)}{\Delta_{s_i} \Delta_{s_j}} = \frac{\Delta_{ij}^2(s)}{\Delta_{s_i} \Delta_{s_j}} \quad (C.9)$$

where $\Delta_{ij}^2(s)$ is the squared sum of the c.o.v.'s of those corrective factors that are the same for both s_i and s_j .

APPENDIX D

MEAN, VARIANCE AND COVARIANCE OF \hat{s}_i BASED
ON REGRESSION ANALYSIS

The estimators \hat{a} and \hat{b}_1 could be treated as random variables denoted by A and B, respectively (Benjamin and Cornell⁴). Then, from Eq. 3.24

$$\hat{s}_i = A + Bz_i \quad (D.1)$$

The expressions for E(A), E(B), VAR(A), VAR(B) and COV(A,B) as obtained from Mood and Graybill⁷² are

$$E(A) = a \quad (D.2a)$$

$$E(B) = b \quad (D.2b)$$

$$\text{VAR}(A) = \frac{\sigma_S^2}{n_s} \left(1 + \frac{\bar{z}^2}{\text{VAR}(z)} \right) \quad (D.2c)$$

$$\text{VAR}(B) = \frac{\sigma_S^2}{n_s \text{VAR}(z)} \quad (D.2d)$$

$$\text{COV}(A,B) = - \frac{\sigma_S^2 \bar{z}}{n_s \text{VAR}(z)} \quad (D.2e)$$

The expected value of \hat{s}_i is

$$\begin{aligned} E(\hat{s}_i) &= E(A) + E(B z_i) \\ &= a + b_1 z_i \end{aligned} \quad (D.3)$$

and the variance

$$\text{VAR} (\hat{s}_i) = \text{VAR} (A) + z_i^2 \text{VAR} (B) + 2 z_i \text{COV} (A,B) \quad (\text{D.4})$$

Using Eqs. D.2c, D.2d and D.2e one gets

$$\text{VAR} (\hat{s}_i) = \frac{\sigma_S^2}{n_s} \left[1 + \frac{(z_i - \bar{z})^2}{\text{VAR} (\bar{z})} \right] \quad (\text{D.5})$$

For two segments (for example i th and j th) within the same stratum

$$\hat{s}_i = A + B z_i$$

$$\hat{s}_j = A + B z_j$$

A first-order approximation of the covariance between \hat{s}_i and \hat{s}_j is (Benjamin and Cornell⁴)

$$\begin{aligned} \text{COV} (\hat{s}_i, \hat{s}_j) &\approx \left(\frac{\partial \hat{s}_i}{\partial A} \right)_0 \left(\frac{\partial \hat{s}_j}{\partial A} \right)_0 \text{COV} (A,A) + \left(\frac{\partial \hat{s}_i}{\partial A} \right)_0 \left(\frac{\partial \hat{s}_j}{\partial B} \right)_0 \text{COV} (A,B) \\ &+ \left(\frac{\partial \hat{s}_i}{\partial B} \right)_0 \left(\frac{\partial \hat{s}_j}{\partial A} \right)_0 \text{COV} (B,A) + \left(\frac{\partial \hat{s}_i}{\partial B} \right)_0 \left(\frac{\partial \hat{s}_j}{\partial B} \right)_0 \text{COV} (B,B) \\ &= \text{VAR} (A) + (z_i + z_j) \text{COV} (A,B) + z_i z_j \text{VAR} (B) \\ &= \frac{\sigma_S^2}{n_s} \left[1 + \frac{(z_i - \bar{z})(z_j - \bar{z})}{\text{VAR} (\bar{z})} \right] \quad (\text{D.6}) \end{aligned}$$

APPENDIX E

RELATION BETWEEN MEAN SAFETY FACTOR AND CORRECTIVE
FACTOR N_f FOR SHORT-TERM SLOPE STABILITY

Consistent with the first-order approximation

$$N_f = \frac{M_R}{M_R^*} \approx \frac{\mu_{M_R}}{M_R^*} \quad (\text{E.1})$$

where \bar{M}_R^* is the mean resisting moment determined from the adopted function \hat{f} and based on the corrected component random variables. Since the slopes have failed, it may be assumed that μ_{M_R} is equal to \bar{M}_0 ; therefore,

$$N_f = \frac{\bar{M}_0}{\bar{M}_R^*} \quad (\text{E.2})$$

Due to detailed soil investigations in the failure cases, the soil strengths at the site are accurately determined, and thus the errors and uncertainties associated with their assessment are reduced to a minimum (Meyerhof⁷¹). Accordingly, the mean safety factors computed for the failure cases, such as those given in Table 4.15, can be expressed in terms of \bar{M}_R^* as

$$\bar{F} = \frac{\bar{M}_R^*}{\bar{M}_0} \quad (\text{E.3})$$

Hence, from Eqs. E.2 and E.3 one gets

$$N_f = \frac{1}{\bar{F}} \quad (\text{E.4})$$

APPENDIX F

COMPUTATION OF THE STATISTICAL PARAMETERS OF s FOR THE
FIRST LAYER BASED ON REGRESSION ANALYSIS

From Eq. D.3

$$\bar{s}_I = -0.051 \times 9.5 + 1.77 = 1.29 \text{ ksf}$$

$$\bar{s}_{II} = -0.051 \times 16.5 + 1.77 = 0.93 \text{ ksf}$$

From Eq. D.4

$$\text{VAR}(\hat{s}_I) = \frac{0.51^2}{38} \left[1 + \frac{(9.5 - 14.0)^2}{3.67^2} \right] = 1.71 \times 10^{-2} (\text{ksf})^2$$

$$\text{VAR}(\hat{s}_{II}) = \frac{0.51^2}{38} \left[1 + \frac{(16.5 - 14.0)^2}{3.67^2} \right] = 1.0 \times 10^{-2} (\text{ksf})^2$$

From Eq. D.6

$$\begin{aligned} \text{COV}(\hat{s}_I, \hat{s}_{II}) &= \frac{0.51^2}{38} \left[1 + \frac{(9.5 - 14.0)(16.5 - 14.0)}{3.67^2} \right] \\ &= 0.12 \times 10^{-2} (\text{ksf})^2 \end{aligned}$$

Since the lengths of the segments within a layer are equal, therefore, for the first layer

$$\hat{s} = \frac{1}{2} (\hat{s}_I + \hat{s}_{II})$$

$$\bar{s} = \frac{1}{2} (1.29 + 0.93) = 1.11 \text{ ksf}$$

$$\begin{aligned}\sigma_s &= \sqrt{\frac{1}{4} [\text{VAR} (\hat{s}_I) + \text{VAR} (\hat{s}_{II}) + 2 \text{COV} (\hat{s}_I, \hat{s}_{II})]} \\ &= \sqrt{\frac{1}{4} [1.71 \times 10^{-2} + 1.0 \times 10^{-2} + 2 \times 0.12 \times 10^{-2}]} \\ &= 0.086 \text{ ksf}\end{aligned}$$

$$\text{c.o.v.} = \frac{0.086}{1.11} = 0.077$$

APPENDIX G

ANALYSIS OF THE COHESIONLESS LAYER

The resultant earth pressure of the cohesionless layer is taken as $1/\cos \alpha_0$ times the horizontal component of earth pressure at rest (Ireland^{4,3}). This could be expressed as (see Fig. G.1)

$$P_0 = \frac{1}{2} \gamma_0 h_0^2 K_0 \frac{1}{\cos \alpha_0} \quad (\text{G.1})$$

where:

γ_0 = average unit weight of the cohesionless layer

h_0 = thickness of the cohesionless layer

K_0 = coefficient of earth pressure at rest

α_0 = angle of inclination of the resultant with respect to the horizontal

The point of application of the resultant is assumed to be the lower third point of the depth of the cohesionless layer ($h_0/3$), and the resultant is assigned an inclination equal to the average friction angle ϕ_0 with the normal to the surface of sliding (Ireland^{4,3}). The resultant shearing strength, S_0 , due to the cohesionless layer is

$$S_0 = P_0 \sin \phi_0$$

or

$$S_0 = \frac{1}{2} \gamma_0 h_0^2 K_0 \frac{1}{\cos \alpha_0} \sin \phi_0 \quad (\text{G.2})$$

and the resisting moment

$$M_{R_0} = \frac{1}{2} \gamma_0 h_0^2 K_0 \frac{1}{\cos \alpha_0} \sin \phi_0 r \quad (G.3)$$

with $\alpha_0 = \beta_0 + \phi_0$ (see Fig. G.1).

The main uncertainty in M_{R_0} is due to the model used in the computation of the resultant earth pressure. In order to account for this modeling error associated with P_0 , a corrective factor, N_{P_0} , will be inserted into Eq. G.3. Accordingly, M_{R_0} can be expressed as

$$M_{R_0} = \frac{1}{2} N_{P_0} \gamma_0 h_0^2 K_0 \frac{1}{\cos (\beta_0 + \phi_0)} \sin \phi_0 r \quad (G.4)$$

Assuming that K_0 and ϕ_0 are statistically independent, the first-order analysis gives

$$\mu_{M_{R_0}} \approx \frac{1}{2} \bar{N}_{P_0} \gamma_0 h_0^2 \bar{K}_0 \frac{1}{\cos (\bar{\beta}_0 + \bar{\phi}_0)} \sin \bar{\phi}_0 r \quad (G.5)$$

$$\Omega_{M_{R_0}}^2 \approx \Omega_{P_0}^2 + \Omega_{K_0}^2 + [\cot \bar{\phi}_0 + \tan \alpha_0]^2 \bar{\phi}_0^2 \Omega_{\phi_0}^2 \quad (G.6)$$

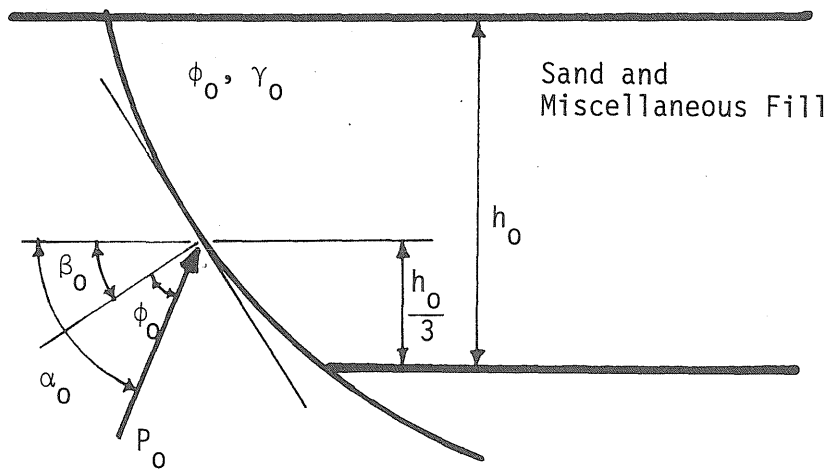


Fig. G.1 Resistance Due to Cohesionless Layer

